MASTERARBEIT / MASTER'S THESIS

Titel der Masterarbeit / Title of the Master's Thesis

„Evaluation of molecular, physiological, and biochemical properties of pathogenic and non-pathogenic *Acanthamoeba* isolates“

verfasst von / submitted by

Maya Alida Ilse Schwarz, B.Sc.

angestrebter akademischer Grad / in partial fulfilment of the requirements for the degree of

Master of Science (MSc)

Wien, 2024 / Vienna 2024

Studienkennzahl lt. Studienblatt / degree programme code as it appears on the student record sheet: UA 066 834

Studienrichtung lt. Studienblatt / degree programme as it appears on the student record sheet: Masterstudium Molekulare Biologie

Betreut von / Supervisor: Univ.-Prof. Mag. Dr. Julia Walochnik

I. Abstract

Background: *Acanthamoeba* spp. are ubiquitous organisms with a high medical relevance, as they can cause *Acanthamoeba* keratitis (AK) and granulomatous amoebic encephalitis (GAE) in humans. It is not fully understood which factors contribute to the pathogenicity of a strain, however, certain genotypes, growth at higher temperatures, the expression of a mannose-binding protein (MBP) and the secretion of several proteases, in particular a mannose-induced protease (MIP), have been reported to be associated with pathogenic strains. It was the aim of this study to compare these properties between clinical and environmental strains in detail.

Methods: Several molecular approaches were applied. The 18S rRNA gene of the pathogenic and environmental strains was sequenced to create a phylogenetic tree. In a temperature tolerance test, the growth at different temperatures of all strains was evaluated. To compare protein and protease patterns, especially of the MBP, amoebae were incubated with mannose and examined with SDS-PAGE and zymography. Furthermore, the expression of MBP and MIP was investigated by quantitative RT-PCR.

Results: The sequencing and phylogenetic analysis revealed that all strains represent genotype T4. This was confirmed by the phylogenetic analysis. The environmental strain E2 showed growth at 37°C, indicating potential pathogenicity. The pathogenic strains differed from the non-pathogenic strains in their protein and protease patterns, but interestingly, no differences in the expression of MBP and MIP were detected. RT-PCR revealed no differences in the expression of MBP between clinical and environmental strains.

Conclusion: Our results clearly support temperature tolerance and a specific protein and protease patterns as pathogenicity markers in *Acanthamoeba* spp. However, pathogenicity was not associated with higher expression of MBP and MIP.

II. Zusammenfassung

Hintergrund: Akanthamöben sind ubiquitäre Organismen mit hoher medizinischer Relevanz, da sie Akanthamöben-Keratitis (AK) und granulomatöse Amöbenenzephalitis (GAE) beim Menschen verursachen können. Es ist nicht vollständig geklärt, welche Faktoren zur Pathogenität eines Stammes beitragen. Es wurde jedoch berichtet, dass bestimmte Genotypen, das Wachstum bei höheren Temperaturen, die Expression eines Mannose-bindenden Proteins (MBP) oder die Sekretion verschiedener Proteasen, insbesondere einer Mannose-induzierten Protease (MIP), mit Pathogenität assoziiert sind. Das Ziel vorliegender Arbeit war, diese Eigenschaften bei klinischen Stämmen und Umweltstämmen vergleichend zu untersuchen.

Methoden: Es wurden mehrere molekulare Techniken angewandt. Das 18S-rRNA-Gen der pathogenen als auch das der apathogenen Umweltisolate wurde sequenziert, um einen phylogenetischen Baum zu erstellen. In einem Temperaturtoleranztest wurde das Wachstum aller Stämme bei verschiedenen Temperaturen untersucht. Zum Vergleich der Protein- und Protease-Muster, insbesondere des MBP, wurden die Amöben mit Mannose inkubiert und mittels SDS-PAGE und Zymographie untersucht. Außerdem wurde die Expression von MBP durch quantitative RT-PCR genauer betrachtet.

Ergebnisse: Die Sequenzierung ergab, dass alle Stämme den Genotyp T4 repräsentieren. Dies wurde durch die phylogenetische Analyse bestätigt. Das Umweltisolat E2 wuchs bei 37°C, was auf eine mögliche Pathogenität hinweist. Die pathogenen Stämme zeigten andere Protein- und Protease-Muster als die nicht-pathogenen Stämme, interessanterweise konnte aber kein Unterschied in der Expression von MBP und MIP gefunden werden. In der RT-PCR zeigten sich keine Expressionsunterschiede von MBP zwischen klinischen Isolaten und Umweltisolaten.

Fazit: Unsere Ergebnisse unterstützen eindeutig die Temperaturtoleranz und ein spezifisches Protein- und Protease-Muster als Pathogenitätsmarker bei Akanthamöben. Die Pathogenität stand jedoch nicht mit einer erhöhten Expression von MBP oder MIP in Zusammenhang.

III. Acknowledgements

An dieser Stelle möchte ich mich bei den Menschen bedanken, die mich in den letzten 1 ½ Jahren begleitet, unterstützt und an mich geglaubt haben und die ich sehr in mein Herz geschlossen habe.

Vielen Dank liebe Julia, für die Ermöglichung meines Projektes und die stetige Unterstützung, immer und zu jedem Thema.

Danke Martina, dafür dass Du nicht nur meine Betreuerin, sondern auch eine Mentorin und vor allem Supporterin warst und immer ein offenes Ohr und einen Rat für mich hattest. Ich hätte mir keine bessere Betreuerin wünschen können. Danke.

Danke Alvie, dafür dass Du dir immer Mühe gegeben hast mir zu helfen.

Danke Ivetta, für die Zigaretten-Pausen und dass Du so bemüht warst mich zu verkuppeln, auch wenn es leider nicht geklappt hat. Das lag aber definitiv an mir.

Danke an Ina für Deine Offenheit und Wärme.

Danke an Kathi, Edwin, Aileen, Iwona und Tania. Danke an das ganze Parasitologie Team für so viel Harmonie im Labor. Ich bin jeden Tag gerne in die Arbeit gekommen und habe mich sehr wohl gefühlt.

Danke Sophia fürs gemeinsam in die Bib gehen und kaffetscherln. Dein Rat und Deine Meinung sind mir sehr viel wert.

Danke Julia fürs für mich Da sein, fürs Unterstützen und für die Bib-Dates.

Danke Tom und Danke Lili, fürs gemeinsame Leiden, Schreiben und in die Bib gehen.

Danke an meine Eltern und Willi, ihr seid super. Habe euch sehr lieb und bin sehr dankbar, so große Fans zu haben.

Danke.

IV. Table of content

V. List of figures

VI. List of tables

VII. List of abbreviations

ADP	Adenosine diphosphate
AIC	Akaike information criterion
AIDS	Acquired immunodeficiency syndrome
AK	*Acanthamoeba* keratitis
AP	*Acanthamoeba* pneumonia
APC	Antigen-presenting cells
APS	Ammonium persulfate
ATP	Adenosine triphosphate
BSA	Bovine serum albumin
CA	Cutaneous acanthamoebiasis
cAMP	Cyclic adenosine monophosphate

cDNA	Complementary DNA
CL	Contact lens
CO_2	Carbon dioxide
CP5	Cysteine protease 5
CPE	Cytopathic effect
CSF	Cerebrospinal fluid
DAMP	Damage-associated molecular pattern
DNA	Desoxyribonucleic acid
gDNA	Genomic DNA
mtDNA	Mitochondrial DNA
rDNA	Ribosomal DNA
dNTP	Deoxyribonucleoside triphosphate
E-64	Trans-epoxy-succinyl-L-leucyl-amido (-4-guanidino)-butane
FISH	Fluorescence in situ hybridisation
GAE	Granulomatous amoebic encephalitis
gDNA	Genomic DNA
HIV	Human immunodeficiency virus
H_2O	Hydrogen oxide
IFNγ	Interferon gamma
IgG/A	Immunoglobulin G/A
IVCM	In vivo confocal microscopy
kDa	Kilo Dalton
Mannose	Methyl alpha-D-mannopyranoside
MBP	Mannose-binding protein
MEGA	Molecular Evolutionary Genetics Analysis
MEM Eagle	Eagle's minimum essential medium
$MgCl_2$	Magnesium chloride
MIP	Mannose-induced protease
ML	Maximum likelihood
MP	Metalloproteinases
mtDNA	Mitochondrial DNA
NaAc	Sodium acetate

NaCl	Sodium chloride
NJ	Neighbour-Joining
PAA	Polyacryamide
PAMP	Pathogen-associated microbial pattern
PBS	Phosphate-buffered saline
PCR	Polymerase chain reaction
Phen	1,10-Phenantroline
PHMB	Poly hexamethylene biguanide
PMSF	Phenylmethanesulfonylfluoride
PYG	Peptone yeast extract glucose
RAPD	Random amplification of polymorphic DNA
rDNA	Ribosomal DNA
RFLP	Restriction fragment length polymorphism
RNA	Ribonucleic acid
rRNA	Ribosomal RNA
RT-PCR	Real-time PCR
SLE	Systemic lupus erythematosus
SP	Serine proteases
Temed	N, N, N′, N′-Tetramethyl ethylenediamine
Th	T-helper cell
w/o M	Without mannose
18S rRNA	18S ribosomal RNA coding DNA

VIII. Introduction

Acanthamoeba spp. are ubiquitous single-celled eucaryotic organisms. The genus *Acanthamoeba* belongs to the family Acanthamoebidae in the Amoebozoa (Protista). They are free-living amoebae (FLA) that are very versatile and can be found in nearly every natural and man-made habitat worldwide, such as soil, freshwater, pools, or contact-lens cases (Marciano-Cabral & Cabral, 2003). Their life cycle is divided into the active trophozoites and the dormant cysts. Cysts can survive for an extended period and are very resistant to chlorine, fungicides, and antibiotics (De Jonckheere & Van De Voorde, 1976).

Acanthamoeba spp. can also be parasitic pathogens, which are able to cause serious diseases in humans, such as *Acanthamoeba* keratitis (AK) and granulomatous amoebic encephalitis (GAE). Furthermore, they can act as vectors and reservoirs for pathogenic bacteria and viruses (Philippe et al., 2023).

Within the genus *Acanthamoeba* various genotypes have been described based on sequencing of the 18S rDNA. To date, 23 genotypes are known (Corsaro, 2020).

Infections caused by *Acanthamoeba* spp. are hard to diagnose and difficult to treat, which requires further research and improved approaches for identification and differentiation, as well as prevention measurements in the future. By giving insights into eucaryotic cell biology, cell-cell interactions, mechanisms of resistance and evolution, amoebae are important model organisms in research.

Several factors have been reported to be associated with pathogenicity, as the respective genotype, growth at higher temperatures, the expression levels of the mannose-binding protein (MBP), and the expression of several proteases, in particular the mannose-induced proteases (MIP), as well as the expression of specific genes. Yet, no reliable and simple differentiation between pathogenic and non-pathogenic strains has been established yet. The aim of this study was, to apply a combination of the above-mentioned methods in order to differentiate pathogenic and environmental isolates and evaluate the differential potential of the applied methods.

8.1. *Acanthamoeba* spp.

The term amoeba was first established by Bory de St. Vincent (1822) and included a large group of polyphyletic and diverse organisms, with no general phenotypic features. Dujardin (1838) established the class Rhizopoda, which included amoebae and foraminifera and was further extended in the same year by Ehrenberg (1838) by the genus *Amoeba*. Specific characters of *Acanthamoeba* spp. are their acanthopodia, which are spiny projections on the cell surface, and their double-layered cyst walls (Marciano-Cabral & Cabral, 2003). Sawyer and Griffin (1975) established the family Acanthamoebidae. Furthermore, Pussard and Pons (1977) separated the *Acanthamoeba* spp. into 18 different species and described three distinct morphologically groups based on cyst morphology. Today 31 *Acanthamoeba* species are known (Connelly et al., 2023).

8.2. Biology

8.2.1. Life cycle and morphology

The life cycles of *Acanthamoeba* spp. consists of two distinct stages: the active trophozoite stage and the dormant cyst (see Figure 1).

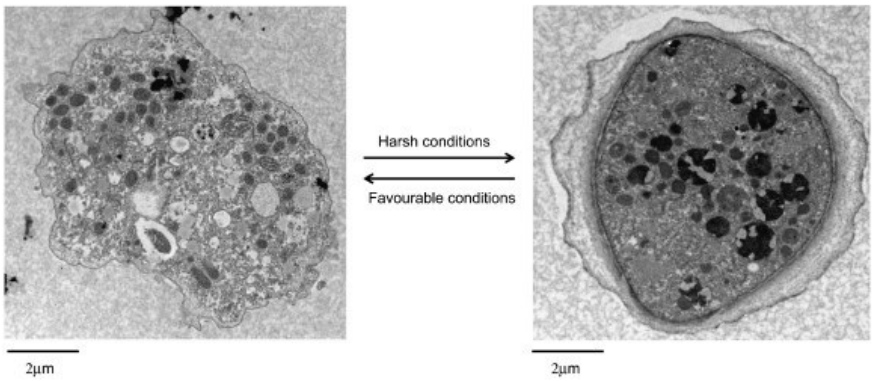

Figure 1. The two stages of Acanthamoeba spp.: trophozoites (left) exist under favourable conditions and cysts (right) under harsh conditions. Image from Siddiqui & Khan (2012).

8.2.1.1. Physiology and morphology of trophozoites

The vegetative stage is the active trophozoite. It has a diameter of 13-23 µm (Siddiqui & Khan, 2012). The trophozoite exists under favourable conditions and exhibits so called acanthopodia, tiny projections from the pseudopods, which are important for feeding and adhesion, for example to contact lenses (Lee et al., 2018; Walochnik & Aspöck, 2002) (see Figure 2).

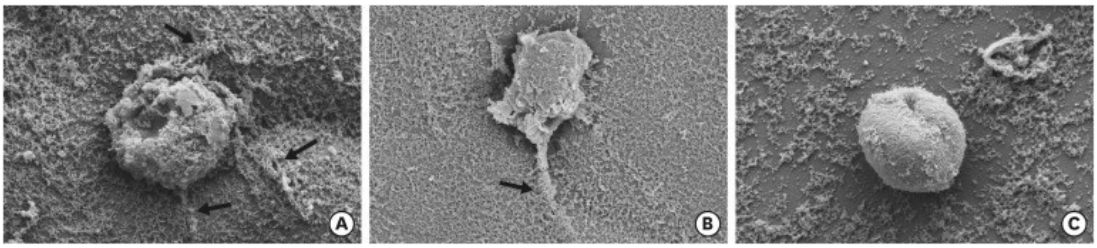

Figure 2. Three different types of cysts from Acanthamoeba spp. Trophozoites can have more than one acanthopod (A), exactly one acanthapod (B) or none (C). Image from Lee et al. (2012).

Amoebae are heterotrophic and mostly feed on bacteria (Doyscher et al., 2013). They prefer coliforms, as *Escherichia coli*, or non-fermentative gram-negative bacteria (Gray et al., 1995). Furthermore, algae, fungi, for example yeast, organic matter, other protozoa as well as keratocytes may serve as food source for the amoeba (Marciano-Cabral & Cabral, 2003; Maycock & Jayaswal, 2016; Neelam & Niederkorn, 2017). The feeding occurs either via phagocytosis or pinocytosis (Alsam et al., 2005; Bowers & Olszewski, 1983; Marciano-Cabral & Cabral, 2003).

The trophozoite moves via the formation of a single pseudopodium anteriorly and smaller acanthopodia on the cell surface (Marciano-Cabral & Cabral, 2003; Preston et al., 2001; Preston & King, 1984).

As in all eukaryotes, typical organelles as a nucleus, smooth and rough endoplasmic reticula, the Golgi apparatus, and mitochondria for energy supply are present (Bowers & Korn, 1968). Furthermore, a rather large contractile vacuole in the cytoplasm is a typical feature for *Acanthamoeba* spp. and important to control the water content (R. F.Carter, 1970; Ma et al., 1990).

The asexual reproduction only occurs in the trophozoite stage via binary fission and mitotic division and requires a favourable environment (Johnston et al., 2009; Marciano-Cabral & Cabral, 2003; Neelam & Niederkorn, 2017; Siddiqui & Khan, 2012). The trophozoite is the infective stage and plays a relevant role in establishing the diseases AK and GAE.

8.2.1.2. Encystment and morphology of cysts

The long-term stage is the resistant and dormant cyst. As a reaction to harsh environmental conditions, for example glucose deficiency, extreme temperatures, non-neutral pH conditions, and/or dryness, trophozoites develop into a double-walled cyst (Bowers & Korn, 1969; Chagla & Griffiths, 1974; Cordingley & Trzyna, 2008). During the encystment process firstly an outer wall, the exocyst, followed by an inner wall, the endocyst, are formed (Weisman, 1976). It is a mechanism to adapt and survive in unfavourable environments. The thicker ectocyst, characterized by laminar fibrous layers and an uneven surface, and the thinner endocyst, composed of fine fibers with a smoother surface, are divided by an intercystic space and connect only at the ostioles. These pores are shielded by opercula, through which *Acanthamoeba* spp. emerge during the excystment process (Chávez-Munguía et al., 2009; Köhsler et al., 2016; Wang et al., 2023).

The ectocyst consists of proteins and several polysaccharides, while the endocyst is composed of 1,4 b-glucan-containing cellulose and xylose (Derda et al., 2009; Dudley et al., 2009; Linder et al., 2002; Tomlinson & Jones, 1962; Weisman, 1976). These components support the stability of the cyst wall and make it more vigorous (Moon et al., 2018; Tomlinson & Jones, 1962). The encystment begins with the trophozoites losing their amoeboid appearance by rounding up, followed by the degradation of glycogen via the glycogen phosphorylase (Bowers & Korn, 1969; Lorenzo-Morales et al., 2008; Moon & Kong, 2012). This is supported by cAMP, which converts the phosphorylase into its active form for glycogen degradation (Siddiqui & Khan, 2012).

During this process, changes in gene expression take place and intracellular macromolecules, as proteins, glycogen, and RNA, decline (Bowers & Korn, 1969). Cysts have a minimal metabolic activity (Siddiqui & Khan, 2012).

The metabolic inactive cysts have been shown to remain viable for up to 24 years in the encysted state and still be infectious after hatching (Sriram et al., 2008). The reason for their extreme endurance is the high resistance against chlorine, as well as fungicides and antibiotics (De Jonckheere & Van De Voorde, 1976). The cysts can survive for a very long period of time in the environment, but also for example on contact lenses or in contact lens cases.

When the environmental conditions are more favourable, the excystment process takes place (Brocious et al., 2018; Marciano-Cabral & Cabral, 2003). Hereby, the operculum is removed, and the outer shell is left behind (Köhsler et al., 2016). While the hatching only takes some minutes, the entire excystment process can take up to 12 hours (Mattar & Byers, 1971).

8.2.2. Distribution and habitats

*Acanthamoeb*a spp. are ubiquitous and versatile organisms and can be found in a variety of places. Because of the very resistant cysts, they are well adapted to unusual and harsh conditions, such as heat and extreme dryness. In the past, many different habitats of *Acanthamoeba* spp. have been documented, including untreated natural freshwater environments, man-made habitats, different types of soil, air, dust, and in samples collected and isolated from humans or animals (De Jonckheere, 1991; Marciano-Cabral & Cabral, 2003; Somani et al., 2023).

In nature, *Acanthamoeba* spp. can be found in natural spring water resources, lakes, fishponds, small streams, and hot springs (Karaman et al., 2022; Lekkla et al., 2005; Majid et al., 2017; Nacapunchai et al., 2014). Moreover, seawaters and fresh waters can be a natural habitat for these organisms, too (Rayamajhee et al., 2023).

They can be present in treated water systems, as swimming pools, hydrotherapy pools, and in tap water (Dini et al., 2000). Furthermore, De Jonckheere (1979) isolated these eukaryotes from aquaria.

Acanthamoeba spp. can be found in different kinds of soil, as agricultural or garden soil, but also in very dry soil and dust (Basher et al., 2018; Meighani et al., 2018).

They can also commonly be found in contact lens cases and on contact lenses, which can be a risk factor for contact lens wearers (Dini et al., 2000; Hassan et al., 2022). Biofilms in general represent a common habitat for *Acanthamoeba* spp. (Barbeau & Buhler, 2001).

Even though *Acanthamoeba* spp. are generally free-living and do not require a host for their life cycle, they have been isolated from humans, various other mammals, and even reptiles, and fish (Dykova et al., 1999; Kamel Abd Ghani et al., 2005; Tuska-Szalay et al., 2022).

In humans, isolates have been collected from corneal scraping, brain tissue, and nasal swaps, as well as from diverse tissues and organs from AK patients and immunocompromised patients (Buerano et al., 2014; Cruz & Rivera, 2014; Marciano-Cabral & Cabral, 2003; Wara-Asawapati et al., 2017).

8.2.3. Identification and differentiation

8.2.3.1. Morphological approaches

According to the morphology of the cysts, *Acanthamoeba* species have been separated into three morphological groups (Pussard & Pons, 1977) (see Figure 3).

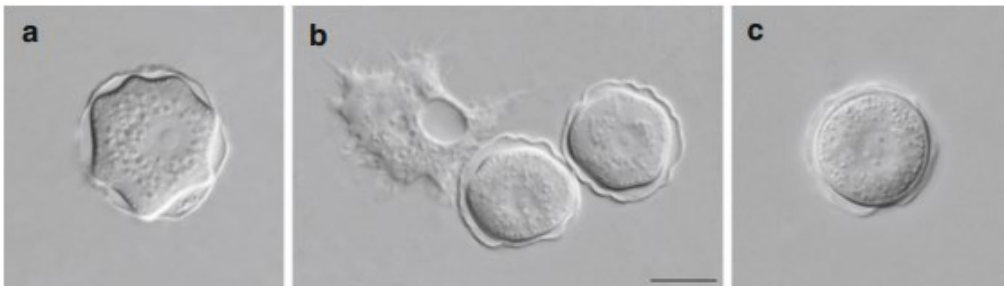

Figure 3. Three different groups of Acanthamoeba spp., according to the morphology of the cysts. Group 1 (a), 2 (b), and 3 (c). Image from Köhsler et al. (2016).

Group 1. Individuals of the first group are the largest, regarding trophozoite and cyst size (see Figure 3a). Cysts have a diameter of more than 18 µm and a rounder outer wall, which is clearly separated from the inner wall (Kong, 2009). Only radiations contribute to a star-shaped structure. The opercula do not penetrate the external cyst wall (Köhsler et al., 2016).

Group 2. Individuals representing the second group are smaller and the shape of the endocyst can vary from polygonal, triangular, or oval to round (see Figure 3b) (Corsaro, 2020). The cysts have a diameter of around 18 µm and while it is possible to detach the ectocyst and endocyst, the ectocyst typically displays wrinkles (Kong, 2009). No apparent radiations are visible, and the opercula are often engulfed into the ectocyst (Köhsler et al., 2016).

Group 3. The individuals of this group exhibit a smaller size, with cysts measuring less than 18 µm, and typically possess poorly defined or no distinct cyst walls (see Figure 3c) (de Lacerda & Lira, 2021; Köhsler et al., 2016). The ectocyst has a very thin and often ripped wall. The endocyst on the other hand has a rounder, triangular or rectangular shape (Kong, 2009).

Moreover, based on morphology the amoebae have been divided into around 25 morphological species (Corsaro & Venditti, 2023). However, classification of *Acanthamoeba* spp. according to trophozoite or cyst morphology alone can be defective because the shape and appearance also depends on several environmental factors, for example culture conditions (Fuerst, 2014; Startford & Griffiths, 1978).

Furthermore, for investigating the pathogenicity of isolates, morphological approaches lack certainty, because experiments showed that different isolates from the same species, here in particular *A. castellanii*, can look morphologically alike, even if their pathogenic potential ranges from non-pathogenic over weakly to highly pathogenic. On the one hand, the Neff strain of *A. castellanii* described by Gunderson & Sogin (1986), exhibits non-pathogenic features (De Jonckheere, 1980). On the other hand, some amoebae that were isolated from an ocular infection were identified as *A. castellanii*, indicating a potential pathogenicity of this species as well (Nagington et al., 1974).

The morphological approach might be helpful for a rough estimation of the respective species. Nowadays, for more detailed investigations and certainty, morphological approaches are usually combined with physiological and molecular methods.

8.2.3.2. Physiological approaches

Early on, physiological approaches to differentiate between strains and to estimate their pathogenic properties were made.

Cursons and Brown (1978) found that pathogenic strains can produce cytopathic effects on targets cells, short CPE, in contrast to non-pathogenic representatives. De Jonckheere (1980) further investigated the CPEs of 19 different *Acanthamoeba* species to identify the pathogenic strains by evaluating the correlation of CPEs, growth characteristics and virulence of the different species in mice.

These studies showed that in many strains appeared to be a correlation between the investigated factors and pathogenicity.

Earlier literature reports the ability of pathogenic isolates to grow at temperatures up to 46°C, which is the temperature of extremely high fever in humans, whereas non-pathogenic isolates lack the ability to grow at temperatures higher than 37°C (Griffin, 1972). Other experiments showed that pathogenic strains can lose their ability to grow at high temperatures after long-term culture, and, on the other hand, non-virulent strains can adapt to higher temperatures (Pumidonming et al., 2010).

Furthermore, pathogenic strains seem to adapt faster to axenic medium that non-pathogenic strains (De Jonckheere, 1980). Pumidonming et al. (2010) separated the strains according to their generation time into fast growing (<20h), moderately growing (20-30h), and slowly growing (>30h) strains at 34°C, 37°C, and 40°C, but did not find a correlation between growth rates and strain properties, such as age, origin, or genotype.

Therefore, physiological approaches alone also seem to be insufficient in differentiating between pathogenic and non-pathogenic isolates. For an estimation of the pathogenic potential of a strain, physiological approaches should be combined with morphological and molecular approaches in order to make more reliable conclusions.

8.2.3.3. Molecular approaches

More recent methods for identification and differentiation of *Acanthamoeba* spp. are molecular approaches, as well as protein-based techniques.

8.2.3.3.1. Protein-based approaches

One protein-based approach is **isoenzyme analysis** that was used either for the identification of a strain or for taxonomy. This method was first applied in 1983 by De Jonckheere (1983), who did an analysis of isoenzyme patterns using agarose isoelectric focusing within a pH range of 3 to 10, as well as protein patterns in a pH range of 5 to 8. He differentiated 30 *Acanthamoeba* strains according to their isoenzyme profile and total protein patterns and classified them into five different species. Two years later, the enzyme activities of 37 representative strains of *Acanthamoeba* spp. against 19 substrates were examined and 13 enzyme complements in total could be found, which were then separated into six larger groups (Costas & Griffiths, 1985). Even a new species, designated *A. healyi*, could be identified by isoenzyme analysis in 1992 (Moura et al., 1992).

Nonetheless, this approach cannot always be used, since it has been shown that it is not applicable for individual species. This was reported by Kong et al. (1995), who found polymorphisms within seven *A. polyphaga* strains.

Another protein-based approach is **SDS-PAGE**, which is short for sodium dodecyl-sulfate polyacrylamide gel electrophoresis and can be used to investigate protein patterns and enzyme activity in general by separation. By initial denaturation of proteins, followed by electrophoresis, protein expression and immunochemical patterns can be analysed (Nowakowski et al., 2014).

Further, **immunoblotting** is an effective method to identify single proteins with the help of antibody specificity. Specific antibodies recognize and bind to the target proteins, thereby detecting their presence or further determining the molecular weight of the protein (Litovchick, 2020).

8.2.3.3.2. DNA-based approaches

One of the most promising approaches for identification of *Acanthamoeba* strains are DNA-based methods.

An important approach was the **restriction fragment length polymorphism**, short **RFLP**. Hereby for example genomic DNA, mitochondrial DNA, ribosomal DNA or other material is incubated with specific restriction enzymes and the resulting fragments are further separated by gel electrophoresis to identify genetic differences (Hames, 1998). Because RFLP was already applied as a useful tool in classifying bacteria, viruses and other pathogens, McLaughlin et al. (1988) characterized several *Naegleria* spp. and *Acanthamoeba* spp. isolates, with the purpose to classify and distinguish between clinical isolates and environmental samples.

Random amplification of polymorphic DNA, short **RAPD** is an approach to analyse and evaluate differences and pairwise similarities of samples, which can be useful regarding diagnostics (Pélandakis et al., 2006).

Hereby no specific DNA segment is targeted, but a long genomic DNA sequence and several short primers are mixed, and random sequences are amplified (Ortega-Rivas et al., 2003). With the resulting patterns a phenogram can be created (Alves et al., 2000).

The most popular technique is the so-called **polymerase chain reaction**, short **PCR**, which was first discovered by Mullis (1990). The conventional PCR assay is known to be a sensitive and reliable approach to detect and identify genes by the rapid amplification of specific DNA fragments (Garibyan & Avashia, 2013). Quantitative measurements of gene expression are possible, as well as the detection of *Acanthamoeba* spp. (Derda et al., 2014). Limitations can be the highly sensitive DNA polymerases and specific primers, for which information of the sequence needs to be available (Garibyan & Avashia, 2013). The most frequently used primers to identify *Acanthamoeba* spp. target the amoebic 18S ribosomal RNA gene (18S rRNA) (Schroeder et al., 2001).

Another PCR approach for DNA amplification and RNA studies that became more and more popular in the last years is the **real-time PCR**, also called quantitative PCR. This method can measure the expression of genes in real-time, detect single nucleotide polymorphisms or can be used for quantitative genotyping (Deepak et al., 2007).

With its improved accuracy and sensitivity, it can be useful for epidemiological surveys and play a key role in the improvement of *Acanthamoeba* infection control (Artika et al., 2022; Lamien-Meda et al., 2022). The first real-time PCR approach for the genus *Acanthamoeba* was established in 2006 by Rivière et al. (2006). The same year, Qvarnstrom et al. (2006) published a multiplex RT-PCR to detect, quantify and differentiate between *Acanthamoeba* spp., *Balamuthia* spp. and *Naegleria* spp. at the same time. This proved, that real-time PCR can be a very effective approach, by combining several working steps into one. Karsenti et al. (2017) developed a RT-PCR assay for the diagnosis of AK with a sensitivity of 100% and a specificity of 94%, contributing to the rapid and effective detection of *Acanthamoeba* spp. Since 2022, even the detection and differentiation of all seven main 18S subtypes (T4A-T4G) of the most abundant genotype T4 by real-time PCR is possible (Azzopardi et al., 2023; Lamien-Meda et al., 2022).

8.3. Phylogeny

The first classification scheme of the genus *Acanthamoeba* spp. was published by Lee et al. (1985) and resembles strongly the later published scheme of Martinez and Visvesvaraz (1997). According to these classification schemes, *Acanthamoeba* are part of the kingdom Protista, subkingom Protozoa, phylum Sacromastigophora, class Lobosea, order Acanthopodia[1]/Amoebida[2], and family Acanthamoebidae.

Pussard and Pons separated *Acanthamoeba* spp. into three different groups according to the morphological properties of the cysts (1977). The classification can be seen in the paragraph "Morphological approaches" (see 8.2.3.1.). To this day, 31 morphological species of *Acanthamoeba* have been identified (Connelly et al., 2023; Corsaro, 2020). When molecular-biological analysis became more popular, sequencing of the entire 18S ribosomal RNA gene (18S rDNA) led to the nowadays widely accepted genotype systems.

[1] According to Lee et al. (1985)
[2] According to Martinez and Visvesvaraz (1997)

This started by the differentiation into four genotypes T1-T4, followed by the differentiation into eight further genotypes (Fuerst, 2014; Gast et al., 1996; Stothard et al., 1998). Today *Acanthamoeba* spp. can be distinguished into 23 genotypes T1-T23, but the number is still increasing (Corsaro, 2021; Corsaro et al., 2015; Köhsler et al., 2016; Putaporntip et al., 2021; Taher et al., 2018). The most abundant genotype, isolated from patients with AK, is the genotype T4, followed by the genotype T3 (Booton et al., 2002, 2005; Walochnik et al., 2015). However, genotype T4 is also the most frequently isolated genotype in environmental samples, without pathogenicity against humans (Booton et al., 2009).

Gast et al. (1996) originally reported that strains in one group differ by at least 6% from all other sequences. Nowadays genotypes differ with a divergence of at least 5% (Stothard et al., 1998). Because of the high divergence within the genotype, Maghsood et al. (2005) divided genotype T2 into the subtypes T2a and T2b. This was followed by the division of genotype T4 into eight subtypes, T4A, T4B, T4C, T4D, T4E, T4F, T4G, and T4Neff (Corsaro & Venditti, 2023; Fuerst, 2014; Fuerst et al., 2015).

8.4. Medical relevance

8.4.1. *Acanthamoeba* keratitis (AK)

Acanthamoeba keratitis is an infection with increasing prevalence. The first case was described in 1974 by Nagington et al. (1974). In the last decades the numbers of infected individuals increased, which is on the one hand connected to the raising number of contact lens wearers and due to improved diagnostic approaches on the other hand (Walochnik & Aspöck, 2021).

8.4.1.1. Epidemiology

In German-speaking countries the incidence of *Acanthamoeba* keratitis is 0.2 cases/100.000 people (Walochnik & Aspöck, 2021). In the Netherlands, the incidence increased from 16 cases in 2009 to 49 cases in 2015, indicating an incidence rate of 1 in 21.000 in soft contact lens wearers in 2015 (Randag et al., 2019). In the USA 372 cases of AK from 1999 to 2011 were reported with a seasonal peak in summer, again with the soft contact lenses as highest risk factor (Page & Mathers, 2013).

Orphanet for rare diseases documented a prevalence of 1-9/100.000 (see ORPHA:67043, Orphanet: Amöbenkeratitis, last checked: 04/01/2024). Büchele et al. (2023) reported, that more frequently female than male patients are infected with an average age of 33.7 years.

8.4.1.2. Risk factors

The risk factors for an infection with AK are dependent on the demographic setting. In developing countries, corneal trauma is the main condition for the establishment of AK, which can be connected to the profession, as for example farming (Jiang et al., 2015). The primary group of patients are non-CL wearers (Agarwal et al., 2014; Arance-Gil et al., 2014; Chynn et al., 1995; Jiang et al., 2015; Raghavan et al., 2018).

In industrialised countries, AK is very often related to the wear of contact lenses (Brown et al., 2018; Cope et al., 2015; Neelam & Niederkorn, 2017; Orosz et al., 2018; Siddiqui et al., 2016; Tanaka et al., 2017). Contact lens wear is therefore the main risk factor for an infection with *Acanthamoeba* spp. besides corneal trauma in general, which may also be related to the wear of contact lenses and/or surgeries (Chin et al., 2015; Gray et al., 1995; Ibrahim et al., 2009; Kilvington, 1993; Lonnen et al., 2014; Lorenzo-Morales et al., 2015; Marciano-Cabral & Cabral, 2003; Mascarenhas et al., 2014; Maycock & Jayaswal, 2016; Reverey et al., 2014; Taher et al., 2018).

The type of contact lenses plays an important role. Amoebae adherence can occur within all types of lenses, including rigid gas permeable lenses, soft lenses, hard lenses, hybrid lenses, orthokeratology lenses, and cosmetic lenses (Chan et al., 2014; Cope et al., 2015; Mascarenhas et al., 2014; McKelvie et al., 2009; Wilhelmus et al., 2008). The highest risk hereby is observed for soft lenses, which also have the highest water content (Chin et al., 2015; Sharma et al., 2000). The predisposition of a contact lens for microbial adherence depends on several factors as surface roughness, the hydrophobicity, the charge of the lens and the composition of the contact lens material (Campolo et al., 2022).

Other risk factors regarding the lenses can be bad hygiene habits in general (Gomes et al., 2016; Marciano-Cabral & Cabral, 2003).

This includes poor hand hygiene, the insufficient cleaning of the lenses with disinfectant, contact to contaminated water, wearing lenses longer than recommended and overnight wear of the lenses (Cope et al., 2015; Kuzman et al., 2014; Mascarenhas et al., 2014; Tan et al., 2018).

The usage of an all-in-one multipurpose solution can decrease the adhesion rate of the amoebae, but correct usage is crucial (S. M. Lee et al., 2018; Lorenzo-Morales et al., 2013; Maycock & Jayaswal, 2016). Factors that can drive an AK are reusing contact lens solutions, topping off, using expired solution, not following the manufacturers protocol correctly or using self-made saline solution and chlorine-based disinfection (Abjani et al., 2016; Carnt et al., 2023; Cope et al., 2015; Niyadurupola & Illingworth, 2006; Por et al., 2009; Radford et al., 2002; Tu & Joslin, 2010a; Willcox, 2010).

AK can also be caused through contact with contaminated water. This includes tap water, water from tanks or lakes, the contact to water during activities as swimming, fishing, snow and water sports, or the daily use of commodities, such as the shower or the hot tub (Arance-Gil et al., 2014; Carnt & Stapleton, 2016; Lindsay et al., 2007; Mirsayafov et al., 2018; Nau & Dhaliwal, 2018; Por et al., 2009; Tan et al., 2018).

Another risk factor can be the contact lens storage case (Larkin et al., 1990; Lonnen et al., 2014). The insufficient cleaning of the case, infrequent replacement, washing with normal tap water, and storage when not air dried, can contribute to an infection (Kuzman et al., 2014; Mirsayafov et al., 2018; Tan et al., 2018; Zimmerman et al., 2017). The presence of bacteria and fungi in the case positively influence the presence of *Acanthamoeba*, as these organisms serve as food source (Matsumoto et al., 2017).

The formation of biofilm on the contact lenses or in the contact lens storage cases represents another risk factor (Bakay & Polat, 2018; Beattie & Tomlinson, 2009).

Regarding the age, younger people under 26 and older people over 55 are more at risk than the rest of the population (Carnt & Stapleton, 2016; Mascarenhas et al., 2014).

General health problems, as an immunosuppression, or diseases such as thyroid disease, as well as genetic mutations, are factors that can contribute to an infection, however, the majority of immunocompromised patients with AK are contact lens wearers (Antonelli et al., 2018; Keay et al., 2009; Lorenzo-Morales et al., 2013; Magnet et al., 2018; Schein et al., 1989; Stapleton & Carnt, 2012).

8.4.1.3. Symptoms

Symptoms of an acute *Acanthamoeba* keratitis can be the feeling of discomfort, blepharospasm, conjunctival hyperaemia, ptosis, excessive tearing, oedema, and/or a foreign body sensation (Siddiqui et al., 2016).

It can also lead to a blurred vision and/or a decreased visual acuity, but the complete loss of vision is an acute problem in a later stage of the infection (Lindsay et al., 2007). Further, ocular pain and/or photophobia are also frequent symptoms (Brown et al., 2018; Chynn et al., 1995; Kaiserman et al., 2012; Lorenzo-Morales et al., 2013, 2015; Neelam & Niederkorn, 2017; Taher et al., 2018; Tanaka et al., 2017). The pain in the eye is related to the inflammation, but the intensity of the pain can differ depending on how much the corneal nerves are affected (Alomar et al., 2009; Stan et al., 2016).

AK mostly occurs unilateral, but can also appear bilateral (Kurna et al., 2012; Wilhelmus et al., 2008).

The symptoms of AK are very similar to those of bacterial, viral, and fungal keratitis, which can complicate the diagnosis (Buchele et al., 2018; Illingworth et al., 1995; Lorenzo-Morales et al., 2013; Niyadurupola & Illingworth, 2006; Stan et al., 2016).

8.4.1.4. Clinical signs

Perineural infiltrates are common during the early stage of an infection and are a pathognomonic sign of AK (Patel & McGhee, 2009). The infiltrates usually appear in a radial form and one or two nerves can be involved (Bacon et al., 1993; Patel & McGhee, 2009). They are caused by trophozoites that migrate via chemotaxis to the neurons, which can destroy the stroma and cause pain for the patient (Clarke & Niederkorn, 2006; Niederkorn et al., 1999). Further, conjunctival hyperaemia, ptosis and/or tearing can be observed (Abjani et al., 2016).

With a progressing infection, neovascularisation, scarring and ring infiltrates can occur (Alomar et al., 2009; Garg et al., 2017; Lorenzo-Morales et al., 2013; Matsumoto et al., 2016). Further, the infection can progress into a scleritis (Carnt & Stapleton, 2016; Lee et al., 2017; Lindsay et al., 2007).

In later stages, trophozoites can attack the corneal nerves, which can lead to neuritis and necrosis (Marciano-Cabral & Cabral, 2003). In rare cases a glaucoma can develop (Illingworth et al., 1995; Lindsay et al., 2007; Taher et al., 2018). Ultimately, surgery or enucleation may be necessary (Bakay & Polat, 2018; Lakhundi et al., 2017).

Tu et al. (2008 a,b) reported five stages of AK starting with stage I. epithelitis and stage II. epithelitis with keratopathy, followed by stage III. anterior stromal involvement and stage IV. deep stromal involvement and ending with stage V. immune ring and scleritis.

8.4.1.5. Differential diagnosis/Diagnostic

Since *Acanthamoeba* keratitis can often be confused with other forms of keratitis, as herpetic simplex keratitis, bacterial, or fungal keratitis, a fast diagnosis and expert know-how are even more important (Illingworth et al., 1995; Niyadurupola & Illingworth, 2006; Stan et al., 2016). To diagnose AK correctly, different techniques are applied.

One approach is **immunohistopathology**, where tissue is stained with specific antibodies against amoebic antigens. This facilitates the identification of morphological structures of trophozoites and cysts under fluorescent microscopy (de Lacerda & Lira, 2021).

Impression **cytology** can be applied as relatively non-invasive and highly specific approach when looking at superficial corneal epithelial tissue, but expertise in cytopathology is needed (Kot et al., 2021).

When the amoebae have infiltrated the cornea deeply, a non-invasive method can be applied, called **in vitro confocal microscopy (IVCM)**.

IVCM has a high specificity and sensitivity and is a rapid tool. However, the microscope is not available everywhere, expensive when purchased, expertise is needed, and only cysts can be detected, which makes it more important in later stages of the infection (Alkatan & Al-Essa, 2019; Kot et al., 2021).

A simple, however, efficient method is the culture on agar-plates seeded with *E. coli* in order to detect and identify the amoebae.

The sample, taken from corneal scrapes, ulcer and/or biopsy, is incubated at 30°C for one week and checked regularly under the phase-contrast microscope (PCM). Trophozoites can appear after 24h, cysts after approximately one week (Walochnik & Aspöck, 2021).

The cysts can be used for morphological identification (see 8.2.3.1.). Also, samples from contact lenses, contact lens cases and cleaning solutions can be checked for pathogens (Illingworth et al., 1995; Lorenzo-Morales et al., 2013; Marciano-Cabral & Cabral, 2003).

A nowadays widely employed molecular technique is the **polymerase chain reaction (PCR)**, that has a high specificity and a higher sensitivity than culture. The results are available rapidly. A powerful PCR protocol employing primers based on the amoebic 18S ribosomal RNA gene (JDP primers, see Table 1; see Appendix, Table 8) enables the identification of all known genotypes, which can all be differentiated with subsequent sequencing (Schroeder et al., 2001). **Real-time PCR** can achieve even more rapid results, with a reduced risk of contaminations, which is very important for a fast and accurate diagnosis in an early stage (Lamien-Meda et al., 2022).

8.4.1.6. Medical and surgical treatment approaches

The treatment of AK should include the eradication of trophozoites and cysts at the same time. Further, the inflammation should be decreased to reduce the pain and to restore comfort (Kaufman & Tu, 2022).

At the moment, different treatment approaches are recommended, starting with topical **biguanides**. These first-line antimicrobial agents can target both trophozoites and cysts at once (Fanselow et al., 2021). The most common ones are polyhexamethylene biguanide (PHMB) and chlorhexidine. Behind the working mechanism are positively charged molecules that are able to bind to *Acanthamoeba* spp. and cause a higher cytoplasmic membrane permeability, which eventually kills the parasites (Lorenzo-Morales et al., 2015). In comparison to PHMB, chlorhexidine seems more effective because of smaller molecules that invade the stroma more effectively (Seal & Hay, 1997).

Side effects of these compounds can be an increased intraocular pressure, as well as toxic keratopathy (Lorenzo-Morales et al., 2015). Biguanides are often used in a combinational therapy together with diamidines (Oldenburg et al., 2011).

A second effective treatment approach are **aromatic diamidines** that bind to the DNA of the pathogen and therefore inhibit its growth (Seal & Hay, 1997). Propamidine isethionate 0.1% and hexamidine 0.1% are the most frequently used representatives and are often employed in combinatory therapy together with biguanides to prevent drug resistance (Fanselow et al., 2021). They can penetrate the pathogen and thereby induce the denaturation of cytoplasmic proteins (Kaufman & Tu, 2022).

Antibiotics, as neomycin, which exhibits a lower cysticidal activity, are very effective against an infection when used in combination with other agents (Fanselow et al., 2021). Neomycin has an indirect effect by reducing the number of bacteria, which normally are ingested by the amoebae, and furthermore prevents a bacterial superinfection (Somani et al., 2023).

Another approach are **azoles**, which are originally used as antifungals. The most prominent azole on the market is voriconazole and has been shown to inhibit the proliferation of *Acanthamoeba* trophozoites (Bagga et al., 2021; Gueudry et al., 2018; Martín-Navarro et al., 2015; Tu et al., 2010 b).

Compounds to decrease both inflammation and pain are **topical corticosteroids** (Fanselow et al., 2021). Steroids target macrophage activity directed towards dead cysts in the stroma, which induces inflammation in the first place before it mitigates the pain (Seal, 2003). Whereas the prescription of corticosteroids is therefore controversial, also **non-steroidal inflammation-decreasing drugs**, as flurbiprofen, are available on the market (Somani et al., 2023).

Other compounds that are not yet licensed in Austria are oral **miltefosine**, an alkylphosphocholine that is primarily used against systemic leishmaniasis and was approved in 2016 by the United Sates Food and Drug Administration (FDA) (fda.gov), as well as **benzalkonium chloride**, short BAK, which is an ammonium surfactant with antimicrobial properties that showed promising amoebicidal activity in vitro (Sundar & Olliaro, 2007; Tu et al., 2013).

In further advanced infections, when treatment attempts were unsuccessful, **surgery** can be performed, such as therapeutic corneal transplantation or keratoplasty (Fanselow et al., 2021). Moreover, corneal cryotherapy or amniotic membrane transplantation are effective approaches (Somani et al., 2023).

New treatment approaches also include **plants derived compounds**. While agents as PHMB, propamidine, and chlorhexidine are the recommended treatment currently, they show considerable toxicity to human keratocytes (Lorenzo-Morales et al., 2015; Niyyati et al., 2016; Seal & Hay, 1997). Candidates for phytotherapy are tea tree oil from the plant *Melaleuca alternifolia*, which has been shown to be effective against cysts and trophozoites in vitro, and *Nigella sativa* aqueous extract, that showed antioxidant properties and does enhance phagocytosis of the parasites (Elkadery et al., 2019; Fanselow et al., 2021; Hadaś et al., 2017).

The challenges in the treatment of AK are to provide rapid diagnosis in general, the duration of treatment, the therapy of choice, the compliance of the patients, as combinational therapy must be applied into to eye hourly, resistance of cysts against several compounds, as well as complications with other pathogens, such as bacterial superinfections.

8.4.2. Granulomatous amoebic encephalitis (GAE)

Another disease entity caused by *Acanthamoeba* spp. is called granulomatous amoebic encephalitis, short GAE. It is a disease of the central nervous system with a low worldwide occurrence, but a mortality rate higher than 90% (Kalra et al., 2020; Kot et al., 2018).

The disease has rarely been reported in immunocompetent individuals but tends to primarily impact immunocompromised individuals, including those undergoing cancer treatment, individuals with human immunodeficiency virus (HIV) or acquired immunodeficiency syndrome (AIDS), organ transplant recipients, and patients with conditions such as diabetes or systemic lupus erythematosus (SLE) (Barete et al., 2007; Brondfield et al., 2017; Carter et al., 2004; Lalitha et al., 1985; Sütçü et al., 2018; Vernon et al., 2005; Wang et al., 2023).

8.4.2.1. Route of infection

The route of infection of GAE has not yet been fully elucidated. An infection can be attributed to the entry of amoebae into the lower respiratory tract or through skin lesions, potentially leading to hematogenous dissemination of the brain (Duggal et al., 2017; Wang et al., 2023).

It is assumed that *Acanthamoeba* spp. enter the central nervous system through the blood-brain-barrier (Kalra et al., 2020; Wang et al., 2023). Further research on the route of infection is needed.

8.4.2.2. Symptoms and clinical signs

First symptoms of GAE are neck stiffness and/or headache (Wang et al., 2023). Neurological symptoms can be seizures, confusion, an altered mental state, hallucinations, focal neurologic signs, cranial nerve palsies, lethargy, ataxia, and/or changes in the personality (Coven et al., 2017; Duggal et al., 2017; Geith et al., 2018).

Regarding the symptoms, the similarity to a bacterial or a viral encephalitis is very high, which can lead to a delayed diagnosis or even a misdiagnosis (Kalra et al., 2020).

8.4.2.3. Diagnosis and treatment

Brain image analysis such as CT and MRI might reveal lesions and provide an initial hint. Subsequently, a combination of immunohistochemistry, cell culture to identify amoebae, and molecular approaches as PCR and real-time PCR are employed. An early diagnosis is crucial for a successful treatment.

Typically, the specimens employed for diagnostic purposes include cerebrospinal fluid (CSF), skin extracted from facial or extremity lesions, sinus or lung biopsy specimens, and brain tissue biopsy acquired through surgery or post-mortem procedures (Parija et al., 2015; Wang et al., 2023). For PCR and real-time PCR samples of brain tissue or CSF are used, to rapidly detect and identify the pathogens (Behera et al., 2016; Coven et al., 2017; Harrison et al., 2018; Walochnik et al., 2015). To culture the cells, brain or skin biopsy samples can be put onto plate culture or in xenic or axenic media (Parija et al., 2015).

Normally, a combination therapy of drugs is applied for treatment. Various drugs have been employed – with varying degrees of success – including liposomal amphotericin B with voriconazole, trimethoprim-sulfamethoxazole with rifampicin, and a combination of meropenem, linezolid, moxifloxacin, fluconazole, and miltefosine. (Kalra et al., 2020; Kidney & Kim, 1998; Walochnik et al., 2008).

Specifically for GAE, the CDC (Centers for Disease Control) recommends the oral use of miltefosine (https://www.cdc.gov/parasites/acanthamoeba/treatment.html).

8.4.3. Interaction between *Acanthamoeba* and bacteria

While bacteria are one of the major food sources of *Acanthamoeba* spp., they can invade and infect the amoebae, which might transmit the pathogens further on to humans (Köhsler, 2007). Normally, *Acanthamoeba* spp. phagocytose and digest bacteria. Some bacteria species can survive the phagocytosis and live on in the cytoplasm, as for example *Legionella pneumophila* or *Legionella*-like pathogens, or within vacuoles of the amoeba, as for example *Burkholderia pickettii*, *Pseudomonas pickettii*, chlamydiales, and bacteriodetes (Fritsche et al., 2000; Horn et al., 1999, 2001; Michel & Hauröder, 1997). It is known, that *Acanthamoeba* and intracellular bacteria, can interact in a symbiosis, whereas the bacteria, that act as endosymbionts, are dependent on the host and cannot be cultured *in vitro* without it (Fritsche et al., 1993). The amoebic host cells protect the bacteria from unfavourable environments, against chemotherapeutic agents, antibiotics, and the human immune system (Barker & Brown, 1994).

Bacteria take advantage by actively infecting *Acanthamoeba* spp. and using them as a vector to invade humans. The amoebae as their host reservoir enable the bacteria to reproduce and grow, which further enhances the growth rate of the bacteria, as well as the motility, intracellular replication, invasion capacity, and the resistance towards antibiotics (Barker et al., 1993, 1995; Cirillo et al., 1994, 1997; Greub & Raoult, 2002; Neumeister et al., 2000).

When the environmental conditions are more favourable, the *Acanthamoeba* cells are lysed by the bacteria, which can reinfect more amoebae and eventually cause disease in humans (Köhsler, 2007).

During an AK, bacterial endosymbionts can enhance the amoebic CPE on human fibroblasts (Fritsche et al., 1998).

8.4.4. Other diseases caused by *Acanthamoeba* spp.

Other diseases caused by *Acanthamoeba* spp. can be a skin disorder, called disseminated or cutaneous acanthamebiasis (CA) and a pulmonary infection, called *Acanthmaoeba* pneumonia (AP). Both are very rare diseases (Wang et al., 2023).

Symptoms of cutaneous acanthamebiasis are the presence of firm papulonodules, that develop into hard erythematous nodules, skin ulcers or cutaneous lesions (Deluoi et al., 1996; May et al., 1992).

When the brain or other organs are involved, the symptoms can occur as a headache, fever, dizziness, nausea, seizures, an altered mental state and/or facial palsies prior to cutaneous manifestations, as well as a disseminated infection, that can include sinuses, skin, and bones (Brondfield et al., 2017; Zhang & Cheng, 2021).

The disease concerns mostly immunocompromised patients and no optimal treatment procedure has been established yet (Chandrasekar et al., 1997; May et al., 1992).

In a case study of a 60-year-old heart recipient, who further suffered from sinusitis and osteomyelitis, the infection could be successfully treated with a combination of flucytosine, fluconazole, miltefosine, and a reduced immunosuppression (Brondfield et al., 2017).

Individuals infected with *Acanthamoeba* pneumonia can show a decrease in the respiratory efficiency and/or the body weight (Im & Kim, 1998; Kot et al., 2021). It affects mostly people suffering from a low immune response (Kaul et al., 2008; Visvesvara et al., 1983).

8.5. Pathogenesis of AK

The pathogenesis of *Acanthamoeba* spp. can be separated into an initial stage, where the infiltration is limited to the corneal epithelium, and into a secondary stage, where the underlying stroma is affected, which can lead to an inflammation (Fanselow et al., 2021; Niederkorn et al., 1999).

An infection usually starts with the adhesion of the amoebae to the contact lens followed by adhesion to the corneal surface or directly to the cornea (Reverey et al., 2014). This is mediated by several processes, such as apoptosis, phagocytosis of host cells, and contact-dependent factors, such as proteases, ecto-ATPases and adhesions (Köhsler, 2007). Adhesions can be separated into two groups: the mannose-binding protein, short MBP, and the laminin-binding protein, short LBP (Corsaro, 2022; Huth et al., 2017).

The mannose-binding protein (MBP) is a transmembrane protein, which consists of 136 kDa subunits and was first described by Yang et al. (1997) (Garate et al., 2006a,b). MBP inherits normal functions of a cell surface receptor and can bind to two glycoproteins of corneal epithelial cells, called mannose bovine serum albumin and purified mannose protein, and can therefore be inhibited when alpha-mannose is present (Da Rocha-Azevedo et al., 2010; Garate et al., 2004; Kim et al., 2012; Yang et al., 1997). Garate et al. (2006b) reported that the pathogenicity of a strain correlates with its expression levels of MBP and established MBP as a potential pathogenicity marker. It was further indicated that the MBP-mediated adhesion is dependent on the MBP expression on the surface, as well as on the mannose-containing glycoproteins that are synthesized by the host cells (Huth et al., 2017; Yoo & Jung, 2012).

The laminin-binding protein facilitates the continued progression of infected tissue (Da Rocha-Azevedo et al., 2009). Laminin is a glycoprotein and part of the extracellular matrix with a molecular weight between 28.2 kDa and 55 kDa (Da Rocha-Azevedo et al., 2009, 2010; Hong et al., 2004). It is crucial during the initial phase when the infiltration is still limited to the corneal epithelium (Gu et al., 2022). The expression of LBP increases in strains with increasing pathogenicity (Garate et al., 2006b; Ng et al., 2017).

Another factor involved in mediating the adhesion process are acanthopodia. Lorenzo-Morales et al. (2013) reported that the number of acanthopodia is correlated to the adhesion rate of the amoebae. Pathogenic isolates develop more than 100 acanthopodia per cell, whereas non-pathogenic isolates do not form more than 20 acanthopodia per cell.

As secondary reaction to the adhesion of pathogenic organisms, the host cells are phagocytosed, which is an actin-dependent process and involves the rearrangement of the cytoskeleton (Wang et al., 2023). Cytochalasin D, a toxin that can inhibit the actin polymerization, can be applied against *Acanthamoeba* mediated host cell death (Alsam et al., 2005; Niederkorn et al., 1999).

The binding of *Acanthamoeba* spp. to the surface induces the secretion of a variety of proteases, such as serine proteases, cysteine proteases and metalloproteinases, which further leads to a cytopathic effect (CPE) (Khan, 2006). These proteases can create pores in the membrane of host cells and degrade the epithelial basement membrane and the stromal matrix, which helps the parasite to infiltrate deeper layers of the cornea and supports the lysis of these cells (Lorenzo-Morales et al., 2013; Niederkorn et al., 1999; Panjwani, 2010).

Serine proteases are the most abundant type of proteases in nearly every genotype and are crucial in host cell injury (Da Rocha-Azevedo et al., 2010; Lorenzo-Morales et al., 2013). These proteases can degrade immunoglobulins (Ig), as IgG and IgA, albumin, and interleukin-1, and further exhibit collagenase properties against collagen I and III (Na et al., 2001; B.-K. Na et al., 2002; Sissons et al., 2006). The mannose-induced protease, short MIP, is a serine protease with a molecular weight of 133 kDa and is therefore also called MIP133 (Hurt et al., 2003a). It can induce lysis of different cells, as iris ciliary body cells, retinal pigment cells, corneal endothelial or epithelial cells, as well as apoptosis of macrophage-like cells (Lorenzo-Morales et al., 2015; Wang et al., 2023).

Cysteine proteases are also believed to contribute to the process of cell degradation (Mitro et al., 1994; Moon et al., 2012; Ramírez-Rico et al., 2015). Moreover, they have been shown to be crucial for the process of encystment and are involved in target cell death (Leitsch et al., 2010; Singh et al., 2004).

Additionally, metalloproteinases, which play a role in cell differentiation, migration, growth factor activity regulation, and angiogenesis, have been reported to induce inflammation (Kot et al., 2021; Parks et al., 2004; Sternlicht & Werb, 2001).

These proteases, either secreted or anchored to the surface of the cell, can exhibit lytic properties that affect the extracellular matrix, in particular collagen I and III, elastin, plasminogen, casein, gelatine, and haemoglobin (Parks et al., 2004; Sissons et al., 2006).

Another aspect of pathogenesis of *Acanthamoeba* infections is apoptosis of the host cells. Apoptosis is the programmed cell death and can be induced by *Acanthamoeba* spp. via three different pathways. The first pathway involves ecto-ATPase-driven cell apoptosis, wherein extracellular ATP and other nucleoside triphosphates undergo hydrolysis, leading to a toxic effect of ADP (Mattana et al., 2002). This is supported by the fact that pathogenic isolates exhibit higher extracellular ATP activities than non-pathogenic isolates (Sissons et al., 2004a). In the second pathway *Acanthamoeba* spp. induce the cell cycle arrest by inhibiting the expression of GADD45A, p130Rb, G1 protein, and cyclin-dependent kinase 6 (Wang et al., 2023). This process is reinforced by the dephosphorylation of the retinoblastoma protein pRb (Sissons et al., 2004b). In the third pathway, the activation of the phosphatidylinositol 3-kinase (PI3K) is crucial for an apoptotic effect (Sissons et al., 2005).

During an infection with *Acanthamoeba* spp. the proteases target immunoglobulins, because the levels of IgA and IgG are lower in AK patients (Carnt & Stapleton, 2016; Neelam & Niederkorn, 2017). This mechanism enables the amoeba to survive long term in the host organism by evading the immune response (Wang et al., 2023).

8.6. Immunobiology

The eyes and the brain are immune privileged areas, exhibiting a weaker immune response of the body in comparison to other body parts. Nevertheless, both the innate and the adaptive immune system are activated and exert several mechanisms in response to an infection with *Acanthamoeba* spp. (Cursons et al., 1980; Niederkorn, 2006).

8.6.1. Innate immune system

When pathogens enter the body, the innate immune system gets activated by the first responses generated by Toll-like receptors (TLRs), recognizing pathogen-associated microbial patterns (PAMPs) or damage-associated molecular patterns (DAMPs) (El-Zayat et al., 2019; Kawasaki & Kawai, 2014). These receptors can be found mainly on phagocytic cells, such as macrophages and neutrophils, as well as on dendritic or mast cells, monocytes, microglia, astrocytes or in neurons (Hurt et al., 2001; Olson & Miller, 2004; Tang et al., 2007).

As cellular response, first neutrophils flow towards the herd of infection, followed by macrophages, which both are able to eliminate *Acanthamoeba* spp. (Carnt et al., 2017). Macrophages are known to play a role in initiating and sustaining the immune response, as well as in tissue repair (Knickelbein et al., 2013; Larkin & Easty, 1991; Mosser & Edwards, 2008). They can either be present as long-lived cells that are responsible for the host tissue as so-called resident macrophages or develop from blood-derived monocytes at the infection site as so-called elicited macrophages (Gordon et al., 2014).

Obviously, also neutrophils are involved in the immune response during AK, since they can be found in lesions and seem to influence the progression of AK (Niederkorn, 2021). Neutrophils are recruited and activated by the macrophage inflammatory protein 2 (MIP-2). The importance of neutrophils was shown by an in vivo examination of neutrophil migration, where intracorneal injection of anti-MIP-2 antibodies resulted in a severe keratitis in animal models, while on the other hand a mitigation of the infection was reported when MIP-2 was injected (Hurt et al., 2001).

Furthermore, TLRs activate the antigen-presenting cell (APC)-cytokines, as interleukins (ILs). Depending on which interleukins are active, the cellular or humoral T-helper cells of the adapted immune system are activated or inhibited (Kot et al., 2021). For the cellular T-helper cells (Th1) IL-12, IL-23, and IL-27 are activated (Robinson & O'garra, 2002). For the humoral T-helper cells (Th2) IL-4 IL-5, and IL-13 are activated (Dabbagh & Lewis, 2003). The role of the parasites regarding the activation and inhibition of TLRs seems to be crucial but is yet not fully examined and further research is necessary (Fouzder et al., 2018).

8.6.2. Adaptive immune system

The response of the adaptive or humoral immune system lags in time until the T-helper and B-helper cells are activated. In healthy individuals, the T-cell responses protect against amoebic pathogens by proliferating and producing interferon γ (IFNγ) (Tanaka et al., 1994). Patients with AK or GAE normally have low levels of serum IgA and IgG, which are important parts of the tear fluid (Neelam & Niederkorn, 2017). Tear fluid is composed of anti-pathogenic substances and is therefore a natural defence against pathogens (de Lacerda & Lira, 2021).

IgA antibodies play an important role at the beginning of infections and have been shown to at least partly inhibit the adhesion of the trophozoites to the corneal epithelium, and therefore contribute to the mitigation of AK (Leher et al., 1998a,b). Serological examinations showed that 90-100% of people with no AK history express serum IgG antibodies, which are specific for *Acanthamoeba* antigens (Cursons et al., 1980; Walochnik et al., 2004). It seems that through frequent environmental exposure to these ubiquitous organisms the adaptive immune system is activated.

8.6.3. Complement pathway

As alternative route the complement system can be activated, which acts as barrier towards microbial infections and kills pathogens in a cascade manner. Both the innate and the adaptive immune system are included into the complement system (Rus et al., 2005). It can be activated through the classical pathway by antigens that trigger specific antibodies or through the alternative pathway by mannosylated glycoproteins, both located on the surface of the *Acanthamoeba* trophozoites (Neelam & Niederkorn, 2017).

The cascade mechanisms are not entirely analysed yet, but it seems that IgA antibodies play a crucial role by triggering neutrophils that further activate the complement pathway (Feng et al., 2015).

8.7. Aims of this study

The aim of this study was to compare pathogenic isolates from patients with AK and potentially non-pathogenic isolates from environmental habitats regarding their biochemical, physiological, and molecular properties.

Several factors that seem to be associated with pathogenicity of an isolate have been previously reported, such as the respective genotype, growth at higher temperatures, the levels of expression of the mannose-binding protein (MBP), expression of several proteases, in particular the mannose-induced proteases (MIP), as well as the expression of specific genes believed to be associated with pathogenicity.

Therefore, by evaluating the 18S rRNA gene sequences of clinical and environmental *Acanthamoeba* isolates the respective genotype and potential subtypes were determined. Additionally, a phylogenetic tree was constructed in order to evaluate the position of these strains within the genus.

In a temperature tolerance test, the ability of the investigated strains to grow at different temperatures was evaluated and compared.

Furthermore, differences in the protein and protease patterns of these strains, incubated with methyl alpha-D-mannopyranoside, were evaluated employing SDS-PAGE and zymography.

In a real-time PCR the expression levels of target genes with specific primers were measured and compared.

IX. Material and Methods

9.1. Strains

9.1.1. Laboratory isolates

The clinical isolates used in this study were previously isolated from patients suffering from *Acanthamoeba* keratitis. These strains were XIN20, SCT21 and JIR22. XIN20 was isolated in 2020, SCT21 was isolated in 2021, and JIR22 was isolated in 2022. Based on previous sequencing of a small fragment, these three strains represented the genotype T4.

The non-pathogenic isolates from the laboratory were *A. castellanii* strain Neff and *A. terricola* strain TT21. Neff (ATCC 30010/EF554328.1) was isolated in 1957 by Robert J. Neff from soil (Neff, 1957). It originally was assigned to the species *A. castellanii*, but sequence similarities of 99.8% indicate that Neff should be placed to the species *A. terricola* (ATCC 30134). In 2013, the first genome was published for *Acanthamoeba* spp. by Clarke et al. (2013). Since then, it has been used as NCBI Reference Sequence: NZ_AHJI00000000.1.

9.1.2. Collecting of environmental samples

Environmental samples were taken from various moist or wet environments, such as the coffee machine tank, several drains, the water bowl of pets, puddles, as well as soil from plant pots. Twelve samples in total were collected.

The samples were taken with a sterile cotton swab and then transferred into tubes containing sodium chloride. Subsequently, the tip was placed on an agar plate coated with *E. coli*.

9.2. Culture of samples

9.2.1. Culture on Agar-Plates

The agar was prepared by dissolving 15 g of agar-agar in 50 ml of Neff-buffer (1.2 g NaCl, 0.04 g $MgSO4{\cdot}7H_2O$, 0.04 g $CaCl2{\cdot}2H_2O$, 1.42 g Na2HPO4 and 1.36 g KH2PO4 dissolved in 500 ml dH_2O) and filled up to 1 L with dH_2O. The mix was sterilized by autoclaving for 45 min at 125 °C.

The liquid agar mix cooled down to 60°C before the plates were filled with 17 ml each. The filled plates were left to solidify overnight at room temperature and were stored in a refrigerator at 4°C the next day. Before applying the collected samples, the plates were coated with 100 µl of a 24h old culture of *E. coli* in a broth consisting of casein-peptone soymeal-peptone (Walochnik et al., 2015).

9.2.2. Preparing amoebae for axenic culture

To transfer cysts from plates into axenic liquid medium, encystment is necessary. On agar plates encystment usually starts after consumption of the bacterial food source. Cysts were scraped from plates with a sterile cotton swab and transferred in the tube containing 3% hydrochloric acid (HCl) and stored for one hour. Then the tubes were centrifuged for 10 minutes at 700 x g. Afterwards, the cells were washed with peptone yeast extract glucose (PYG) medium and transferred to fresh flasks, where the growth of trophozoites was monitored regularly under the microscope. It can take several weeks for these cysts to develop into an amoebae culture with sufficient cell density for further experiments.

9.2.3. Culture in axenic medium

The PYG medium used for culturing the cells was prepared freshly. It consisted of 10 g protease-peptone, 10 g yeast extract, 5 g sodium chloride (NaCl), 0.7 g Na_2HPO_4, 0.7 g KH_2PO_4, 5 g glucose, and 10 ml mix of antibiotics and antimycotics (10.000 units penicillin, 10 mg streptomycin, and 25 µg/ml amphotericin B) . The broth was filled up to 1 L with dH_2O. The medium was filtered using a sterile microfiltration unit. It was stored at 4°C.

9.2.4. Harvesting cells from liquid cultures and from plates

Cells from liquid cultures were harvested by transferring the medium into a fresh tube after shaking the flask. Amoebae were pelleted at 700 x g for 10 minutes and washed once with PBS. When the cells were harvested from plates for DNA isolation or else, the cells were scraped and transferred with a sterile cotton swab into a tube with NaCl or PBS. This tube was centrifuged at 700 x g for 10 minutes to collect the pellet.

9.3. Analysis of 18S rRNA gene sequences

9.3.1. DNA-Isolation

The DNA was isolated and purified with the the DNeasy ® Blood & Tissue Kit by QIAGEN (Hilden, Germany). Every step was carried out at room temperature. 20 µl Proteinase K was pipetted into fresh 1.5 ml Eppendorf tubes, before 200 µl containing amoebae were pipetted on top. If there was less sample available, 100 - 200 µl saline solution could be added. 200 µl AL buffer was added and the sample was vortexed for 15 seconds, before being incubated for 20 minutes at 56°C. After spinning the samples down, 200 µl of 96-100% ethanol was added, followed by vortexing and spinning down. A maximum of 700 µl could be transferred into QIAmp Mini spin columns.
The samples were centrifuged at 6000 x g for 1 minute. The filtrate was discarded, and the collection tube exchanged. 500 µl AW1 buffer was pipetted into the column and the sample was centrifuged again for 1 minute at 6000 x g. In the next step 500 µl AW2 buffer was added, and the tubes were centrifuged for 3 minutes at full speed. Next, the samples were centrifuged empty in a fresh collection tube for 1 minute at full speed, to discard the leftovers. The column was transferred again into to a fresh 1.5 ml Eppendorf tube and 100 µl AE buffer were pipetted in the middle of the matrix. The incubation step should last at least one minute, but a longer amount of time (up to five minutes) can increase the DNA concentration. The final centrifugation step lasted 1 minute at 6000 x g, before the samples were stored at -20°C or further processed.

9.3.2. Conventional polymerase chain reaction (PCR)

For the conventional PCR the Eppendorf Mastercycler (Eppendorf AG, Hamburg, Germany) was used. One reaction consisted of 50 µl, composed of 5 µl 10 x reaction buffer B, 5 µl magnesium chloride (MgCl2), 1 µl dNTPs, 0.25 µl HOT FIREPol ® as polymerase, 5 µl forward primer, 5 µl reverse primer, 1 - 3 µl of DNA and water, filled up to 50 µl. A negative control with water instead of DNA was added for every PCR run. The program was adjusted to the annealing temperatures of the used primers. To amplify the 18S rRNA gene, the primers SSU1-1rev, 1fw-2rev, 2fw-3rev and 3fw-SSU2 were used with the program “GastB/54” (see Appendix, Table 8) (Koehsler et al., 2007). To specifically detect *Acanthamoeba* spp., the genus-specific primers JDP1-JDP2 with the program “JDP” were used (see Appendix, Table 9). The primers are shown in the following table (see Table 1).

Table 1. The primer sequences of the Rhiz primers SSU1, 1fw, 1rev, 2fw, 2rev, 3fw, 3rev, and SSU2 and the primers JDP1 and JDP2, used in this study for conventional PCR.

Name	Primer	Primer Sequence (5'-3')	Amplicon Length (bp)	Average Tm (°C)
SSU1-1rev	SSU1	CGACTGGTTGATCCTGCCAGTAG	617	66.6
	1rev	GCTGCTGGCACCAGACTTG		61.6
1fw-2rev	1fw	CAAGTCTGGTGCCAGCAGC	587	61.6
	2rev	GACTACGACGGTATCTGATCG		61.2
2fw-3rev	2fw	CGATCAGATACCGTCGTAGTC	627	61.2
	3rev	CTAAGGGCATCACAGACCTG		60.5
3fw-SSU2	3fw	CAGGTCTGTGATGCCCTTAG	409	60.5
	SSU2	TCCTGATCCTTCCGCAGGTTCAC		66.6
JDP	JDP1	GGCCCAGATCGTTTACCGTGAA	423 to 551	56.7
	JDP2	TCTCACAAGCTGCTAGGGAGTCA		57.1

9.3.3. Visualization on Agarose-Gel

To separate the DNA products after PCR by electrophoresis, a 2% agarose gel was prepared. It consisted of agarose and 1 x TAE and was stained with GelRed ® Nucleic Acid Stain by Biotium (Fremont, CA, USA). To apply the samples to the chambers 6 µl Gel Loading Buffer G2526-5ML by Sigma-Aldrich and 24 µl of the sample were mixed. As a marker the 50 bp DNA Step Ladder (S7025) by Sigma-Aldrich was used. The bands were visualized with the BIO RAD Molecular Imager Gel Doc™ XR+.
The bands were cut out from the gel and purified using the GFX™ PCR DNA and Gel Band Purification Kit by cytiva (Marlborough, MA, USA).

9.3.4. Sanger sequencing

To prepare a sequencing PCR, 2 µl primer (either forward or reverse), 2 µl AB-mix, 2 µl sequencing buffer and 1 - 4 µl of purified PCR product were filled up with water to 10 µl in total. The used device was the Eppendorf Mastercycler (Eppendorf AG, Hamburg, Germany).
The program for the thermocycler can be found in the appendix under the name "SequNeu" (see Appendix, Table 7).
After the PCR, fresh sequencing tubes were prepared with 1 µl sodium acetate (NaAc) each. The samples were transferred to the sequencing tubes and 33 µl 100% cold ethanol was added. The samples were put on ice (-20°C) for 20 minutes.

Afterwards, the tubes were centrifuged for 30 minutes at 4°C at 12.000 U (g). The supernatant was discarded, and the sample was washed with 90 µl 70% cold ethanol, before being centrifuged again for 10 minutes. The alcohol was discarded, the samples were air dried for five minutes and 20 µl formamide (HIDI) were added to the dried sample, followed by heating for 5 minutes at 94°C. The samples were put on ice for 5 minutes, before being transferred to the sequencing tubes. Before the samples were placed into the device, empty tubes needed to be filled with HIDI.
The device used for Sanger sequencing was the Applied Biosystems SeqStudio Genetic Analyzer (Thermo Fisher Scientific, Waltham, MA, USA).

9.3.5. Data analysis

To generate consensus sequences of the entire 18S rRNA genes, the DNA sequence analysis tools GeneDoc 2.7.0 and ClustalX 2.1 were used. At least two sequences of each strand were used. The sequences were aligned in GeneDoc and exported as FASTA files for phylogenetic analysis.

9.3.6. Phylogenetic analysis

The alignments for the phylogenetic analysis were performed using Muscle in Molecular Evolutionary Genetics Analysis (MEGA) software version 11.

The first tree compared 18S rRNA genes to see potential clusters of pathogenic and non-pathogenic strains. For reference, 18S rRNA gene sequences from other *Acanthamoeba* strains, either from literature or from GenBank were added (Corsaro, 2020). As outgroup, sequences representing the genotype T3 (T3AgriffH37 and T3Panola) and the genotype T11 (T114RE and T11 RB:F:1) were used.

The bootstrap was set to 1000 replicas and the Kimura 2 model specifying a gamma distribution and invariable sites was applied, based on the best-fit evolutionary model selection and according to the model with the highest Akaike information criterion (AIC). The algorithms used for the phylogenetic analysis were the Maximum Likelihood (ML) and the Neighbour-Joining method (NJ).

To determine the 18S subtypes within genotype T4 after Corsaro et al. (2020; 2023), the sequences were aligned to previous determined samples representing the subtypes T4A to T4H. For this analysis two samples representing the genotype T11 (T11 ZOO9 and T11 A2) were used as outgroup. Based on the best-fit evolutionary model selection and the highest AIC, Jukes-Cantor model specifying a gamma distribution and invariant sites was applied and the bootstrap was set to 1000. For the phylogenetic analysis the algorithms ML and NJ were used.

9.4. Temperature tolerance test

To examine the temperatures for optimal growth of pathogenic and non-pathogenic isolates, six different strains were grown at 25°C, 34°C and 37°C for seven days each.

9.4.1. Preparation of the plates

For this experiment, fresh agar-plates were prepared with concentric circles on the bottom using a stencil. The smallest circle had a radius of 0.9 cm, the second one 1.5 cm, the third a radius of 2.25 cm and the biggest one a radius of 3 cm (see Figure 4). For each strain and temperature two independent experiments in duplicate were performed.

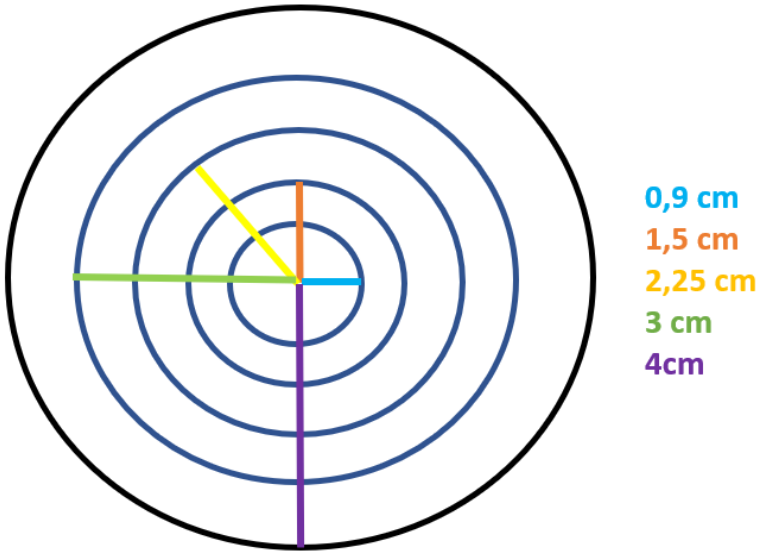

Figure 4. Radiuses of circles, painted on the back of the plate.

9.4.2. Preparation of the samples

The strains were grown in 12.5 cm flasks (4 ml) for several days. The cells were counted and 10^4 cells/2 µl were inoculated onto the agar plates.

To count the cells the Fuchs-Rosenthal counting chamber was used with a magnification of 40x of the light microscope. The cells of four squares with 16 subdivisions each were counted. The average of these numbers was determined, and the following equation was used to identify the number of cells per µl.

$$\frac{Average\ x\ 16}{3{,}2\mu l} = cells\ per\ \mu l$$

Alternatively, the Corning Cell counter REF 6749 was used.

9.4.3. Temperature tolerance test

After the plates were coated with ~100 µl of *E. coli*, 2 µl containing 10^4 cells of each sample were pipetted in the middle of the plate. Two replicates for each isolate were incubated at 25°C, 34°C, and 37°C. The plates were checked after 24h, 48h and 72h and again after six and seven days, to evaluate the growth radius. This was noted on a prepared Excel sheet. On the seventh day the cells were harvested in 2 ml NaCl and counted as described before.

9.5. Analysis of proteins

The compare protein patterns of pathogenic and non-pathogenic isolates, SDS-PAGE was performed.

9.5.1. Preparation of samples for SDS-PAGE

For the experiment a 1M methyl alpha-D-mannopyranoside (mannose) solution was prepared. 1.94 g methyl alpha-D-mannopyranoside by Sigma-Aldrich were dissolved in PYG and filled up to a volume of 10 ml and stored at 4°C.

In order to compare protein profiles of amoebae with and without exposure to methyl alpha-D-mannopyranoside, the cells of the six pathogenic and non-pathogenic isolates were incubated for 48h with 100 mM mannose. Untreated cells were used as control. For a 100 mM concentration 200 µl of the mannose-PYG mix were added to 3.8 ml liquid culture. After 48h, the cells were counted to harvest 10^6 cells for each sample. After harvesting, the cells were resuspended in 200 µl PBS each. 15 ml of PBS were mixed with 1 tablet of the cOmplete™ Protease Inhibitor Cocktail by CO-RO Roche. This was supposed to inhibit the proteases that were released after homogenization, to prevent the proteins from breaking down.

To establish the best working technique for homogenization, three different approaches were applied.

For the first approach to break up the cells, liquid nitrogen was used. The cells in a 1.5 ml tube were put into a container with liquid nitrogen for five minutes two times consecutively. In between, the cells were defrosted once, before being put on -20°C.

For the second approach the cells were mechanically broken up with an electric hand homogenizer for 30 seconds.

For the third approach the homogenizer Precellys® 24 was employed. The cells were put in special tubes with glass beads. The machine was started with 5500 X for 10 seconds. Afterwards 100 µl PBS were added into the tube to transfer the sample into a fresh Eppendorf tube before freezing it at -20°C.

For SDS-PAGE, the concentration of the samples was measured and adjusted to 50 µg/µl and then resuspended 1:4 with 4 x Laemmli buffer (2 ml 1 M Tris-HCl (pH 6.8), 0.8 g SDS, 610 mg DTT, 4 ml glycerine, 3.8 ml dH2O, 40 µg bromophenol blue).

The samples were incubated at 95°C for five minutes. When the gel solidified, 7 µl of the samples were loaded onto the gel. Either the PageRuler™ Plus Prestained Protein Ladder or the PageRuler™ Prestained Protein Ladder, both by Thermo Fisher Scientific (prev. Fermentas), were used as weight standard (5-10 µl).

9.5.2. Preparation of SDS-Gels

For the SDS-PAGE, a stacking and a separating gel were prepared. The separating gels were always prepared with a final concentration of 10% Polyacrylamide (PAA). The separating gel consisted of 2.5 ml 1.5 M lower Tris, 3.3 ml 30% PAA, and 4 ml H_2O.

40 µl 10% ammonium persulfate (APS) and 10 µl N, N, N′, N′-Tetramethyl ethylenediamine (Temed) by Sigma-Aldrich were added, before the solution had to be pipetted immediately into the gel form. Isopropanol was applied on top to avoid any air bubbles. The gel solidified after 30 minutes. At this point, the stacking gel could be prepared, which consisted of 1.25 ml 0,5 M upper Tris, 0.83 ml 30% PAA, 3.25 ml H_2O, 40 µl APS, and 5 µl Temed. Again, after 30 minutes the gel solidified.

9.5.3. Running of SDS-Gels

The gels were run for 15 minutes with a current of 15 mA, before increasing it to 25 mA. If the bands were running very slow, the amperage was increased up to 50 mA.

9.5.4. Staining of SDS-Gels

After gel electrophoresis, the gels were stained immediately for at least one hour with Coomassie staining solution (0.1% Coomassie R-250 by Thermo Fisher Scientific in 40% ethanol, 10% acetic acid, dH_2O) und destained afterwards with destaining solution (10% ethanol, 7.5% acetic acid, dH_2O). When the bands were visible, an image of the protein patterns was taken with the BIO RAD Molecular Imager Gel Doc™ XR+.

9.6. Analysis of proteases

To compare protease patterns of pathogenic and non-pathogenic isolates, zymography was performed.

9.6.1. Preparation of samples for Zymography

The effect of mannose on excreted proteases of *Acanthamoeba* was analysed, by adding 50 mM and 100 mM mannose to every isolate for 24h, 48h, and 72h.

Untreated cells were used as control. Afterwards, the cells were counted, and 10^6 cells were pipetted in a 6- or 12-well plate. This plate was prepared by pipetting of sterile filtered Minimum Essential Medium (MEM) Eagle (Sigma-Aldrich) (2 - 5 ml), substituted with 1.1 g $NaHCo_3$ and 0.061 g Na_3Po_4, in every well.

The plate was then incubated in the CO_2 incubator for 24h. After this time, only the supernatant was collected carefully. To remove remaining cells, the samples were centrifuged for 10 minutes at 700 x g. The supernatant was transferred into the Vivaspin® 6 tubes by Sartorius, to increase the protease concentration.

The tubes were centrifuged for 30 - 60 minutes at 8.000 x g, until less than 200 µl of the filtered sample were collected. The exact concentration of the proteases could not be determined, but adjustment of all samples to the same concentration of 2.5 µg/µl, the concentration of proteins (A-260) was measured via the NanoDrop.

9.6.2. Preparation of gels for Zymography

For zymography a stacking gel and a separating gel with a polyacrylamide (PAA) concentration of 10% were prepared.
The content of the gels has been described previously in paragraph 7.5.2.
For the separating gel, 100 µl 10% gelatine per gel were added, before the addition of APS and Temed. The stacking gel was prepared as described above as well.

9.6.3. Running of Zymography gels

The gels were run for 15 minutes with a current of 15 mA, before increasing it to 25 mA. If the bands were running very slow, the amperage was increased up to 50 mA.

9.6.4. Staining of Zymography gels

After gel electrophoresis, the gels were shaken for one hour in Triton-X 100, which needed to be changed after 30 minutes. Next, developing buffer was added, again for one hour. After renewing the buffer, the plates with the gels were incubated at 37°C for 18h. The next day, the gels were stained with Coomassie for about 2 h on a shaking plate.

Finally, destaining solution was added and the gels were destained until the proteases would appear as light bands on the gel. Then, images of the protease patterns were taken with the BIO RAD Molecular Imager Gel Doc™ XR+.

9.6.5. Protease identification by inhibition

In order to identify the protease class in the supernatant of the samples, protease inhibitors and samples of untreated amoebae were used.

To check for serine proteases, phenylmethanesulfonylfluoride, short PMSF, an irreversible inhibitor with a final concentration 2 mM was used.

The second chemical compound was 1,10-phenanthroline (Phen), which targets metalloproteases. The final concentration used was 10 mM (Sissons et al., 2006). Since it is a reversible inhibitor, it had to be included in the running and developing buffer.

The third inhibitor E-64 targets and inhibits cysteine proteases irreversibly. E-64 is short for trans-epoxy-succinyl-L-leucyl-amido-(4-guanidino) butane. The final concentration applied was 100 µM (Na et al., 2001).

The samples were prepared and mixed with the respective inhibitors and incubated for 30 minutes, after which 4 x Laemmli buffer was added in a 1:4 ratio, and the samples were loaded onto the gel. For control a sample without inhibiting agents mixed with the buffer was loaded as well. The gels for zymography were prepared and the gel electrophoresis was run as described previously.

9.7. Quantitative real-time PCR

9.7.1. Primer design

To target the genes of interest, primers were established and tested in conventional PCRs. We focused on potential pathogenicity markers, such as acanthaporine (AcPo), metalloproteases (MP), serine proteases (SP), cysteine protease 5 (CP5) and especially the mannose-binding protein (MBP).

For every target, several specific primer pairs were designed according to sequences in the nucleotide data bank of the National Library of Medicine (nih.gov). The primers were synthesized by Microsynth (Balgach, Switzerland).

Table 2. All RT-PCR primers used in this study.

Name	Primer	Sequence ID	Target gene	Primer Sequence (5'-3')	Amplicon Length (bp)	Average Tm (°C)
SP1	680 fw	XM_004340589.1	Serine protease	GTA ACG AGA ACA CCG ACG C	120	59.5
	800 rev			GCT TCA GCA ACT TTG GCA AG		58.4
SP2	800 fw	XM_004356920.1	Encystation-mediating serine proteinase	CTT GCC AAA GTT GCT GAA GC	180	58.4
	980 rev			GAA CTT GGG GTA CTG GCT C		59.5
SP3	680 fw	XM_004340589.1	Serine protease	GTA ACG AGA ACA CCG ACG C	300	59.5
	980 rev			GAA CTT GGG GTA CTG GCT C		59.5
AcPo	AcPo fw	JF514558.1	Acantha-porin precursor	CAA GTG CTC TTC CGA GAT CT	210	58.4
	AcPo rev			CCT TCT TAA GAA CGC TGC AC		58.4
MBP1	2450 fw	AY604040.1	Mannose-binding protein	CTA CCA GTG GAA CTA CAA CGG	240	61.2
	2690 rev			GGT GTT CCA GTA GAA GTT ACC		59.5
MBP2	2690 fw	AY604040.1	Mannose-binding protein	GGT AAC TTC TAC TGG AAC ACC	230	59.5
	2920 rev			GCA GTA GAA CTG CTT GCA CG		60.5
MBP3	2920 fw	AY604040.1	Mannose-binding protein	CGT GCA AGC AGT TCT ACT GC	155	60.5
	3075 rev			CTT GTA GTC GTC GCA GCA G		59.5
MBP4	3075 fw	AY604040.1	Mannose-binding protein	CTG CTG CGA CGA CTA CAA G	245	59.5
	3320 rev			CTT GTT GAG CAT CCT GTA CAG		59.5
MBP5	3320 fw	AY604040.1	Mannose-binding protein	CTG TAC AGG ATG CTC AAC AAG	100	59.5
	3420 rev			CAC AAG AAC GAG ATC GAG ATG		59.5
MBP6	2920 fw	AY604040.1	Mannose-binding protein	CGT GCA AGC AGT TCT ACT GC	400	60.5
	3320 rev			CTT GTT GAG CAT CCT GTA CAG		59.5
MBP7	3075 fw	AY604040.1		CTG CTG CGA CGA CTA CAA G	345	59.5

	3420 rev		Mannose-binding protein	CAC AAG AAC GAG ATC GAG ATG		59.5
CP5.1	380 fw	LC472811.1	mRNA for cysteine proteinase 5	CAC GTC AAG AAC CAG GGT CA	170	60.5
	550 rev			GTA CTC GAA GGC GTA GTC C		59.5
CP5.2	550 fw	LC472811.1	mRNA for cysteine proteinase 5	GGA CTA CGC CTT CGA GTA C	350	59.5
	900 rev			CGC CCC ACG AGT TCT TGA C		61.6
MP1	1160 fw	XM_004334649.1	Metallo-peptidase (ACA1_091940)	CTC ACT CAC GGA TTT GAT GAC	100	59.5
	1260 rev			CAT TGA GTT CGC TCA ACG AAG		59.5
MP2	1260 fw	XM_004334649.1	Metallo-peptidase (ACA1_091940)	CTT CGT TGA GCG AAC TCA ATG	160	59.5
	1420 rev			GTT GAT GCC AGG AAT CAC TTC		59.5
MP3	1160 fw	XM_004334649.1	Metallo-peptidase (ACA1_091940)	CTC ACT CAC GGA TTT GAT GAC	260	59.5
	1420 rev			GTT GAT GCC AGG AAT CAC TTC		59.5
18S	18S fw	OR564022.1	18S-rRNA-gene	CCCAGATCGTTTA CCGTGAA	180	58.4
	18S rev			TAAATATTAATGC CCCCAACTATCC		60.9
HPVT	HPVT fw	XM_004337011.1	Hypo-xanthine-guanine phospho-ribosyl-transferase (ACA1_214340)	GGAGCGGATCGT TCTCTG	201	58.4
	HPVT rev			ATCTTGGCGTCGA CGTGC		58.4

9.7.2. Testing primers in conventional PCRs

In conventional PCRs, the primer pairs were tested with cDNA of the strain JEA19, a clinical laboratory strain.

Based on amplifications of the initial PCR, where the primer sets for the amplification of serine proteases and the mannose-binding protein resulted in multiple unspecific bands, in a following PCR the program “GastB/54” (see Appendix, Table 8) was optimized according to Asif et al. (2021), to increase the yield and reduce unspecific bands (see Appendix, Table 10).

Adjustments for the second PCR included shorter annealing and elongation times, as well as lower annealing temperature and more cycles were made (see Appendix, Table 10). The elongation and the annealing time were reduced from one minute each to 25 s and to 45 s. The annealing temperature was increased from 54°C to 56°C and the number of cycles was increased from 35 times to 40 times. The adjusted PCR revealed specific bands for five of the MBP primer pairs.

For the serine proteases no specific primer pairs could be found. The reason for this could be an inadequate design of the primers. It is possible that they have interacted with each other by dimerization, the formation of hairpins, or sticky ends that indicate a low internal stability (Judelson & Al-Mohanna, 2014). Further, the primers could not only be specific to the target genes, but also to other sequence parts in the genome and therefore bind more than once, which results in unspecific bands and would ultimately affect real-time PCR. The GC-content or the melting temperatures could be further reasons for an unspecific binding and weak bands (Asif et al., 2021).

9.7.3. Sample preparation for RT-PCR

To determine potential differences in the RNA content of pathogenic and non-pathogenic isolates, the laboratory strains XIN20 and TT21 were used.

The cells were incubated in PYG in fresh flasks. Six flasks for each isolate were prepared, to harvest cells after 24h, 48h and 72h after mannose-addition, as well as without mannose. On day one, 100 mM mannose was added, and the cells were incubated at room temperature.

After counting, a total of 10^6 cells/ml for each strain, with and without mannose, was harvested, centrifuged for 10 minutes at 700 x g and washed one time with PBS before the pellet was either frozen at -20°C or resuspended in a lysis buffer to isolate the RNA directly.

9.7.4. RNA-Isolation

The RNA was isolated with the Thermo Scientific GeneJET RNA Purification Kit. To isolate the RNA, 20 µl 2-mercaptoethanol were added per 980 µl lysis buffer and vortexed. 600 µl lysis buffer was added to every sample, before transferring the samples to a Qiagen shredder. The tubes were centrifuged for two minutes at 12.000 x g and 360 µl of cold 100% ethanol were added to the flow-through. The samples were transferred to RNA columns and centrifuged, before the flow-through was discarded. First, 700 µl of washing buffer 1, then 500 µl and 250 ml of washing buffer 2 were added in three steps, before the columns were placed into fresh collection tubes, to dry spin the tubes. Finally, the columns were put into fresh, RNase-free 1.5 ml Eppendorf tubes. 30 ml of RNase-free water was pipetted carefully in the middle of the filter.
The yield could be increased by letting the water soak in. The tubes were spinned one last time before the RNA concentration was measured via the NanoDrop.
Between the centrifugation steps the samples were kept on ice.
To eliminate leftovers of genomic DNA (gDNA), 1 µl DNase per 9000 ng RNA was added. The tubes were incubated at 37°C for 20 minutes, at 25°C for 40 minutes and at 70°C for five minutes. 1/10 auf 3M NaAc and three times 100% ethanol were added, before the samples were stored at -80°C overnight for RNA precipitation.
The next day, the samples were centrifuged for 20 minutes at 4°C, the supernatant was discarded, and the pellets were washed with 95 µl 70% ethanol, before being centrifuged again for 20 minutes. In the last step, the supernatant was discarded, and the pellet was airdried to let the remaining alcohol evaporate. The pellet was dissolved in 30 µl nuclease-free water and the final RNA concentration was measured. The RNA was stored at -80°C or at -20°C if used timely.

9.7.5. Complementary DNA (cDNA) synthesis

To transcribe cDNA from a single-strand RNA template for real-time PCR the Maxima First Strand cDNA Synthesis Kit for RT-PCR from Thermo Fisher Scientific was used. According to the protocol, per reaction 4 µl 5x Reaction Mix, 2 µl Maxima Enzyme Mix and 1 µg template RNA were mixed and filled up with nuclease-free water to reach a volume of 20 µl in total.
The mix was incubated for 10 minutes at 25°C, 30 minutes at 60°C and 5 minutes at 85°C. Afterwards the concentration of the DNA was measured via the NanoDrop.

The sample was diluted to 20 µg/µl for the real-time PCR. The cDNA was used as fast as possible, as it is very unstable.

9.7.6. Quantitative real-time PCR

As mastermix, the Takyon No ROX SYBR 2x MasterMix blue dTTP by Eurogentec (Seraing, Belgium) was used. 7.5 µl mastermix was prepared in advance with 0.25 µl forward and reverse primer each. The cDNA was diluted to 20 µg/µl in water. Via Excel the pipetting scheme was prepared.

Per sample, 8 µl mastermix and 7 µl cDNA were added to a total volume of 15 µl. For the negative controls water was used instead of DNA. The reference primers were HPT and QV 18S (see Table 2). The device used for RT-PCR was the CFX Connect real-time PCR detection system (BioRad Laboratories, Inc., Singapore).

The program can be found in the appendix (see Appendix, Table 11). The scan mode for all channels was activated.

After selecting nine primer pairs, a real-time PCR with the cDNA of JIR22 was performed.

9.7.7. Analysis of RT-PCR

The results of the RT-PCR were analysed with the CFX Manager by BioRad.

X. Results

10.1. Sequencing and phylogenetic analysis

In total, twelve environmental samples were collected with cotton swabs and cultured on agar plates seeded with *E. coli*. When growth of amoebae was detected by microscopic observation, the amoebae were cut out and subcultured on fresh agar plates. Isolates of the genus *Acanthamoeba* spp. could be clearly distinguished by the distinctive form of the cysts. For these isolates, a PCR specific for *Acanthamoeba* spp. was performed amplifying initially the diagnostic JDP fragment, which was sequenced subsequently (Schroeder et al., 2001). Other amoebae were further analysed by sequencing of a fragment of the 18S rRNA gene.

The following table shows the sampling location and the sequenced genus or the respective *Acanthamoeba* genotype (see Table 3).

Table 3. Table of location and species/genotype of the collected environmental isolates.

Abbreviation	**Location**	**Genus/Genotype**
AD	Shower Drain	*Acanthamoeba* spp./T4
AK	Drain Kitchen Sink	*Acanthamoeba* spp. & *Flamella* spp.
ASZ	Sink RNA Lab	*Acanthamoeba* spp./T4
AWC	Drain Sink WC	*Stemonitis* spp.
E2	Plant Pot Home	*Acanthamoeba* spp./T4
EK1	Plant Pot Kitchen 1	*Acanthamoeba* spp./T4
EK2	Plant Pot Kitchen 2	*Thecamoeba* spp.
KA	Cat water bowl	*Naegleria* spp.
KM	Coffee machine water tank	*Vermamoeba* spp.
M	Moss balcony	*Vanella* spp.
MSK1	Guinea pig water bowl	*Hyperamoeba* spp. & *Guttulinopsis* spp.
P	Water puddle balcony	*Hartmanella* spp.

All three environmental *Acanthamoeba* strains E2, ASZ, and EK1 were attempted to be transferred from xenic culture to liquid culture, but only cysts from isolate E2 excysted and would grow to sufficient densities in axenic culture. This strain was used for further studies (see SDS-PAGE and zymography). The complete 18S rRNA gene sequences of all *Acanthamoeba* strains collected during sampling (E2, ASZ, EK1) and of three AK strains (XIN20, SCT21, JIR22) from the laboratory archive were selected and identified as belonging to genotype T4, based on BLAST searches that showed the highest similarities in comparison with published stains representing genotype T4. A phylogenetic tree was calculated with clinical and environmental representatives of genotype T4. The following figure shows a Maximum Likelihood tree created with MEGA 11 (see Figure 5).

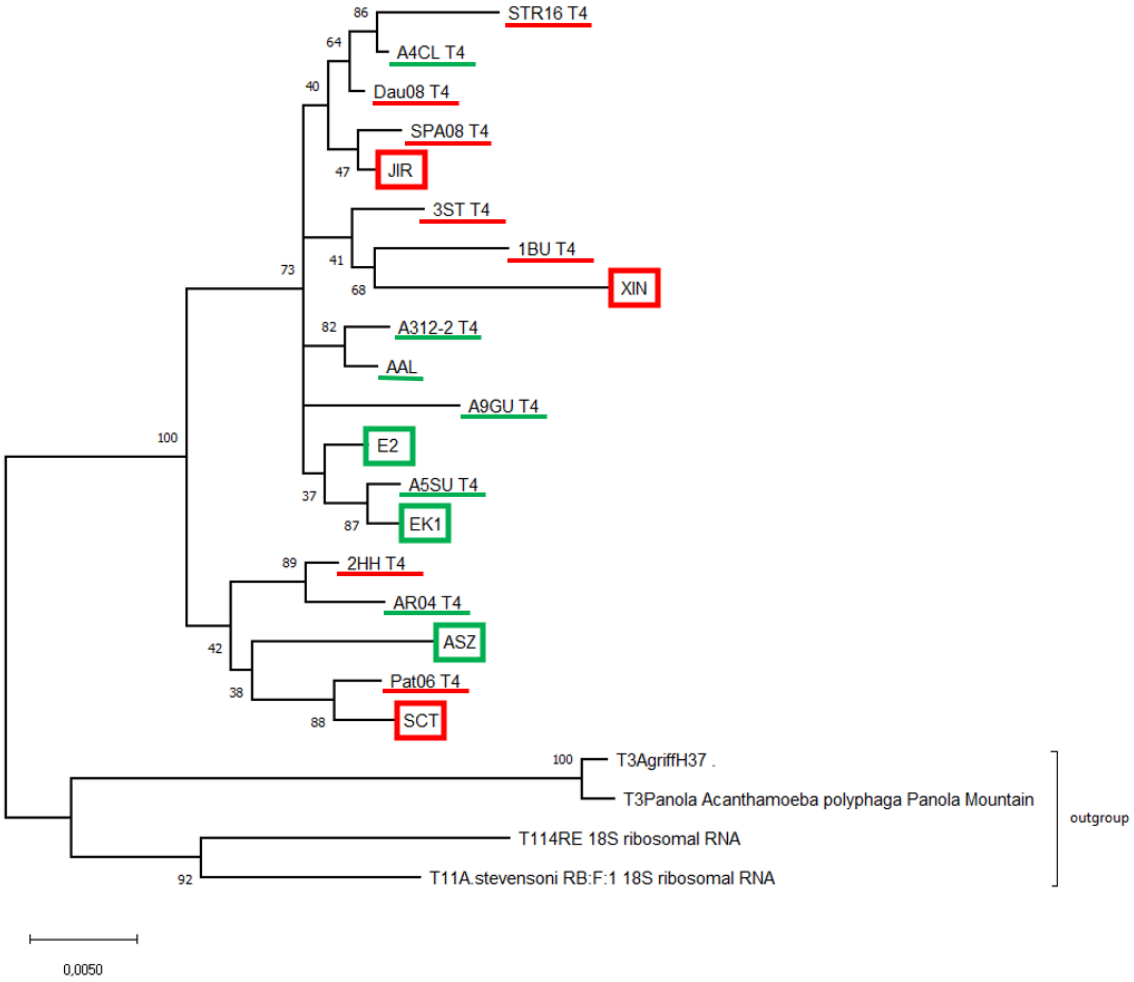

Figure 5. Rooted phylogenetic maximum likelihood tree using K2+GI (Kimura2-parameter specifying a gamma distribution and invariable sites) model created with sequences of the clinical and the environmental isolates representing genotype T4 (ASZ, EK1, E2, XIN20, SCT21, JIR22). The tree is drawn to scale, with branch lengths measured in the number of substitutions per site. Sequences representing genotypes T3 and T11 are used as outgroup. Bootstrap values are based on 1.000 replicates and are given at the nodes Bar: 0.0050 substitutions per site. All pathogenic strains are marked in red, all non-pathogenic strains are marked in green. The sequences of the environmental and the clinical strains investigated in this study are circled with a box, the remaining strains with an underline.

All isolates investigated in this study clearly represent genotype T4, which is supported by high bootstrap values. Although, it appears as if a sub-cluster of pathogenic strains is indicated including the strains XIN20 and JIR22, as well as a non-pathogenic sub-cluster with the strains E2 and EK1, clinical and environmental isolates can in general not be differentiated based on phylogenetic analysis, since several clusters are a mixture of both. At least some of these mixed clusters have a high bootstrap support.

To identify subtypes of the genotype T4, the sequences were analysed together with sequences of isolates that represent the subtypes T4A to T4H and sequences representing genotype T11 as outgroup (see Figure 6) (Corsaro, 2020).

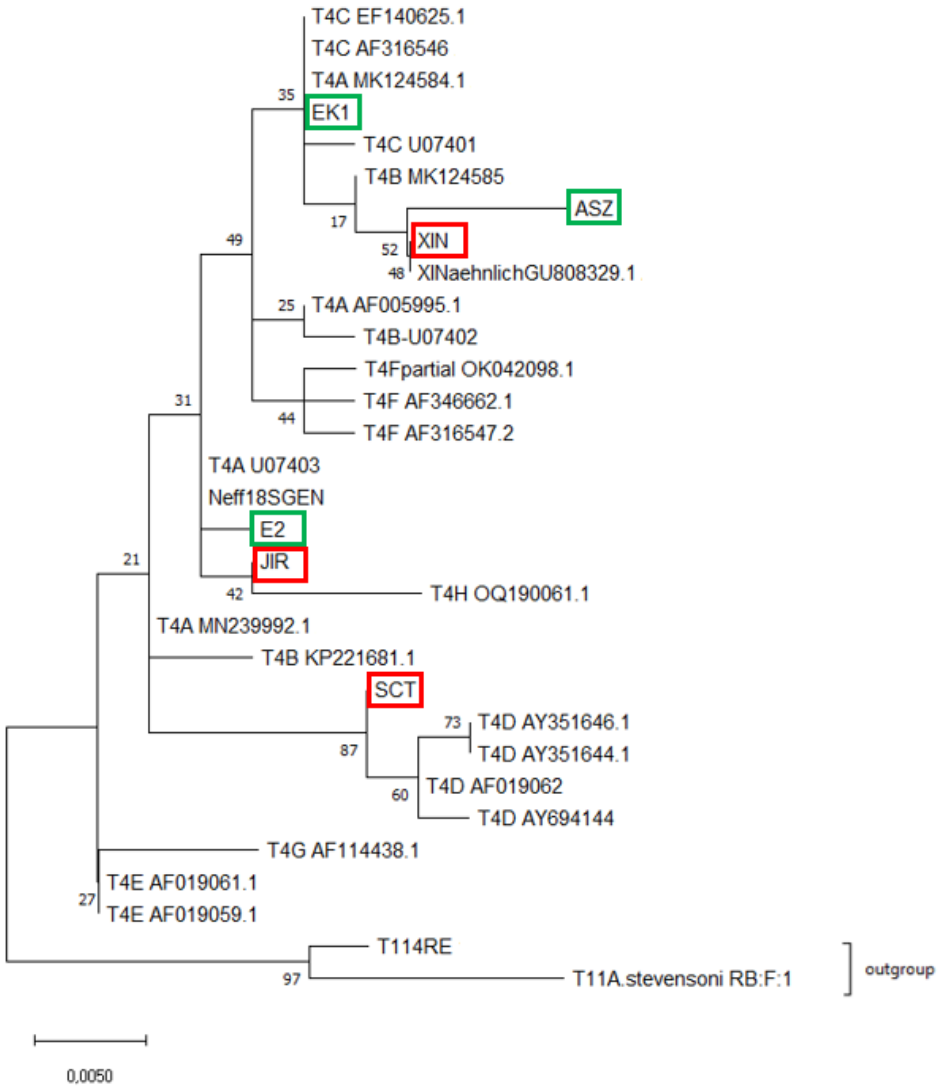

Figure 6. The phylogenetic tree with the JC+GI model is created with the sequences isolates and sequences representing the subtypes T4A to T4H after Corsaro (2020) and Corsaro & Venditti (2023) and genotype T11 as outgroup.

Strain EK1 is clusters closely to sequences representing the subtypes T4C and one sequence of T4A. Strain E2 clusters together with the reference strain Neff, which is representing subtype Neff. Strain JIR22 is clustering together with a sequence representing subtype T4H.

Environmental strain ASZ forms a cluster together with a pathogenic strain in a subcluster with T4B. Strain SCT21 clusters with sequences representing the subtype T4D with a bootstrap of 87.

10.2. Temperature tolerance tests

Since only strain E2 of the collected environmental isolates was able to grow in axenic culture, for subsequent experiments, in order to the same culture conditions for all strains, the non-pathogenic *A. terricola* strain TT21 and *A. castellanii* strain Neff (Ef554328.1) were chosen as non-pathogenic strains and investigated together with strain E2. As pathogenic representatives the clinical strains XIN20, SCT21, and JIR22 were used.

The following figures show the growth curves of these six different pathogenic and non-pathogenic strains at 25°C (Figure 7), 34°C (Figure 8), and 37°C (Figure 9).

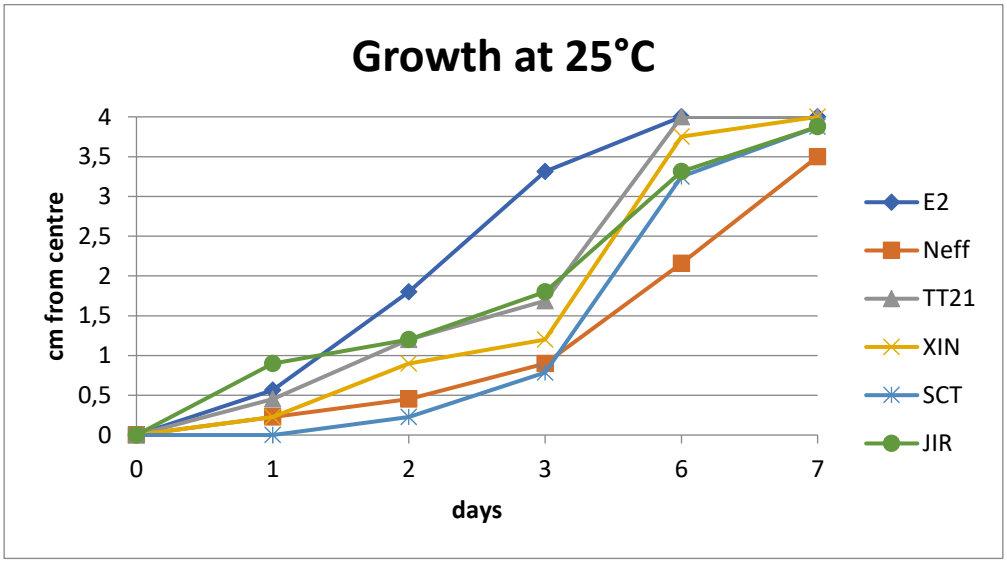

Figure 7. Growth in cm from the centre of the plate of the non-pathogenic strains (E2, Neff, TT21) and pathogenic strains (XIN20, SCT21, JIR22) at 25°C for seven days. The smallest circle on the plate had a radius of 0.9 cm, the second one 1.5 cm, the third a radius of 2.25 cm and the biggest one 3 cm (see Figure 4). The total radius of a plate is 4 cm.

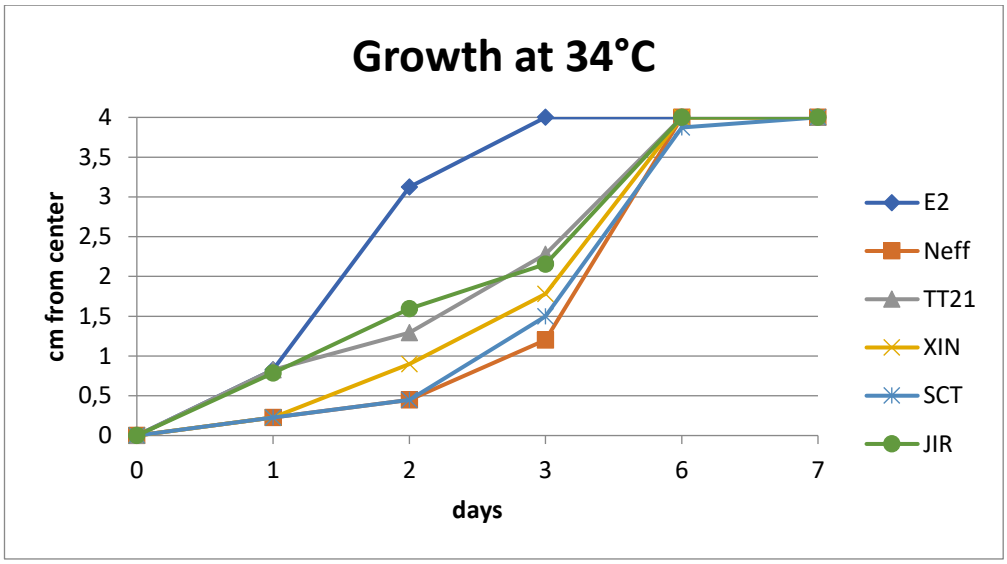

Figure 8. Growth in cm from the centre of the plate of the non-pathogenic strains (E2, Neff, TT21) and pathogenic strains (XIN20, SCT21, JIR22) at 34°C for seven days. The smallest circle on the plate had a radius of 0.9 cm, the second one 1.5 cm, the third a radius of 2.25 cm and the biggest one 3 cm (see Figure 4). The total radius of a plate is 4 cm.

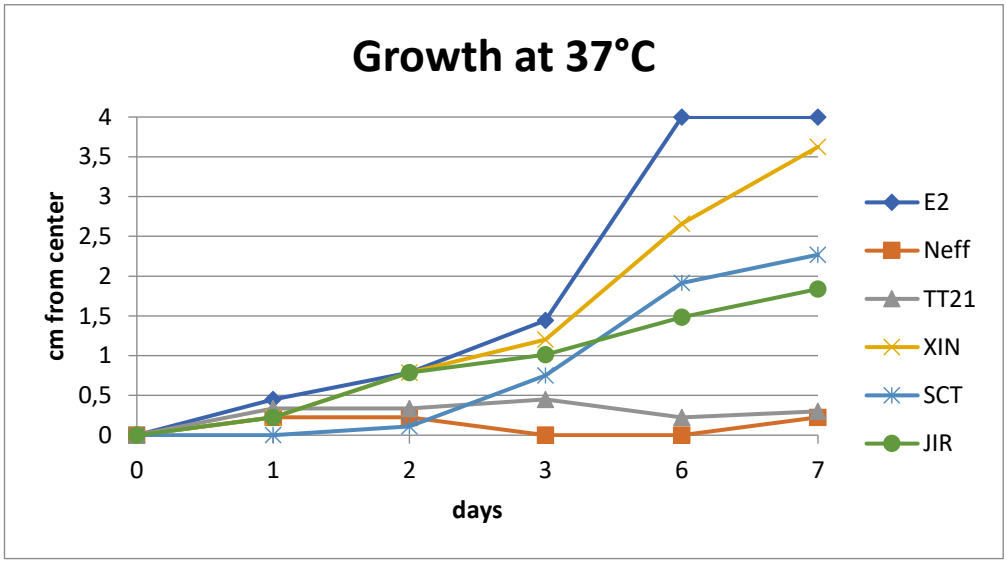

Figure 9. Growth in cm from the centre of the plate of the non-pathogenic strains (E2, Neff, TT21) and pathogenic strains (XIN20, SCT21, JIR22) at 37°C for seven days. The smallest circle on the plate had a radius of 0.9 cm, the second one 1.5 cm, the third a radius of 2.25 cm and the biggest one 3 cm (see Figure 4). The total radius of a plate is 4 cm.

The non-pathogenic strain Neff grew at 25°C and 34°C after two days. After seven days at 25°C the end of the plate was nearly reached. At 34°C the cells grew fast between the third and the sixth day and the end of the plate was reached after four to six days. No growth could be detected at 37°C for the non-pathogenic isolate Neff.

The non-pathogenic isolate TT21 grew equally successful at 25°C and 34°C. The cells grew faster at 34°C, but at both temperatures the end of the plate was reached between the third and the sixth day. At 37°C no growth could be detected for TT21.

The cells of the environmental isolate E2, collected from a plant pot, reached the end of the plate between the third and the sixth day at every temperature. Furthermore, at all three temperatures the cells grew nearly equally fast within 24 hours. At 25°C the cells crossed the fourth ring at 3 cm after three days. On day two, the cells had already crossed the fourth ring when being incubated at 34°C, which indicates a very fast growth. At 37°C, the growth was slower, but the end of the plate was reached between day three and six.

The pathogenic isolate XIN20 grew well at all temperatures. The fastest growth was observed at 34°C. At 34°C, the end of the plate was reached between day three and six and at 25°C the end of the plate was reached on day seven. At 37°C, the cells grew slower and came only close to the edge of the plate on day seven.

The pathogenic isolate SCT21 grew at every temperature. The cells reached the border of the plate at 25°C and 34°C on day seven, but grew only close the third ring at 2.25 cm at 37°C. The fastest growth was detected at 34°C.

The pathogenic strain JIR22 showed growth at every temperature. At 25°C the cells reach the end of the plate on day seven. The fastest growth was detected at 34°C, where the edge of the plate was reached between the third and the sixth day. At 37°C, the cells crossed the second ring at 1.5 cm.

10.3. SDS-Page

In figure 10, the protein patterns of the three pathogenic isolates XIN20, SCT21, and JIR22 grown in PYG and in PYG supplemented with 100 mM mannose are shown.

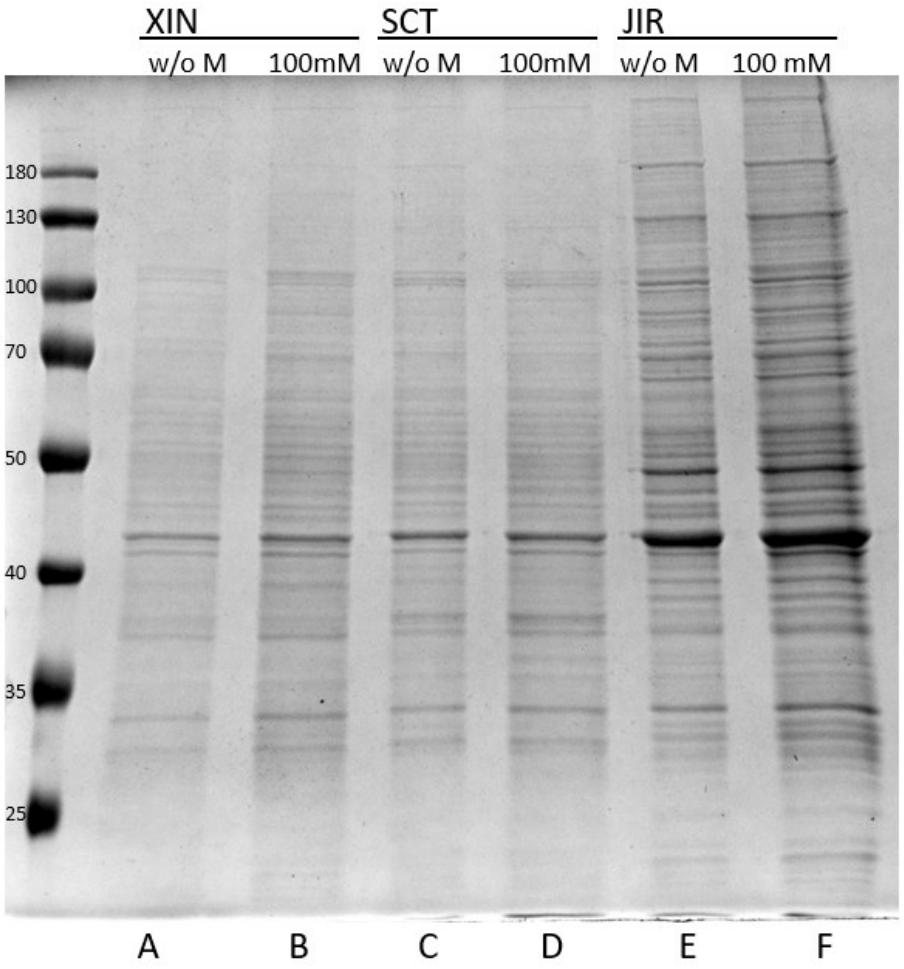

Figure 10. Protein patterns of the strains XIN20, SCT21, and JIR22 with and without the incubation of 100 mM mannose for 48h, visualized via SDS-PAGE. Columns A and B show the bands of XIN20 without (A) and with a 100 mM mannose incubation for 48h (B). Columns C and D show the bands of SCT21 without (C) and with a 100 mM mannose incubation for 48h (D). Columns E and F show the bands of JIR22 without (E) and with a 100 mM mannose incubation for 48h (F).

The protein band patterns vary to some extend in all three strains. Many weak bands were present that are not mentioned particularly in the following paragraphs.

The resulting bands indicate a similar protein content in all strains. Strong bands in all three isolates are visible at ~105 kDa, ~44 kDa, ~42 kDa, ~37 kDa, ~33 kDa, and ~30 kDa.

The bands of the strain JIR22 appear to be overall stronger expressed. The band patterns of XIN20 and SCT21 seem weaker, but most bands that are visible in strain JIR22 appear to be expressed too, however, with lower intensity.

At ~185 kDa, ~130 kDa, and ~50 kDa are strong bands in the band pattern of JIR22, that seem significantly less pronounced in XIN20 and SCT21.

In SCT21 at ~38 kDa bands, in both samples, incubated with and without mannose, are present. These bands appear to be unique and cannot be found in the other isolates.

In general, no differences in the protein band patterns of untreated cells and cells incubated with 100 mM mannose are visible in all strains investigated in this study.

The following figure shows the results of the SDS-PAGE of the three non-pathogenic isolates Neff, E2, and TT21 (see Figure 11).

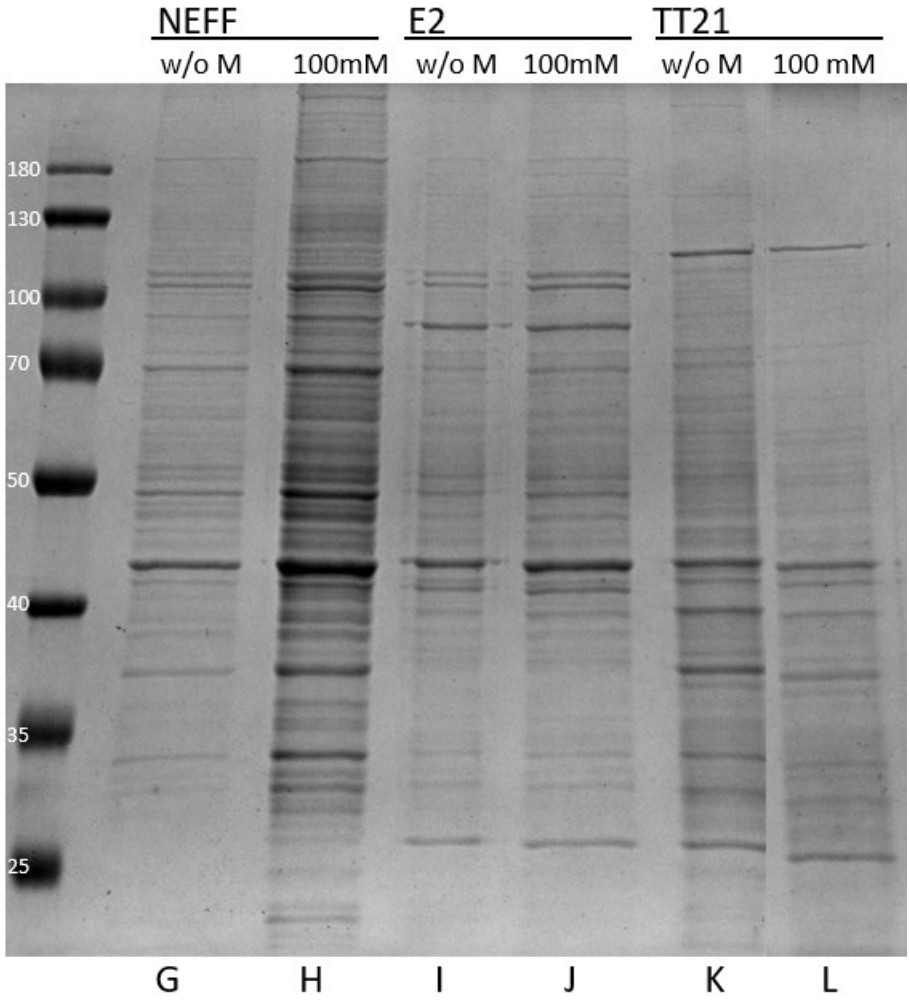

Figure 11. Protein patterns of the strains Neff, E2, and TT21 with and without the incubation of 100 mM mannose for 48h, visualized via SDS-PAGE. Columns G and H show the bands of Neff without (G) and with a 100 mM mannose incubation for 48h (H). Columns I and J show the bands of E2 without (I) and with a 100 mM mannose incubation for 48h (J). Columns K and L show the bands of TT21 without (K) and with a 100 mM mannose incubation for 48h (L).

The protein band patterns vary in all the three strains to a certain extend. Many weak bands are present that are not mentioned in the following paragraph.

In the protein patterns of Neff, strong bands are present at ~185 kDa, ~130 kDa, ~107 kDa, ~105 kDa, ~90 kDa, ~70 kDa, ~52 kDa, ~50 kDa, ~49 kDa, ~44 kDa, ~ 42 kDa, ~37 kDa, and ~33 kDa.

In E2 the bands at ~185 kDa, ~70 kDa, ~50 kDa, ~49 kDa, ~44 kDa, ~42 kDa, and ~33 kDa are also present, but noticeable weaker than in pathogenic strain JIR22. The bands at ~107 kDa, ~105 kDa, ~90 kDa, and ~44 kDa are just as strong as in the pattern of strain JIR22. Additionally, bands at ~87 kDa and ~27 kDa are present. A weak band at ~130 kDa is present.

At ~38 kDa and at ~110 kDa strong bands are visible in the pattern of TT21. Weaker expressed band are visible at ~44 kDa, 42 kDa, and ~33 kDa. The band at ~27 kDa as in E2 is present in TT21 as well. At ~37 kDa the same band is visible than in the pattern of Neff.

The following table shows all expressed protein from the pathogenic and non-pathogenic strains in comparison (see Table 4).

Table 4. Overview over the expressed proteins of the six investigated strains.

Protein weight	**XIN20**	**SCT21**	**JIR22**	**Neff**	**E2**	**TT21**
185 kDa		x	x	x	x	
130 kDa	x	x	x	x	x	x
110 kDa						x
107 kDa				x	x	
105 kDa	x	x	x	x	x	
90 kDa				x	x	
87 kDa					x	
70 kDa				x	x	
50 kDa		x	x	x	x	
49 kDa				x	x	
44 kDa	x	x	x	x	x	x

42 kDa	x	x	x	x	x	x
38 kDa		x				x
37 kDa	x	x	x	x		x
33 kDa	x	x	x	x	x	x
30 kDa	x	x	x			
27 kDa					x	x

10.4. Zymography

To investigate differences in the protease expression of strains grown with and without mannose, protease patterns of all pathogenic and non-pathogenic strains were evaluated (see Figures 10 & 11).

The following figure shows the results of the zymography of the three pathogenic isolates XIN20, SCT21, and JIR22 (see Figure 12).

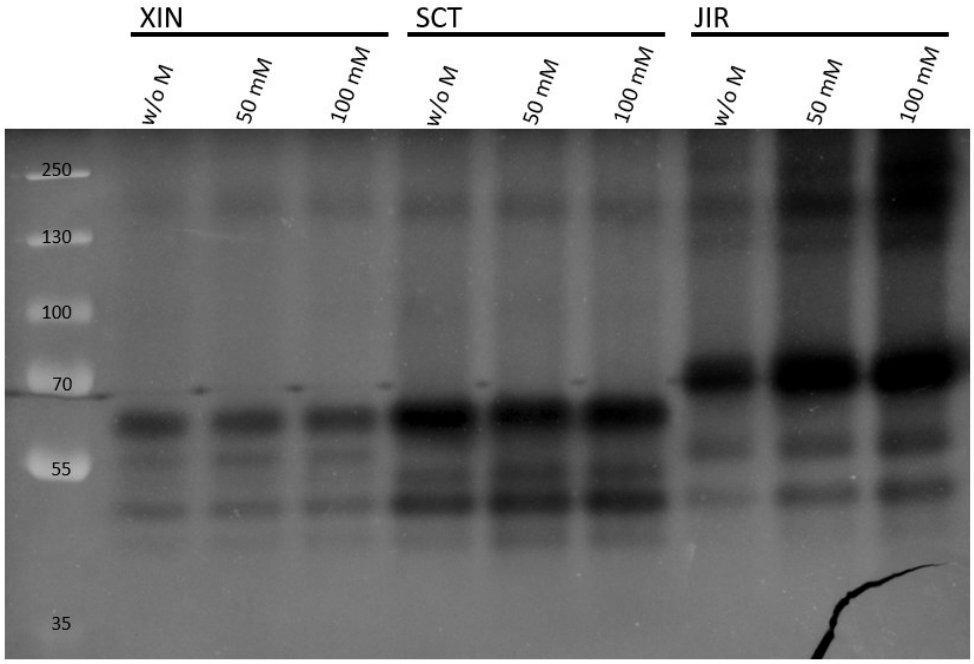

Figure 12. The gel picture shows the protease patterns of the pathogenic isolates XIN20, SCT21, and JIR22 without the addition of mannose, a 50 mM and a 100 mM concentration of mannose for 24h.

In the protease patterns of the strain XIN20 strong bands at ~60 kDa and less strong bands at ~49 kDa are present. Weak bands at ~188 kDa, ~55 kDa, and ~47 kDa are visible.

For the strain SCT21 strong bands can be seen at ~60 kDa and ~49 kDa. At ~188 kDa, ~54 kDa, and ~47 kDa weaker bands are present.

The band pattern of the strain JIR22 shows a strong band at ~72 kDa. Other bands can be observed at ~230 kDa, ~188 kDa, ~133 kDa, ~55 kDa, and ~49 kDa.

The protease patterns show no differences for the individual pathogenic strains when incubated with 50 mM, 100 mM or without mannose.

In general, the protease patterns of the strains XIN20 and SCT21 appear to be almost identical, while the pattern of the strain JIR22 shows various different bands that are not presetn in both other strains.

The following figure shows the results of the zymography of the three non-pathogenic isolates Neff, E2, and TT21 (see Figure 13).

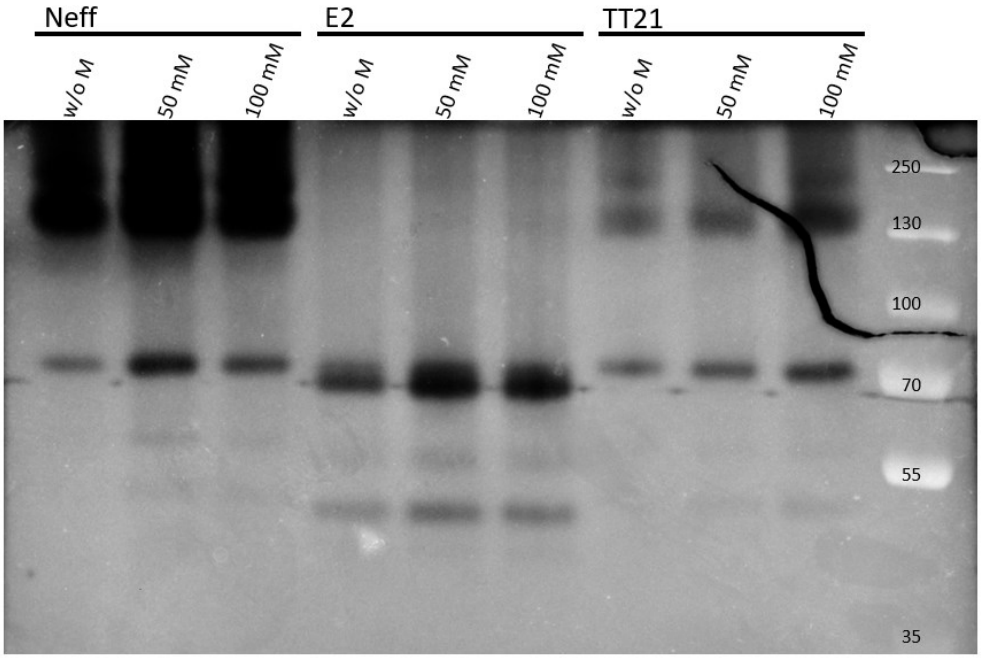

Figure 13. The gel picture shows the protease patterns of the pathogenic isolates Neff, E2, and TT21 without the addition of mannose, a 50 mM and a 100 mM concentration of mannose for 24h.

For the strain Neff, the protein pattern shows strong bands at ~75 kDa. Weak bands can be observed at ~60 kDa and ~49 kDa. The smears from ~133 kDa upwards are too strong to identify specific bands. In a follow-up experiment less than 2.5 µg/µl of the sample had to be applied.

For the strain E2 strong bands at ~72 kDa and weaker bands at ~ 55 kDa and ~47 kDa are present. Weaker bands at higher molecular weight are indicated.

Strong bands for the strain TT21 can be observed at ~133 kDa and ~75 kDa. Weaker bands are present at ~230 kDa, ~60 kDa, and ~49 kDa.

Although differneces in the intensity of protease bands are obvious, strains Neff and TT21 exhibit a more similar pattern, while strain E2 appears to express a different set of proteases, except for a protease at ~47 kDa, that is also expressed in TT21.

The gel picture shows no differences for the individual non-pathogenic strains when incubated with 50 mM, 100 mM or without mannose.

The following table shows all expressed proteases from the pathogenic and non-pathogenic strains in comparison (see Table 5).

Table 5. Comparison of the molecular weight of serine proteases found in this study with the molecular weight of proteases reported in literature.

Protease weight	**XIN20**	**SCT21**	**JIR22**	**Neff**	**E2**	**TT21**
47 kDa	x	x			x	
49 kDa	x	x	x	x		x
54 kDa		x				
55 kDa	x		x		x	
60 kDa	x	x		x		x
72 kDa			x		x	
75 kDa				x		x
133 kDa			x			x
188 kDa	x	x	x			x
230 kDa			x			x

To identify the types of proteases, individual protease inhibitors were applied, which is shown in Figure 14.

As controls, samples of the strains E2, TT21, Neff, SCT21, and JIR22 are applied without the addition of any protease inhibitor (A).

The second image shows the inhibiton with the metalloprotease inhibitor 1,10-phenantroline (B). The band patterns do not vary much from the band patterns of the gel without any inhibition and are visible for every of the five strains.

The third image shows the inhibiton with the cysteine peptidase inhibitor E-64 (C). The band patterns do not vary much from the band patterns of the gel without any inhibition and are visible for every of the five strains.

The following fourth image shows the inhibiton with the serine protease inhibitor phenylmethanesulfonylfluoride (D). When PMSF is added before the samples are applied to the gel, no bands are visible, except for the strain SCT21.

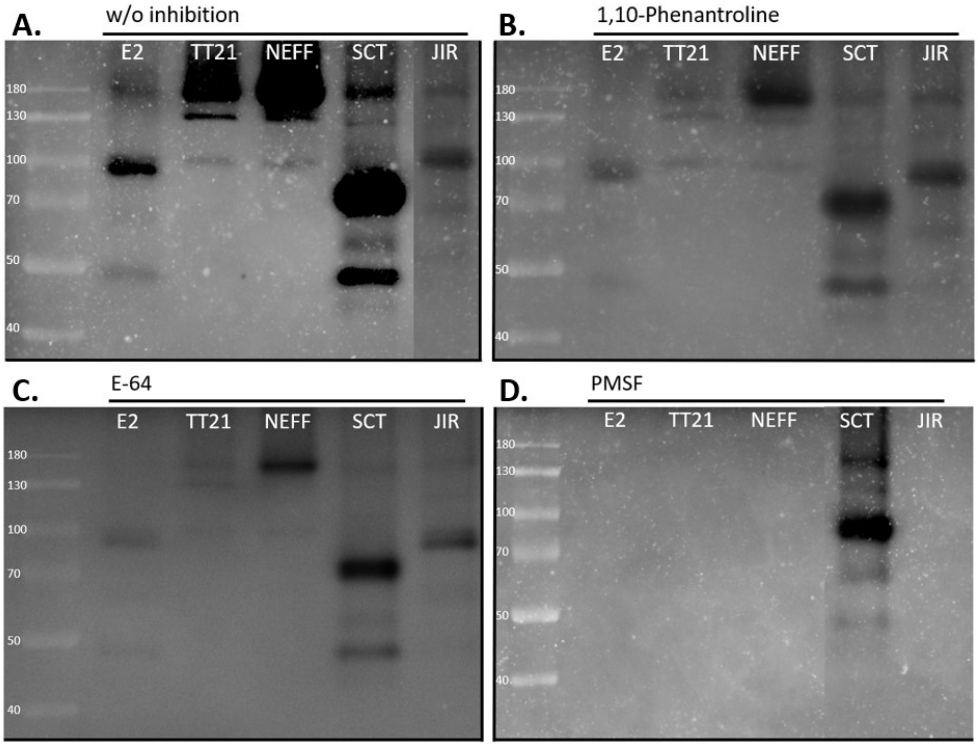

Figure 14. Protease patterns of the strains E2, TT21, Neff, SCT22, and JIR21, without the addition of protease inhibitors (A), incubated with 1,10-Phenantroline (B), with E-64 (C), and with PMSF (D), visualized via zymography.

The expression of different proteases of each strain is visible in Figure 14A. The strains TT21 and Neff show similarities, as well as the strains E2 and JIR22, whereas the strain SCT21 has an individual band pattern.

Because the previous results after inhibition with PMSF showed a differing band pattern of SCT21 in contrast to all other strains, the experiment was repeated for this strain only.

The supernatant of the strain SCT21, visualized in a zymography, without any inhibitors showed the normal band pattern (see Figure 15). The same pattern is present when phenantroline and E-64 are added. After inhibition with PMSF no bands are visible.

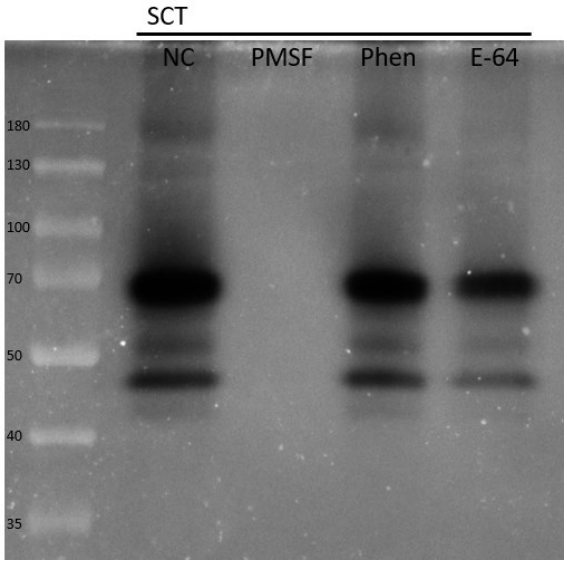

Figure 15.Protease pattern of the incubation without any protease inhibitor, PMSF, 1,10-Phenantroline, and E-64 for the strain SCT21, visualized via zymography.

For the strain XIN20 a separate zymography gel is shown (see Figure 16).

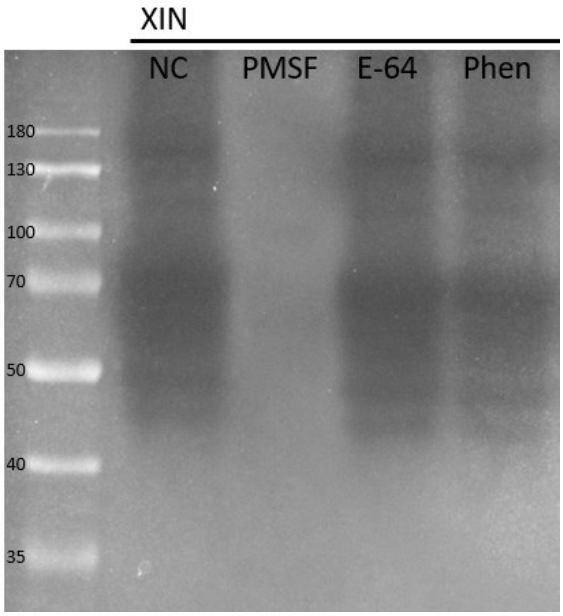

Figure 16. Protease pattern of the incubation without any protease inhibitor, PMSF, E-64, and 1,10-Phenantroline for the strain XIN20, visualized via zymography.

The supernatant of the strain XIN20, visualized in a zymography, without any inhibitors shows the normal band pattern. The same pattern is present when phenantroline and E-64 are added. After inhibition with PMSF no bands are visible.

10.5. Real-time PCR

In a conventional PCR with DNA of the strain JIR22 the designed primers were tested for their efficiency (see Figure 17, see Table 2).

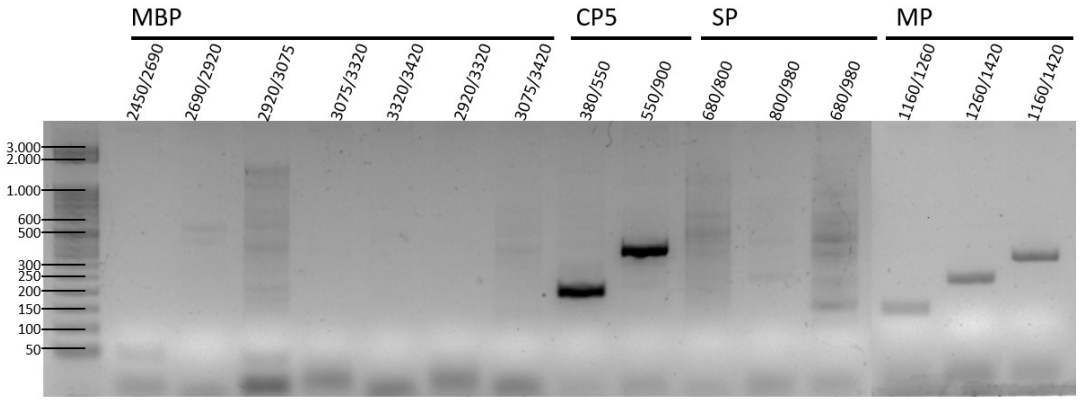

Figure 17. Band patterns from a conventional PCR with isolated DNA of the strain JIR22 with several primer pairs, targeting genes that act as potential pathogenicity markers, as the mannose-binding protein (MBP), serine proteases (SP), cysteine protease 5 (CP5), and metalloproteinases (MP).

The gel picture shows specific bands, several unspecific bands, as well as no bands for some primer pairs. For the metalloproteinase, specific bands can be seen with the primer pairs 1160/1260 (~150 abp), 1260/1420 (~250 abp), and 1160/1420 (~300 abp). The cysteine protease 5 was specifically targeted with the primer pairs 380/550 with a band at ~190 abp and 550/900 with a band at ~350 abp.

The primers targeting serine proteases reveal several unspecific bands and the primers targeting the MBP reveal either unspecific bands or no bands at all.

The primers that showed no specific bands in the first PCR were used again in a conventional PCR with cDNA of the strain JEA19 (see Figure 18). The annealing and elongation time, the cycles and the temperature were adjusted in order to reduce unspecific bands and increase sensitivity.

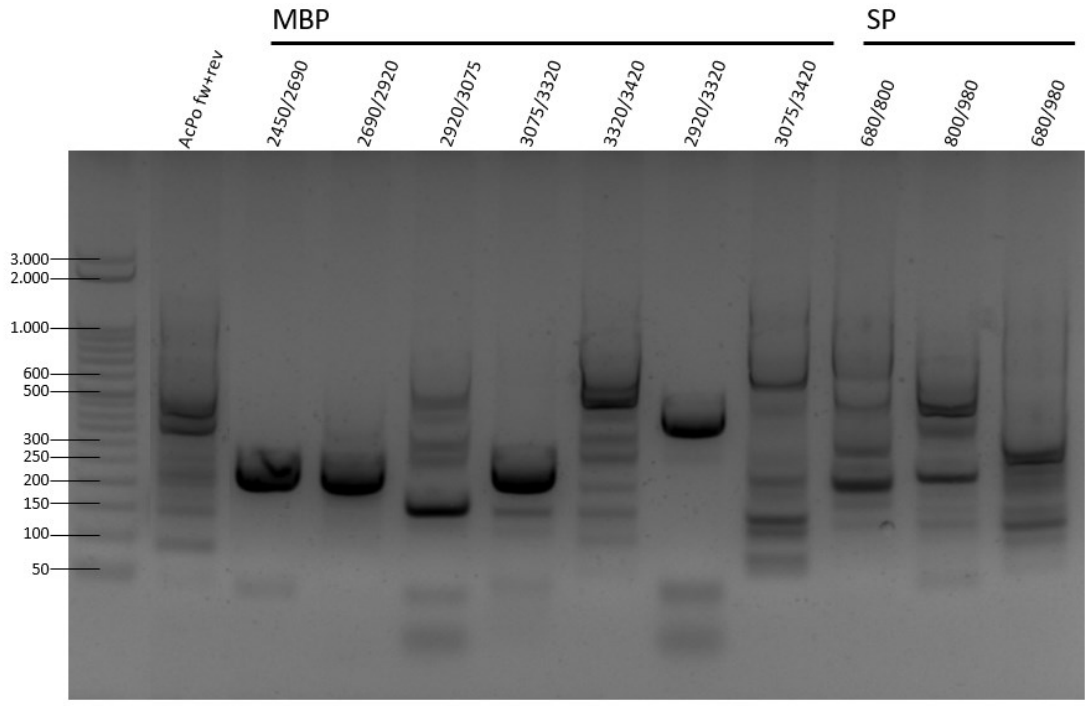

Figure 18. Band patterns from a conventional PCR with cDNA of the strain JEA19 with adjusted PCR settings and several primer pairs, targeting genes that act as potential pathogenicity markers, as MBP, AcPo and CP5.

No specific bands were detected with the primers targeting acanthaporine.

For the mannose-binding protein the adjustments showed specific bands for the primer pairs 2450/2690 (~190 abp), 2690/2920 (~180 abp), and 2920/3320 (~300 abp).

Eight primer pairs show a specificity for the potential pathogenicity markers: MBP1, MBP2, MBP4, MBP6, MP1, MP2, MP3, CP5.1, and CP5.2 (see Table 2).

The test-RT-PCR with cDNA of the strains XIN20 and TT21 together with the reference primers for HPT and 18S revealed that the primers 3075/3320 for the MBP (MBP4), the primers 1260/1420 for the MP (MP3), and the primers 380/550 for the CP5 (CP5.1) show promising ct-values and melt curves and can be used in expression studies in the future (see Table 2).

XI. Discussion

Acanthamoeba spp. are ubiquitous organisms that can be found in natural and man-made habitats all around the world. While these FLA can cause *Acanthamoeba* keratitis and granulomatous amoebic encephalitis in humans, it is not known what makes a specific strain pathogenic, while another strain representing the same morphology and genotype exhibits non-pathogenic properties. Hadaś and Mazur (1993) reported, that several properties contribute to the pathogenicity of an *Acanthamoeba* spp. isolate. These properties include the ability to have a higher temperature tolerance, the growth in defined media, the expression of the mannose-binding protein (MBP), and inducing cytopathic effects by the expression of several proteases, in particular the mannose-induced protease (MIP) (Cursons & Brown, 1978; De Jonckheere, 1977; De Jonckheere, 1980; Griffin, 1972; Hurt et al., 2003a; Yang et al., 1997). Other reported characteristics are the tolerance towards high osmolarity and a higher locomotive ability (De Jonckheere, 1980; Khan et al., 2001; Thong & Ferrante, 1986). The main findings of this study regarding potential pathogenicity factors are the differences of pathogenic and non-pathogenic strains regarding their physiological characteristics. Further, no significant genetical differences regarding the analysis of the 18s rRNA gene sequences, as well as no noticeable differences in the expression of the mannose-binding protein (MBP) and mannose-induced protease (MIP) were determined.

Temperature tolerance has been reported to be an important trait in pathogenicity (Gianinazzi et al., 2009; Griffin, 1972). For the temperature tolerance test, three different temperatures have been chosen. 25°C represents room temperature, 34°C is the temperature of the outer human eye, which is an important factor in the pathogenesis of AK, and 37°C represents the temperature of the human body and is relevant for GAE in the human brain (Efron et al., 1989). Griffin (1972) assumed that the virulence of *Naegleria* spp. and *Acanthamoeba* spp. strains was directly related to their growth at distinctive temperatures. The findings of this study show that the non-pathogenic isolates TT21 and Neff grow well at 25° and 34°C, but are not able to grow at 37°C. This indicates that they may be able to grow in the human eye and cause AK but cannot multiply inside the human body. Through encystment, these strains can still survive at higher temperatures, but they cannot grow (Griffin, 1972). All three pathogenic isolates, strain XIN20, SCT21, and JIR22 did grow well at all temperatures, which agrees with observations made in previous studies. Walochnik et al. (2001) demonstrated that pathogenic strains exhibit thermophilic properties by growing at 40°C, while non-pathogenic strains grew significantly less at the same temperature. Khan et al. (2001) were able to confirm the same properties for pathogenic strains at 37°C or higher, as well as Niyyati et al. (2013), who further differentiated strains that grew at 37°C as weakly pathogenic. Griffin (1972) reported that non-pathogenic strains are usually not able to grow at higher temperatures, in particular 37°C, which is crucial for causing GAE, and pathogenic strains can grow up to 46°C, which enables them to multiply in a host and to survive a fever. This agrees with the findings of this study. The environmental isolate E2, that was collected from soil and could be successfully transferred into liquid culture, showed strong and fast growth at all temperatures as well. Although strain E2 was not isolated from a clinical specimen, its growth behaviour does indicate a potential pathogenicity. This behaviour has been described before (Walochnik et al., 2000). Growth at 37°C on the one hand and ability to grow without bacteria as food source on the other are traits previously described for pathogenic strains, what agrees with the findings of this study (Megha et al., 2017; Schuster, 2002). Niyyati et al. (2013) also found strains with high pathogenic properties in soil, as the environmental strain E2 in the current study. The strain EK1, however, which was also isolated from plant pot soil, did not grow axenically, and thus was excluded from further examinations.

The slower growth rates at high temperatures of clinical isolates SCT21 and JIR22 may be explained by adaptions to the long-term axenic culture in the laboratory, which seems to affect physiological properties of strains, however, it obviously does not affect all strains equally as observed for isolate XIN20 (Pumidonming et al., 2010). Also, Stevens & O'Dell (1974) reported that strains, which are frequently transferred in axenic culture, seem to lose their pathogenic features. Köhsler et al. (2008) found that strains can lose their ability to encyst after prolonged axenic culture. Thereby the strains change their properties after a few months and the decrease continues for years before it remains constant at a very low level. A possible reason for this could be the adaption of the strains to their environment in the medium, which guarantees their survival and makes the encystment redundant. Eventually, the expression of specific genes, that are not needed anymore, is downregulated. This behaviour further indicates the involvement of epigenetic mechanisms (Köhsler et al., 2008). The phenomenon, that certain properties are lost, has been observed it other single-celled organisms, regarding the loss of locomotive action, the loss of virulence in *Naegleria fowleri*, or the changed patterns of expression of proteinases in cultures of *Trichomonas vaginalis* (Neale & Alderete, 1990; Thong & Ferrante, 1986; Wong et al., 1977). The prolonged axenic culturing of strains may therefore also affect the pathogenicity of *Acanthamoeba* isolates. This correlates to the finding that the freshly isolated and cultured strain E2 grew clearly faster than the pathogenic strains, indicating a higher flexibility, reactivity, and adaptability. The other environmental strains ASZ and EK1 did not grow in liquid culture. Megha et al. (2017) explained the inability of environmental strains to grow in axenic culture with a dependency of these amoebae and on bacteria as food source, maybe also specific endosymbionts being involved. For older strains with an impaired encystment potential, media with higher alkaline pH are used for support, which could be further applied in the future to support the excystation in axenic media as well. All this can be summed up in the hypothesis that only strains which are readily adaptable to various conditions and can grow without bacteria as food source, can cause an infection in human tissues (Köhsler et al., 2008).

Currently, 31 *Acanthamoeba* spp. species have been described in the literature. They are separated into 23 genotypes T1-T23, based on the sequences of their 18S rRNA genes (Connelly et al., 2023; Corsaro, 2020). The most frequent represented genotype, according to the results of the sequencing and phylogenetic analysis in this study is genotype T4, which agrees with literature, where the most abundant genotype in clinical isolates, as well as environmental isolates, is genotype T4 (Booton et al., 2004; Corsaro, 2020; Fuerst et al., 2015; Stothard et al., 1998). According to the results of the 18S rRNA gene sequencing, all collected environmental *Acanthamoeba* isolates, as well as the laboratory strains isolated from patients with AK, represent the genotype T4. Sequencing of the 18S rRNA gene does not enable a differentiation of pathogenic and non-pathogenic strains, as indicated in the constructed phylogenetic tree. As expected, no true clusters of pathogenic and non-pathogenic isolates were observed, although some subclusters appeared to consist of mostly either pathogenic or non-pathogenic representatives. However, do the findings of this study not entirely agree with the results published by Walochnik et al. (2000), who could identify clusters of isolates with no clinical relevance. Representatives of the genotype T4 mostly belong into the morphological group II, which is the most abundant group and includes clinical, as well as in environmental strains, which is supported by the fact that all isolates investigated in this study represent genotype T4 and a group II morphology (data not presented) (Stothard et al., 1998). Another model in MEGA-X might support a more precise differentiation. As the genotype T4 is very abundant and diverse, Corsaro et al. (2020; 2023) further classified it into eight subtypes T4A-T4H and T4Neff. Not all strains representing the same subtype cluster together, which can be observed when focusing on the reference strains of the subtype T4A, that are widely distributed throughout the tree (see Figure 6). T4A seems also to be the most frequent subtype in the study of Connelly et al. (2023), which agrees with the phylogenetic analysis of this study: two of six analysed strains, in particular the environmental strains EK1 and E2, seem to represent the subtype T4A. However, it has been shown that subtype T4A does not group into a single clade in most other studies and might be more spread within phylogenetic trees than other subtypes (Connelly et al., 2023; Corsaro, 2020). Corsaro (2020) reported that the reference strain Neff, that was used for the genome project, forms its own branch as subtype T4G and clearly is separated from the other subtypes.

In the current study, the strain Neff was closely located to the subtype T4A and the environmental strain E2. In the phylogenetic tree generated in this study, the sequence representing the subtype T4G is further closely related to T4E sequences, which does not fully agree with the study by Corsaro (2020). Probably, in a tree with more representatives of each subtype this could be better dissolved. The classification of strains into subtypes is not always possible, as there is no clear definition for the subtypes. One reason for this is that only a small number of strains has been classified into subtypes yet, which is relevant for reference and makes it more difficult to classify new strains. Another aspect is that not all strains representing the genotype T4 can be clearly assigned to an already specified subtype and many sequences published in GenBank are unique and do not fit into one of the established subtypes (Fuerst, 2014).

Concerning proteins, SDS-PAGE revealed a ~42 kDa protein band for every of the six pathogenic and non-pathogenic strains. This band most likely represents actin, which was described by Gordon et al., (1976) to make up 20% of the total protein content in *Acanthamoeba* spp. Other studies reported the weight of actin varying from 44 kDa for *Acanthamoeba* spp. to 45 kDa for *Naegleria fowleri* and *Entamoeba histolytica* (González-Robles et al., 2008). Interestingly, a band at 44 kDa was found for all strains as well. Actin is an important part of the cytoskeleton and relevant for cell motility, the transport of organelles, endocytosis, and exocytosis (Bader et al., 2004; Pollard & Borisy, 2003; Snider et al., 2004; Yarar et al., 2005). It has further been shown that actin is present in acanthopodia, lamellipodia and additional endocytic structures in *Acanthamoeba* spp., which supports these findings (González-Robles et al., 2008). In the current study, bands at ~33 kDa and ~44 kDa were found for every of the six strains investigated. Bands with a weight of ~50 kDa were weakly present in the strains SCT21, JIR22, Neff, and E2. At ~62 kDa no distinctive band for any of the strains was found. For genotype T4, protein bands at 33 kDa, 44 kDa, 50 kDa, and 62 kDa have been shown (Pumidonming et al., 2014). The protein patterns did show similarities between all strains, independently of their pathogenicity, which does partly agree with the findings by Pumidonming et al., (2014), which say that pathogenic and non-pathogenic strains representing the same genotype rather vary regarding the expression levels than the protein patterns.

Since all strains examined in this study belong to morphological group II and the banding pattern is supposed to correlate with groups, this is not surprising. The protein expression only seemed stronger in strain JIR22 in comparison to the strains XIN20 and SCT21. However, despite similarities, all strains revealed slight differences and thus their individual protein patterns. Variations were found for all strains. Reasons for the this could be differences in the growth rates and other cell physiological characteristics of the strains, as well as changes of the strains properties due to a long-term axenic culture, as mentioned earlier (Becker-Finco et al., 2013; Pumidonming et al., 2010). Noticeable is the very similar protein pattern of the environmental strains E2 and Neff, which would indicate similar cell physiological characteristics. Interestingly, in the phylogenetic analysis of T4 subtypes these two strains also grouped closely together. Also, the pathogenic strains SCT21 and JIR22 expressed nearly identical protein patterns. Higher similarity was also reflected in their similar growth rates at higher temperatures. In the current study, the pathogenic strain JIR22 exhibited a strong band at ~130 kDa. The strains XIN20, SCT21, Neff, E2, and TT21 only revealed a very weak, but clearly present band at ~130 kDa. This most likely to be the mannose-binding ptotein (MBP), which weights ~400 kDa and consists of multiple 130 kDa subunits (Garate et al., 2004). Yang et al. (1997) identified this protein earlier as 136 kDa extracellular membrane-related protein. It is known that trophozoites express the MBP on the cell surface, which mediates the adhesion to the host cells and is therefore a potential pathogenicity marker (Cao et al., 1998; Garate et al., 2004; Yang et al., 1997). The adherence of *Acanthamoeba* trophozoites to host cells induces a cytopathic effect, depending on the pathogenicity of the strain (Cao et al., 1998; Larkin & Easty, 1991). Garate et al. (2006) reported that the pathogenicity of a strain and its ability to produce a CPE when adhered to host cells is directly correlated to the expression levels of the mannose-binding protein. They deduced from their results that a strong pathogenicity is correlated with a strong CPE and high MBP expression, whereas strains with a weaker pathogenicity also express lower levels of MBP and therefore a weaker CPE (Garate et al., 2006). In this study, no differences in the expression of MBP between the pathogenic and non-pathogenic strains were observed. The non-pathogenic strains Neff, TT21, and E2 showed the same low expression of MBP as the pathogenic strains XIN20 and SCT21.

Thus, the assumption, that pathogenic strains would express higher levels of MBP was not supported by my study. Additionally, growth in the presence of methyl alpha-D-mannopyranoside did not show an impact on the expression of MBP and other proteins. Interestingly, Garate et al. (2006) found that the strain *A. royreba* has a CPE twice as high as *A. palestinensis*, while both strains express the same amount of MBP and are non-pathogenic. This corroborates that non-pathogenic isolates are able to express the mannose-binding protein. This indicates that the pathogenicity might be influenced by factors that either control the expression of MBP or stabilize the produced protein (Garate et al., 2006). My findings support this statement. The mannose concentration and incubation time applied might not have been sufficient to induce expression changes of MBP, although the applied protocols were similar to previously described experiments in other studies (Garate et al., 2006). However, the selection of the *Acanthamoeba* strains might also contribute to a different outcome. The cells of the strains AZ and EK1 did not grow sufficiently on the plates to carry out further experiments. Also, as these strains did not grow without bacteria, bacterial proteins would have been present in protein and protease pattern analyses. All proteases detected by zymography were completely inhibited by PMSF, an inhibitor specific for serine proteases. This indicates that all pathogenic and non-pathogenic isolates investigated secrete serine proteases of different weights. Also, other studies reported serine proteases to be the most common extracellular proteases in *Acanthamoeba* spp., which supports my findings (Omaña-Molina et al., 2013). However, besides serine proteases, also cysteine proteases and metalloproteases have been identified in *Acanthamoeba* spp. (Alfieri et al., 2000; Cao et al., 1998; Khan, 2006; Khan et al., 2000; Mitro et al., 1994). No cysteine proteases or metalloproteinases were detected in the current study. Khan et al. (2000) reported that 1 mM PMSF and 1 mM aprotonin deleted serine proteases in pathogenic isolates completely, whereas in non-pathogenic isolates only a partial deletion of the proteases was observed. In this study, with only PMSF, the proteases were inhibited completely, independently of the pathogenicity of the strain. Strains with the same or a similar pathogenicity have been described to exhibit a similar protease pattern (Mahdavi Poor et al., 2017). This would further argue for a potential pathogenicity of strain E2, as its protease pattern shows specific similarities with the pattern of the pathogenic strain JIR22 (see Table 5).

The pathogenic strains XIN20 and SCT21 also exhibited very similar protease patterns, supporting this theory. In the literature several serine proteases with different molecular weights have been reported (see Table 6).

Table 6. Molecular weight of reported serine proteases in literature.

Molecular weight	**Reference**
12 kDa	Na et al., 2001
27 kDa	Alfieri et al., 2000
33 kDa	Kim et al., 2003
34 kDa	Serrano-Luna et al., 2006
35 kDa	Hadaś & Mazur, 1993
36 kDa	Mitro et al., 1994
40 kDa	Mitra et al., 1995
42 kDa	Cho et al., 2000
47 kDa	Alfieri et al., 2000
49 kDa	Mitro et al., 1994
50 kDa	Serrano-Luna et al., 2006
53 kDa	Serrano-Luna et al., 2006
54 kDa	Park & Song, 1996
55 kDa	Cao et al., 1998
60 kDa	Alfieri et al., 2000
62 kDa	Serrano-Luna et al., 2006
64 kDa	Mahdavi Poor et al., 2017
65 kDa	Hadaś & Mazur, 1993
66 kDa	Mitro et al., 1994
72 kDa	Serrano-Luna et al., 2006
75 kDa	Alfieri et al., 2000
85 kDa	Sissons et al., 2006
97 kDa	Cao et al., 1998
100 kDa	Alfieri et al., 2000
107 kDa	Khan et al., 2000
130 kDa	Sissons et al., 2006
133 kDa	Hurt, Niederkorn, et al., 2003

148 kDa	Mahdavi Poor et al., 2017
157 kDa	Serrano-Luna et al., 2006
188 kDa	Serrano-Luna et al., 2006
230 kDa	Cao et al., 1998

Da Rocha-Azevedo and Costa Silva-Filho (2007) differentiated strains into pathogenic and non-pathogenic according to the number of bands revealed by zymography. Clinical strains produced six bands, whereas environmental strains only produced two bands. In this study, the three pathogenic isolates XIN20, SCT21, and JIR22 produced six bands. The non-pathogenic strain Neff produced at least four bands, TT21 three strong and two weaker bands, and the strain E2 three clearly visible bands, generally agreeing with this theory, although more weak bands were found. Mahdavi Poor et al. (2017) did not confirm this theory, in their study clinical isolates produced bands in a range of 37 kDa to 177 kDa and environmental isolates in a range of 39 kDa to 184 kDa. The most frequently detected protease had a molecular weight of 148 kDa, followed by one with a weight of 64 kDa. The range in this study reached from ~47 kDa to ~230 kDa for both pathogenic and non-pathogenic strains, with individual bands for each strain, the most common expressed protease being a ~49 kDa protease, directly followed by a ~60 kDa protease. Mitro et al. (1994) discovered a protease at 49 kDa related to the degradation of type I collagen, which is one of the main components of the stromal matrix. They assumed that this protease contributes to the pathogenicity against the cornea during an infection with AK. Except for the environmental strain E2, every other strain, independently of its pathogenicity, expressed this protease. This indicates that even non-pathogenic strains may have a potential for degrading collagen. The proteases visible at 47 kDa, 60 kDa, and 75 kDa have previously been described by Alfieri et al. (2000), reporting properties identical to the properties of serine proteases that have been described before. In the current study, a protease visible at ~60 kDa was expressed by two pathogenic and two non-pathogenic strains, with no potential indication of pathogenicity. Park and Song (1996) described the protease at 54 kDa, which was expressed in the strain SCT21, to degrade type I collagen and fibronectin. According to their study, not degraded by this serine protease are bovine serum albumin (BSA), haemoglobin, lysozymes, immunoglobulin A and G, which probably also applies for all other proteases.

Another protease that has the property to degrade human type I and type IV collagen has been described to weight 133 kDa and was called mannose-induced protease (MIP) (Hurt et al., 2003a). Its production seems to be necessary for the induction of corneal infections. The contact with methyl-α-mannopyranoside led to higher amounts of MIP in the study by Hurt et al. (2003b). In the current study, after incubation with 50 mM and 100 mM mannose, no stronger expression of MIP was found than without mannose, thus indicating no correlation between the expression of MIP and growth in the presence of methyl-α-mannopyranoside. The protease at ~188 kDa was only expressed in the pathogenic strains XIN20, SCT21, and JIR22. This protease has been reported as secreted serine protease from *A. castellanii* by Serrano-Luna et al. (2006). Another protease at ~72 kDa has been described by the same authors, to be a secreted serine protease from *A. polyphaga*. This protease was found to be expressed by strain E2. For the proteases at ~55 kDa and ~230 kDa no further information on their properties was found in the literature. However, they also have been reported by Cao et al. (1998) and it can be assumed that they have similar properties to the serine proteases already mentioned. Park & Song (1996) identified a serine protease at 54 kDa with a substrate specificity against type I collagen and fibronectin, which in the current study was detected in the strains Neff and SCT21 (~54 kDa). Khan et al. (2000) discovered a serine protease at 107 kDa that was strongly expressed exclusively in pathogenic isolates. However, my results do not agree with these findings, as no band in either the pathogenic or the non-pathogenic strains was visible. Overall, it appears as if not one single or even some specific proteases are clearly responsible for a strain's pathogenic potential, and although the data obtained are in general agreement with previously published studies there were several discrepancies to previous data and also within the set of strains investigated.

XII. Conclusion

The sequencing of the 18S rRNA gene of the clinical and environmental strains showed that all strains do represent the genotype T4.

The phylogenetic analysis did not reveal any clusters of pathogenic and non-pathogenic strains regarding their 18S rRNA gene sequences, however subtypes within the genotype T4 could be distinguished.

The temperature tolerance test revealed that the non-pathogenic strains did not grow at 37°C in comparison to the clinical strains. Only the environmental strain E2 showed the ability to grow fast at high temperatures, which indicates a potential pathogenicity.

SDS-PAGE and zymography showed that all strains express individual protein and protease patterns.

A quantitative real-time PCR was established to investigate the expression of potential pathogenicity markers, including a metalloproteinase, the cysteine protease 5, and the mannose-binding protein (MBP). However, in this study, all expressed proteases were identified as serine proteases by inhibition with PMSF and the expression of the assumed pathogenicity markers MBP and MIP did not correlate to pathogenicity.

Interestingly, the environmental isolate E2 exhibited a protein pattern similar to the non-pathogenic strain Neff, but a protease pattern similar to pathogenic strain JIR22.

In summary, the results of the current study clearly support temperature tolerance and protein and protease patterns to correlate with pathogenicity in *Acanthamoeba* spp., but further investigations are needed to identify true virulence markers.

XIII. References

Abjani, F., Khan, N. A., Yousuf, F. A., & Siddiqui, R. (2016). Targeting cyst wall is an effective strategy in improving the efficacy of marketed contact lens disinfecting solutions against Acanthamoeba castellanii cysts. *Contact Lens and Anterior Eye*, *39*(3), 239–243. https://doi.org/10.1016/j.clae.2015.11.004

Agarwal, R. K., Mittal, G., Raj, A., & Gupta, S. (2014). Acanthamoeba detection in the anterior chamber after therapeutic penetrating keratoplasty. *Journal of Clinical and Diagnostic Research*, *8*(6). https://doi.org/10.7860/JCDR/2014/8366.4457

Alfieri, S. C., Correia, C. E., Motegi, S. A., & Pral, E. M. (2000). Proteinase activities in total extracts and in medium conditioned by Acanthamoeba polyphaga trophozoites. *The Journal of Parasitology*, *86*(2), 220–227. https://doi.org/10.1645/0022-3395(2000)086[0220:PAITEA]2.0.CO;2

Alkatan, H. M., & Al-Essa, R. S. (2019). Challenges in the diagnosis of microbial keratitis: A detailed review with update and general guidelines. *Saudi Journal of Ophthalmology*, *33*(3), 268–276. https://doi.org/10.1016/j.sjopt.2019.09.002

Alomar, T., Matthew, M., Donald, F., Maharajan, S., & Dua, H. S. (2009). In vivo confocal microscopy in the diagnosis and management of acanthamoeba keratitis showing new cystic forms. *Clinical and Experimental Ophthalmology*, *37*(7), 737–739. https://doi.org/10.1111/j.1442-9071.2009.02128.x

Alsam, S., Sissons, J., Dudley, R., & Khan, N. A. (2005). Mechanisms associated with Acanthamoeba castellanii (T4) phagocytosis. *Parasitology Research*, *96*(6), 402–409. https://doi.org/10.1007/s00436-005-1401-z

Alves, J. M. P., Gusmão, C. X., Teixeira, M. M. G., Freitas, D., Foronda, A. S., & Affonso, H. T. (2000). Random amplified polymorphic DNA profiles as a tool for the characterization of Brazilian keratitis isolates of the genus Acanthamoeba. *Brazilian Journal of Medical and Biological Research*, *33*(1), 19–26.

Antonelli, A., Favuzza, E., Galano, A., Montalbano, M., Filippo, D., Ciccone, N., Berrilli, F., Mencucci, R., Cave, D. Di, & Rossolini, G. M. (2018). Regional spread of contact lens-related Acanthamoeba keratitis in Italy. *New Microbiologica*, *41*(1), 1121–7138.

Arance-Gil, Á., Gutiérrez-Ortega, Á. R., Villa-Collar, C., Nieto-Bona, A., Lopes-Ferreira, D., & González-Méijome, J. M. (2014). Corneal cross-linking for Acanthamoeba keratitis in an orthokeratology patient after swimming in contaminated water. *Contact Lens and Anterior Eye*, *37*(3), 224–227. https://doi.org/10.1016/j.clae.2013.11.008

Artika, I. M., Dewi, Y. P., Nainggolan, I. M., Siregar, J. E., & Antonjaya, U. (2022). Real-Time Polymerase Chain Reaction: Current Techniques, Applications, and Role in COVID-19 Diagnosis. In *Genes* (Vol. 13, Issue 12). MDPI. https://doi.org/10.3390/genes13122387

Asif, S., Khan, M., Waqar Arshad, M., & Shabbir, M. I. (2021). PCR Optimization for Beginners: A Step by Step Guide. *Research in Molecular Medicine*, *9*(2), 81–102. https://doi.org/10.32598/rmm.9.2.1189.1

Azzopardi, M., Chong, Y. J., Ng, B., Recchioni, A., Logeswaran, A., & Ting, D. S. J. (2023). Diagnosis of Acanthamoeba Keratitis: Past, Present and Future. *Diagnostics*, *13*(16), 2655. https://doi.org/10.3390/diagnostics13162655

Bacon, A. S., Frazer, D. G., Dart, J. K. G., Matheson, M., Ficker, L. A., & Wright, P. (1993). A REVIEW OF 72 CONSECUTIVE CASES OF ACANTHAMOEBA KERATITIS, 1984-1992. *Eye*, *7*, 719–725.

Bader, M. F., Doussau, F., Chasserot-Golaz, S., Vitale, N., & Gasman, S. (2004). Coupling actin and membrane dynamics during calcium-regulated exocytosis: A role for Rho and ARF GTPases. *Biochimica et Biophysica Acta - Molecular Cell Research*, *1742*(1–3), 37–49. https://doi.org/10.1016/j.bbamcr.2004.09.028

Bagga, B., Sharma, S., Gour, R. P. S., Mohamed, A., Joseph, J., M Rathi, V., & Garg, P. (2021). A randomized masked pilot clinical trial to compare the efficacy of topical 1% voriconazole ophthalmic solution as monotherapy with combination therapy of topical 0.02% polyhexamethylene biguanide and 0.02% chlorhexidine in the treatment of Acanthamoeba keratitis. *Eye* , *35*(5), 1326–1333. https://doi.org/10.1038/s41433-020-1109-4

Bakay, B. B., & Polat, Z. A. (2018). In Vitro Evaluation of Adhesion of Two Acanthamoeba Strains to Cosmetic Contact Lenses. *Eye & Contact Lens*, *44*, S241–S246. https://doi.org/10.1097/ICL.0000000000000457

Barbeau, J., & Buhler, T. (2001). Biofilms augment the number of free-living amoebae in dental unit waterlines. *Res. Microbiol*, *152*, 753–760.

Barete, S., Combes, A., De Jonckheere, J. F., Datry, A., Varnous, S., Martinez, V., Ptacek, S. G., Caumes, E., Capron, F., Francès, C., Gibert, C., & Chosidow, O. (2007). Fatal Disseminated Acanthamoeba lenticulata Infection in a Heart Transplant Patient. *Emerging Infectious Diseases*, *13*(5), 736–738. www.cdc.gov/eid

Barker, J., & Brown, M. R. W. (1994). Trojan Horses of the microbial world: protozoa and the survival of bacterial pathogens in the environment. *Microbiology*, *140*, 1253–1259.

Barker, J., Lambert, P. A., & Brown, M. R. W. (1993). Influence of Intra-Amoebic and Other Growth Conditions on the Surface Properties of Legionella pneumophila. *Infection and Immunity*, *61*(8), 3503–3510.

Barker, J., Scaife, H., & Brown, A. M. R. W. (1995). Intraphagocytic Growth Induces an Antibiotic-Resistant Phenotype of Legionella pneumophila. *ANTIMICROBIAL AGENTS AND CHEMOTHERAPY*, *39*(12), 2684–2688. https://journals.asm.org/journal/aac

Basher, M. H. A., Ithoi, I., Mahmud, R., Abdulsalam, A. M., Foead, A. I., Dawaki, S., Atroosh, W. M. M., Nissapatorn, V., & Abdullah, W. O. (2018). Occurrence of Acanthamoeba genotypes in Central West Malaysian environments. *Acta Tropica*, *178*, 219–228. https://doi.org/10.1016/j.actatropica.2017.11.015

Beattie, T. K., & Tomlinson, A. (2009). The Effect of Surface Treatment of Silicone Hydrogel Contact Lenses on the Attachment of Acanthamoeba castellanii Trophozoites. *Eye & Contact Lens: Science & Clinical Practice*, *35*(6), 316–319. https://doi.org/10.1097/ICL.0b013e3181becce6

Becker-Finco, A., Costa, A. O., Silva, S. K., Ramada, J. S., Furst, C., Stinghen, A. E., De Figueiredo, B. C., De Moura, J., & Alvarenga, L. M. (2013). Physiological, morphological, and immunochemical parameters used for the characterization of clinical and environmental isolates of Acanthamoeba. *Parasitology*, *140*(3), 396–405. https://doi.org/10.1017/S0031182012001746

Behera, H. S., Satpathy, G., & Tripathi, M. (2016). Isolation and genotyping of Acanthamoeba spp. from Acanthamoeba meningitis/ meningoencephalitis (AME) patients in India. *Parasites and Vectors*, *9*(1). https://doi.org/10.1186/s13071-016-1729-5

Booton, G. C., Joslin, C. E., Shoff, M., Tu, E. Y., Kelly, D. J., & Fuerst, P. A. (2009). Genotypic identification of acanthamoeba sp. isolates associated with an outbreak of acanthamoeba keratitis. *Cornea*, *28*(6), 673–676. https://doi.org/10.1097/ICO.0b013e31819342a7

Booton, G. C., Kelly, D. J., Chu, Y. W., Seal, D. V., Houang, E., Lam, D. S. C., Byers, T. J., & Fuerst, P. A. (2002). 18S ribosomal DNA typing and tracking of Acanthamoeba species isolates from corneal scrape specimens, contact lenses, lens cases, and home water supplies of Acanthamoeba keratitis patients in Hong Kong. *Journal of Clinical Microbiology*, *40*(5), 1621–1625. https://doi.org/10.1128/JCM.40.5.1621-1625.2002

Booton, G. C., Rogerson, A., Bonilla, T. D., Seal, D. V., Kelly, D. J., Beattie, T. K., Tomlinson, A., Lares-Villa, F., Fuerst, P. A., & Byers, T. J. (2004). Molecular and physiological evaluation of subtropical environmental isolates of Acanthamoeba spp., causal agent of Acanthamoeba keratitis. *Journal of Eukaryotic Microbiology*, *51*(2), 192–200. https://doi.org/10.1111/j.1550-7408.2004.tb00545.x

Booton, G. C., Visvesvara, G. S., Byers, T. J., Kelly, D. J., & Fuerst, P. A. (2005). Identification and distribution of Acanthamoeba species genotypes associated with nonkeratitis infections. *Journal of Clinical Microbiology*, *43*(4), 1689–1693. https://doi.org/10.1128/JCM.43.4.1689-1693.2005

Bowers, B., & Korn, E. D. (1968). THE FINE STRUCTURE OF ACANTHAMOEBA CASTELLANII I. The Trophozoite. *THE JOURNAL OF CELL BIOLOGY*, *39*, 95–111.

Bowers, B., & Korn, E. D. (1969). THE FINE STRUCTURE OF ACANTHAMOEBA CASTELLANII (NEFF STRAIN) II. Encystment. *THE JOURNAL OF CELL BIOLOGY*, *41*, 786–805.

Bowers, B., & Olszewski, T. E. (1983). Digestible and Discriminates Internally Indigestible Particles between. *THE JOURNAL OF CELL BIOLOGY*, *97*, 317–322.

Brocious, J., Tarver, M. E., Hampton, D., & Eydelman, M. (2018). Acanthamoeba: An overview of the challenges to the development of a consensus methodology of disinfection efficacy testing for contact lens care products. *Eye and Contact Lens*, *44*(6), 351–354. https://doi.org/10.1097/ICL.0000000000000470

Brondfield, M. N., Reid, M. J. A., Rutishauser, R. L., Cope, J. R., Tang, J., Ritter, J. M., Matanock, A., Ali, I., Doernberg, S. B., Hilts-Horeczko, A., DeMarco, T., Klein, L., & Babik, J. M. (2017). Disseminated Acanthamoeba infection in a heart transplant recipient treated successfully with a miltefosine-containing regimen: Case report and review of the literature. *Transplant Infectious Disease*, *19*(2). https://doi.org/10.1111/tid.12661

Brown, A. C., Ross, J., Jones, D. B., Collier, S. A., Ayers, T. L., Hoekstra, R. M., Backensen, B., Roy, S. L., Beach, M. J., & Yoder, J. S. (2018). Risk Factors for Acanthamoeba Keratitis-A Multistate Case-Control Study, 2008-2011. *Eye & Contact Lens*, *44*, S173–S178. https://doi.org/10.1097/ICL.0000000000000365

Büchele, M. L. C., Nunes, B. F., Filippin-Monteiro, F. B., & Caumo, K. S. (2023). Diagnosis and treatment of Acanthamoeba Keratitis: A scoping review demonstrating unfavorable outcomes. *Contact Lens and Anterior Eye*, *46*, 1–8. https://doi.org/10.1016/j.clae.2023.101844

Buchele, M. L. C., Wopereis, D. B., Casara, F., de Macedo, J. P., Rott, M. B., Monteiro, F. B. F., Bazzo, M. L., dos Reis Spada, F., dos Santos, J. I., & Caumo, K. S. (2018). Contact lens-related polymicrobial keratitis: Acanthamoeba spp. genotype T4 and Candida albicans. *Parasitology Research*, *117*(11), 3431–3436. https://doi.org/10.1007/s00436-018-6037-x

Buerano, C. C., Trinidad, A. D., Fajardo, L. S. N., Cua, I. Y., Baclig, M. O., & Natividad, F. F. (2014). Isolation of acanthamoeba genotype t4 from a non-contact lens wearer from the Philippines. *Tropical Medicine and Health*, *42*(4), 145–147. https://doi.org/10.2149/tmh.2014-15

Campolo, A., Pifer, R., Shannon, P., & Crary, M. (2022). Microbial Adherence to Contact Lenses and Pseudomonas aeruginosa as a Model Organism for Microbial Keratitis. *Pathogens*, *11*, 1–15. https://doi.org/10.3390/xxxxx

Cao, Z., Jefferson, D. M., & Panjwani, N. (1998). Role of Carbohydrate-mediated Adherence in Cytopathogenic Mechanisms of Acanthamoeba* Characterization of the Carbohydrate-binding Specificity of Acanthamoeba Lectin. *THE JOURNAL OF BIOLOGICAL CHEMISTRY*, *273*(25), 15838–15845. http://www.jbc.org

Carnt, N., Minassian, D. C., & Dart, J. K. G. (2023). Acanthamoeba Keratitis Risk Factors for Daily Wear Contact Lens Users: A Case–Control Study. *Ophthalmology*, *130*(1), 48–55. https://doi.org/10.1016/j.ophtha.2022.08.002

Carnt, N., Montanez, V. M., Galatowicz, G., Veli, N., & Calder, V. (2017). Tear Cytokine Levels in Contact Lens Wearers With Acanthamoeba Keratitis. *Cornea*, *36*(7), 791–798. https://doi.org/10.1097/ICO.0000000000001238

Carnt, N., & Stapleton, F. (2016). Strategies for the prevention of contact lens-related Acanthamoeba keratitis: A review. *Ophthalmic and Physiological Optics*, *36*(2), 77–92. https://doi.org/10.1111/opo.12271

Carter, R. F. (1970). Description of a Naegleria sp. isolated from two cases of primary amoebic meningo-encephalitis, and of the experimental pathological changes induced by it. *The Journal of Pathology*, *100*(4), 217–244. https://doi.org/10.1002/path.1711000402

Carter, W., Gompf, S., Toney, J., Greene, J., & Cutolo, E. (2004). Disseminated Acanthamoeba Sinusitis in a Patient with AIDS: A Possible Role for Early Antiretroviral Therapy Patient care View project Review of Appendicitis in Neutropenic Patients View project. *The AIDS Reader*, *14*, 41–49. https://www.researchgate.net/publication/7864431

Chagla, A. H., & Griffiths, A. J. (1974). Growth and Encystation of Acanthamoeba castellanii. *Journal of General Microbio/Ogy*, *85*, 139–145.

Chan, T. C. Y., Li, E. Y. M., Wong, V. W. Y., & Jhanji, V. (2014). Orthokeratology-associated infectious keratitis in a tertiary care eye hospital in Hong Kong. *American Journal of Ophthalmology*, *158*(6), 1130-1135.e2. https://doi.org/10.1016/j.ajo.2014.08.026

Chandrasekar, P. H., Nandi, P. S., Fairfax, M. R., & Crane, L. R. (1997). Cutaneous infections due to Acanthamoeba in patients with acquired immunodeficiency syndrome. *Archives of Internal Medicine*, *157*(5), 569–572.

Chávez-Munguía, B., Omaña-Molina, M., Castañón, G., Bonilla, P., González-Lázaro, M., Hernández-Martínez, D., Salazar-Villatoro, L., Esparza-García, A., Martínez-Palomo, A., & Ortega-Pierres, G. (2009). Ultrastructural study of the encystation and excystation processes in Naegleria sp. *Journal of Eukaryotic Microbiology*, *56*(1), 66–72. https://doi.org/10.1111/j.1550-7408.2008.00372.x

Chin, J., Young, A. L., Hui, M., & Jhanji, V. (2015). Acanthamoeba keratitis: 10-Year study at a tertiary eye care center in Hong Kong. *Contact Lens and Anterior Eye*, *38*(2), 99–103. https://doi.org/10.1016/j.clae.2014.11.146

Cho, J. H., Na, B. K., Kim, T. S., & Song, C. Y. (2000). Purification and characterization of an extracellular serine proteinase from Acanthamoeba castellanii. *IUBMB Life*, *50*(3), 209–214. https://doi.org/10.1080/152165400300001534

Chynn, E. W., Lopez, M. A., Pavan-Langston, D., & Talamo, J. H. (1995). Acanthamoeba Keratitis Contact Lens and Noncontact Lens Characteristics. *Ophthalmology*, *102*, 1369–1373.

Cirillo, J. D., Falkow, † Stanley, Tompkins, L. S., & Bermudez, L. E. (1997). Interaction of Mycobacterium avium with Environmental Amoebae Enhances Virulence. *INFECTION AND IMMUNITY*, *65*(9), 3759–3767.

Cirillo, J. D., Falkow, S., & Tompkins, L. S. (1994). Growth of Legionella pneumophila in Acanthamoeba castellanii Enhances Invasion. *INFECTION AND IMMUNITY*, 3254–3261. https://journals.asm.org/journal/iai

Clarke, D. W., & Niederkorn, J. Y. (2006). The pathophysiology of Acanthamoeba keratitis. *Trends in Parasitology*, *22*(4), 175–180. https://doi.org/10.1016/j.pt.2006.02.004

Clarke, M., Lohan, A. J., Liu, B., Lagkouvardos, I., Roy, S., Zafar, N., Bertelli, C., Schilde, C., Kianianmomeni, A., Bürglin, T. R., Frech, C., Turcotte, B., Kopec, K. O., Synnott, J. M., Choo, C., Paponov, I., Finkler, A., Heng Tan, C. S., Hutchins, A. P., … Loftus, B. J. (2013). Genome of Acanthamoeba castellanii highlights extensive lateral gene transfer and early evolution of tyrosine kinase signaling. *Genome Biology*, *14*(2), R11. https://doi.org/10.1186/gb-2013-14-2-r11

Connelly, L., Anijeet, D., Tole, D., & Alexander, C. L. (2023). Acanthamoeba keratitis: Molecular typing of Acanthamoeba species directly from ocular tissue. *Current Research in Parasitology and Vector-Borne Diseases*, *4*. https://doi.org/10.1016/j.crpvbd.2023.100141

Cope, J. R., Collier, S. A., Rao, M. M., Chalmers, R., Lynn Mitchell, ; G, Richdale, K., Wagner, H., Kinoshita, B. T., Lam, D. Y., Sorbara, L., Zimmerman, A., Yoder, J. S., & Beach, M. J. (2015).

Contact Lens Wearer Demographics and Risk Behaviors for Contact Lens-Related Eye Infections - US, 2014. *MMWR Morb Mortal Wkly Rep*, *64*(32), 865–870. http://www.cdc.gov/mmwr/cme/conted_info.html#weekly.http://www.cdc.gov/contactlenses.

Cordingley, J. S., & Trzyna, W. C. (2008). Multiple Factors Affecting Growth and Encystment of Acanthamoeba castellanii in Axenic Culture Endocytosis View project Signal transduction View project. *Acta Protozoologica*, *47*, 307–316. http://www.hgsc.bcm.tmc.edu/

Corsaro, D. (2020). Update on Acanthamoeba phylogeny. *Parasitology Research*, *119*, 3327–3338. https://doi.org/10.1007/s00436-020-06843-9/Published

Corsaro, D. (2021). On the diversity and clinical importance of Acanthamoeba spp. from Group 1. *Parasitology Research*, *120*, 2057–2064. https://doi.org/10.1007/s00436-021-07171-2/Published

Corsaro, D. (2022). Acanthamoeba Mannose and Laminin Binding Proteins Variation across Species and Genotypes. *Microorganisms*, *10*(11). https://doi.org/10.3390/microorganisms10112162

Corsaro, D., & Venditti, D. (2023). Molecular evidence for a new lineage within the Acanthamoeba T4 genotype. *Parasitology Research*, *122*(6), 1445–1450. https://doi.org/10.1007/s00436-023-07844-0

Corsaro, D., Walochnik, J., Köhsler, M., & Rott, M. B. (2015). Acanthamoeba misidentification and multiple labels: redefining genotypes T16, T19, and T20 and proposal for Acanthamoeba micheli sp. nov. (genotype T19). *Parasitology Research*, *114*(7), 2481–2490. https://doi.org/10.1007/s00436-015-4445-8

Costas, M., & Griffiths, A. J. . (1985). Enzyme Composition and the Taxonomy of Acanthamoeba. *The Journal of Protozoology*, *32*(4), 604–607. https://doi.org/10.1111/j.1550-7408.1985.tb03086.x

Coven, S. L., Song, E., Steward, S., Pierson, C. R., Cope, J. R., Ali, I. K., Ardura, M. I., Hall, M. W., Chung, M. G., & Bajwa, R. P. S. (2017). Acanthamoeba granulomatous amoebic encephalitis after pediatric hematopoietic stem cell transplant. *Pediatric Transplantation*, *21*(8). https://doi.org/10.1111/petr.13060

Cruz, A. R. S., & Rivera, W. L. (2014). Genotype analysis of Acanthamoeba isolated from human nasal swabs in the Philippines. *Asian Pacific Journal of Tropical Medicine*, *7S1*, S74-8. https://doi.org/10.1016/S1995-7645(14)60206-6

Cursons, R. T. M., & Brown, T. J. (1978). Use of cell cultures as an indicator of pathogenicity of free-living amoebae. *Journal of Clinical Pathology*, *31*, 1–11.

Cursons, R. T. M., Brown, T. J., Keys, E. A., Moriarty, K. M., & Till, D. (1980). Immunity to Pathogenic Free-Living Amoebae: Role of Humoral Antibody. *INFECTION AND IMMUNITY*, *29*(2), 401–407. https://journals.asm.org/journal/iai

Da Rocha-Azevedo, B., & Costa E Silva-Filho, F. (2007). Biological characterization of a clinical and an environmental isolate of Acanthamoeba polyphaga: Analysis of relevant parameters to decode pathogenicity. *Archives of Microbiology*, *188*(5), 441–449. https://doi.org/10.1007/s00203-007-0264-3

Da Rocha-Azevedo, B., Jamerson, M., Cabral, G. A., & Marciano-Cabral, F. (2010). Acanthamoeba culbertsoni: Analysis of amoebic adhesion and invasion on extracellular matrix components collagen I and laminin-1. *Experimental Parasitology*, *126*(1), 79–84. https://doi.org/10.1016/j.exppara.2009.08.004

Da Rocha-Azevedo, B., Jamerson, M., Cabral, G. A., Silva-Filho, F. C., & Marciano-Cabral, F. (2009). Acanthamoeba interaction with extracellular matrix glycoproteins: Biological and biochemical characterization and Role in Cytotoxicity and Invasiveness. *Journal of Eukaryotic Microbiology*, *56*(3), 270–278. https://doi.org/10.1111/j.1550-7408.2009.00399.x

Dabbagh, K., & Lewis, D. B. (2003). Toll-like receptors and T-helper-1/T-helper-2 responses. *Current Opinion in Infectious Diseases*, *16*(3), 199–204. https://doi.org/10.1097/00001432-200306000-00003

De Jonckheere. (1983). Isoenzyme and Total Protein Analysis by Agarose Isoelectric Focusing, and Taxonomy of the Genus Acanthamoeba. *The Journal of Protozoology*, *30*(4), 701–706. https://doi.org/10.1111/j.1550-7408.1983.tb05346.x

De Jonckheere, J. (1977). Use of an Axenic Medium for Differentiation Between Pathogenic and Nonpathogenic Naegleria fowleri Isolates. *APPLIED AND ENVIRONMENTAL MICROBIOLOGY*, *33*(4), 751–757.

De Jonckheere, J. F. (1979). Occurrence of Naegleria and Acanthamoeba in Aquaria. *APPLIED AND ENVIRONMENTAL MICROBIOLOGY*, *38*(4), 590–593.

De Jonckheere, J. F. (1980). Growth Characteristics, Cytopathic Effect in Cell Culture, and Virulence in Mice of 36 Type Strains Belonging to 19 Different Acanthamoeba spp. *APPLIED AND ENVIRONMENTAL MICROBIOLOGY*, *39*(4), 681–685.

De Jonckheere, J. F. (1991). Ecology of Acanthamoeba. *Reviews of Infectious Diseases*, *13 Suppl 5*, S385-7. https://doi.org/10.1093/clind/13.supplement_5.s385

De Jonckheere, J., & Van De Voorde, H. (1976). Differences in Destruction of Cysts of Pathogenic and Nonpathogenic Naegleria and Acanthamoeba by Chlorine. *APPLIED AND ENVIRONMENTAL MICROBIOLOGY*, 294–297.

de Lacerda, A. G., & Lira, M. (2021). Acanthamoeba keratitis: a review of biology, pathophysiology and epidemiology. *Ophthalmic and Physiological Optics*, *41*(1), 116–135. https://doi.org/10.1111/opo.12752

de St. Vincent, B. (1822). Amibe. *Dict. Class d'Hist. Nat.*, *1*, 260–262.

Deepak, S. A., Kottapalli, K. R., Rakwal, R., Oros, G., Rangappa, K. S., Iwahashi, H., Masuo, Y., & Agrawal, G. K. (2007). Real-Time PCR: Revolutionizing Detection and Expression Analysis of Genes. In *Current Genomics* (Vol. 8).

Deluoi, A., Teilhac, M., Poirot, J., Maslo, C., Luboinski, J., Rozenbaum, W., & Chatelet, F. (1996). Cutaneous Lesions Due to Acanthamoeba sp in a Patient with AIDS. *Journal of Eukaryotic Microbiology*, *43*(5). https://doi.org/10.1111/j.1550-7408.1996.tb05043.x

Derda, M., Winiecka-Krusnell, J., Linder, M. B., & Linder, E. (2009). Labeled Trichoderma reesei cellulase as a marker for Acanthamoeba cyst wall cellulose in infected tissues. *Applied and Environmental Microbiology*, *75*(21), 6827–6830. https://doi.org/10.1128/AEM.01555-09

Derda, M., Wojtkowiak-Giera, A., & Hadaś, E. (2014). Comparative analyses of different genetic markers for the detection of Acanthamoeba spp. isolates. *Acta Parasitologica*, *59*(3), 472–477. https://doi.org/10.2478/s11686-014-0267-6

Dini, L. A., Cockinos, C., Frean, J. A., Niszl, I. A., & Markus, M. B. (2000). Unusual Case of Acanthamoeba polyphaga and Pseudomonas aeruginosa Keratitis in a Contact Lens Wearer from Gauteng, South Africa. *JOURNAL OF CLINICAL MICROBIOLOGY*, *38*(2), 826–829.

Doyscher, D., Fieseler, L., Dons, L., Loessner, M. J., & Schuppler, M. (2013). Acanthamoeba feature a unique backpacking strategy to trap and feed on Listeria monocytogenes and other motile bacteria. *Environmental Microbiology*, *15*(2), 433–446. https://doi.org/10.1111/j.1462-2920.2012.02858.x

Dudley, R., Jarroll, E. L., & Khan, N. A. (2009). Carbohydrate analysis of Acanthamoeba castellanii. *Experimental Parasitology*, *122*(4), 338–343. https://doi.org/10.1016/j.exppara.2009.04.009

Duggal, S. D., Rongpharpi, S. R., Kumar Duggal, A., Kumar, A., Biswal, I., Duggal, A. K., & Neurology, D. M. (2017). Role of Acanthamoeba in Granulomatous Encephalitis: A Review. *J Infect Dis Immune Ther*, *1*(1).

Dujardin, F. (1838). Recherches sur les organisms inférieurs. *Ann Sco Nat Zool.*, *2*, 343–377.

Dykova, I., Lomn, J., Schroeder-Diedrich, J. M., Booton, G. C., & Byers, T. J. (1999). ACANTHAMOEBA STRAINS ISOLATED FROM ORGANS OF FRESHWATER FISHES. *Amoebae, Including Acanthamoeba (Fig*, *85*(6), 1106–1113. www.biosci.

Efron, N., Young, G., & Brennan, N. A. (1989). Ocular surface temperature. *Current Eye Research*, *8*(9), 901–906.

Ehrenberg, G. C. (1838). Die Infusionsthierchen als vollkommene Organismen. Ein Blick in das tiefere organische Leben der Natur I+II. *L. Voss. Leipzig*, 547.

Elkadery, A. A. S., Elsherif, E. A., Ezz Eldin, H. M., Fahmy, I. A. F., & Mohammad, O. S. (2019). Efficient therapeutic effect of Nigella sativa aqueous extract and chitosan nanoparticles against experimentally induced Acanthamoeba keratitis. *Parasitology Research*, *118*(8), 2443–2454. https://doi.org/10.1007/s00436-019-06359-x

El-Zayat, S. R., Sibaii, H., & Mannaa, F. A. (2019). Toll-like receptors activation, signaling, and targeting: an overview. *Bulletin of the National Research Centre*, *43*(1). https://doi.org/10.1186/s42269-019-0227-2

Fanselow, N., Sirajuddin, N., Yin, X. T., Huang, A. J. W., & Stuart, P. M. (2021). Acanthamoeba keratitis, pathology, diagnosis and treatment. *Pathogens*, *10*(3), 1–11. https://doi.org/10.3390/pathogens10030323

Feng, X., Zheng, W., Wang, Y., Zhao, D., Jiang, X., & Lv, S. (2015). A Rabbit Model of Acanthamoeba Keratitis That Better Reflects the Natural Human Infection. *Anatomical Record*, *298*(8), 1509–1517. https://doi.org/10.1002/ar.23154

Fouzder, C., Mukhuty, A., Das, S., & Chattopadhyay, D. (2018). TLR Signaling on Protozoan and Helminthic Parasite Infection. In *Toll-like Receptors*. www.intechopen.com

Fritsche, T. R., Gautom, R. K., Seyedirashti, S., Bergeron, D. L., And, I., & Lindquist2, T. D. (1993). Occurrence of Bacterial Endosymbionts in Acanthamoeba spp. Isolated from Corneal and Environmental Specimens and Contact Lenses. *JOURNAL OF CLINICAL MICROBIOLOGY*, *31*(5), 1122–1126.

Fritsche, T. R., Horn, M., Wagner, M., Herwig, R. P., Schleifer, K.-H., & Gautom, R. K. (2000). Phylogenetic Diversity among Geographically Dispersed Chlamydiales Endosymbionts Recovered from Clinical and Environmental Isolates of Acanthamoeba spp. *APPLIED AND ENVIRONMENTAL MICROBIOLOGY*, *66*(6), 2613–2619. https://journals.asm.org/journal/aem

Fritsche, T. R., Sobek, D., & Gautom, R. K. (1998). Enhancement of in vitro cytopathogenicity by Acanthamoeba spp. following acquisition of bacterial endosymbionts. *FEMS Microbiology Letters*, *166*(2), 231–236. https://doi.org/10.1111/j.1574-6968.1998.tb13895.x

Fuerst, P. A. (2014). Insights from the DNA databases: Approaches to the phylogenetic structure of Acanthamoeba. *Experimental Parasitology*, *145*(S), S39–S45. https://doi.org/10.1016/j.exppara.2014.06.020

Fuerst, P. A., Booton, G. C., & Crary, M. (2015). Phylogenetic Analysis and the Evolution of the 18S rRNA Gene Typing System of Acanthamoeba. *Journal of Eukaryotic Microbiology*, *62*(1), 69–84. https://doi.org/10.1111/jeu.12186

Garate, M., Cao, Z., Bateman, E., & Panjwani, N. (2004). Cloning and characterization of a novel mannose-binding protein of Acanthamoeba. *Journal of Biological Chemistry*, *279*(28), 29849–29856. https://doi.org/10.1074/jbc.M402334200

Garate, M., Cubillos, I., Marchant, J., & Panjwani, N. (2005). Biochemical characterization and functional studies of Acanthamoeba mannose-binding protein. *Infection and Immunity*, *73*(9), 5775–5781. https://doi.org/10.1128/IAI.73.9.5775-5781.2005

Garate, M., Marchant, J., Cubillos, I., Cao, Z., Khan, N. A., & Panjwani, N. (2006). In vitro pathogenicity of Acanthamoeba is associated with the expression of the mannose-binding protein. *Investigative Ophthalmology and Visual Science*, *47*(3), 1056–1062. https://doi.org/10.1167/iovs.05-0477

Garg, P., Kalra, P., & Joseph, J. (2017). Non-contact lens related Acanthamoeba keratitis. *Indian Journal of Ophthalmology*, *65*(11), 1079. https://doi.org/10.4103/ijo.IJO_826_17

Garibyan, L., & Avashia, N. (2013). Polymerase chain reaction. *Journal of Investigative Dermatology*, *133*(3), 1–4. https://doi.org/10.1038/jid.2013.1

Gast, R. J., Ledee, D. R., Fuerst, P. A., & Byers, T. J. (1996). Subgenus Systematics of Acanthamoeba: Four Nuclear 18S rDNA Sequence Types. *Journal of Eukaryotic Microbiology*, *43*(6), 498–504. https://doi.org/10.1111/j.1550-7408.1996.tb04510.x

Geith, S., Walochnik, J., Prantl, F., Sack, S., & Eyer, F. (2018). Lethal outcome of granulomatous acanthamoebic encephalitis in a man who was human immunodeficiency virus-positive: A case report. *Journal of Medical Case Reports*, *12*(1). https://doi.org/10.1186/s13256-018-1734-8

Gianinazzi, C., Schild, M., Wüthrich, F., Müller, N., Schürch, N., & Gottstein, B. (2009). Potentially human pathogenic Acanthamoeba isolated from a heated indoor swimming pool in Switzerland. *Experimental Parasitology*, *121*(2), 180–186. https://doi.org/10.1016/j.exppara.2008.11.001

Gomes, T. D. S., Magnet, A., Izquierdo, F., Vaccaro, L., Redondo, F., Bueno, S., Sánchez, M. L., Angulo, S., Fenoy, S., Hurtado, C., & Aguila, C. Del. (2016). Acanthamoeba spp. in Contact Lenses from Healthy Individuals from Madrid, Spain. *PLoS ONE*, *11*(4). https://doi.org/10.1371/journal.pone.0154246

González-Robles, A., Castañón, G., Hernández-Ramírez, V. I., Salazar-Villatoro, L., González-Lázaro, M., Omaña-Molina, M., Talamás-Rohana, P., & Martínez-Palomo, A. (2008). Acanthamoeba castellanii: Identification and distribution of actin cytoskeleton. *Experimental Parasitology*, *119*(3), 411–417. https://doi.org/10.1016/j.exppara.2008.04.004

Gordon, D. J., Eisenberg, E., & Korn, E. D. (1976). Characterization of cytoplasmic actin isolated from Acanthamoeba castellanii by a new method. *The Journal of Biological Chemistry*, *251*(15), 4778–4786.

Gordon, S., Plüddemann, A., & Martinez Estrada, F. (2014). Macrophage heterogeneity in tissues: phenotypic diversity and functions. *Immunological Reviews*, *262*, 36–55.

Gray, T. B., Cursons, R. T. M., Sherwan, J. F., Rose, P. R., & Gray, T. B. (1995). Acanthamoeba, bacterial, and fungal contamination of contact lens storage cases. *British Journal of Ophthalmology*, *79*, 601–605.

Greub, G., & Raoult, D. (2002). Parachlamydiaceae: Potential Emerging Pathogens. *Emerging Infectious Diseases* •, *8*(6).

Griffin, J. L. (1972). Temperature Tolerance of Pathogenic and Nonpathogenic Free-Living Amoebas. *Science*, *178*(4063), 869–870. https://doi.org/10.1126/science.178.4063.869

Gu, X., Lu, X., Lin, S., Shi, X., Shen, Y., Lu, Q., Yang, Y., Yang, J., Cai, J., Fu, C., Lou, Y., & Zheng, M. (2022). A Comparative Genomic Approach to Determine the Virulence Factors and Horizontal Gene Transfer Events of Clinical Acanthamoeba Isolates. *Microbiology Spectrum*, *10*(2). https://doi.org/10.1128/spectrum.00025-22

Gueudry, J., Goff, L. Le, Compagnon, P., Lefevre, S., Colasse, E., Aknine, C., Duval, F., François, A., Razakandrainibe, R., Ballet, J. J., Muraine, M., & Favennec, L. (2018). Evaluation of voriconazole anti-Acanthamoeba polyphaga in vitro activity, rat cornea penetration and efficacy against experimental rat Acanthamoeba keratitis. *Journal of Antimicrobial Chemotherapy*, *73*(7), 1895–1898. https://doi.org/10.1093/jac/dky094

Gunderson, J. H., & Sogin, M. L. (1986). Length variation in eukaryotic rRNAs: small subunit rRNAs from the protists Acanthamoeba castellanii and Euglena gracilis. *Gene*, *44*(1), 63–70. https://doi.org/10.1016/0378-1119(86)90043-0

Hadaś, E., Derda, M., & Cholewiński, M. (2017). Evaluation of the effectiveness of tea tree oil in treatment of Acanthamoeba infection. *Parasitology Research*, *116*(3), 997–1001. https://doi.org/10.1007/s00436-017-5377-2

Hadaś, E., & Mazur, T. (1993). Biochemical markers of pathogenicity and virulence of Acanthamoeba sp. strains. *Parasitology Research*, *79*(8), 696–698. https://doi.org/10.1007/BF00932513

Hames, B. D. (1998). An introduction to polyacrylamide gel electrophoresis. *ISMN*, *39*.

Harrison, W. T., Lecky, B., & Hulette, C. M. (2018). Fatal granulomatous amebic encephalitis in a heart transplant patient: Clinical, radiographic, and autopsy findings. *Journal of Neuropathology and Experimental Neurology*, *77*(11), 1001–1004. https://doi.org/10.1093/jnen/nly089

Hassan, F. A., Tolba, M., Omar, H., Abdel-Hakeem, S. S., & Abed, G. H. (2022). Isolation and identification of free-living amoeba from contact lenses: Thermal and osmotic tolerance in relation to their pathogenicity. *Assiut University Journal of Multidisciplinary Scientific Research (AUNJMSR)*, *51*(1), 40–56. https://www.researchgate.net/publication/360860868

Hong, Y. C., Lee, W. M., Kong, H. H., Jeong, H. J., & Chung, D. Il. (2004). Molecular cloning and characterization of a cDNA encoding a laminin-binding protein (AhLBP) from Acanthamoeba healyi. *Experimental Parasitology*, *106*(3–4), 95–102. https://doi.org/10.1016/j.exppara.2004.01.011

Horn, M., Fritsche, T. R., Gautom, R. K., Schleifer, K. H., & Wagner, M. (1999). Novel bacterial endosymbionts of Acanthamoeba spp. related to the Paramecium caudatum symbiont Caedibacter caryophilus. *Environmental Microbiology*, *1*(4), 357–367. https://doi.org/10.1046/j.1462-2920.1999.00045.x

Horn, M., Harzenetter, M. D., Linner, T., Schmid, E. N., Müller, K. D., Michel, R., & Wagner, M. (2001). Members of the Cytophaga-Flavobacterium-Bacteroides phylum as intracellular bacteria of Acanthamoebae: Proposal of "Candidatus Amoebophilus asiaticus." *Environmental Microbiology*, *3*(7), 440–449. https://doi.org/10.1046/j.1462-2920.2001.00210.x

Hurt, M., Apte, S., Leher, H., Howard, K., Niederkorn, J., & Alizadeh, H. (2001). Exacerbation of acanthamoeba keratitis in animals treated with anti-macrophage inflammatory protein 2 or antineutrophil antibodies. *Infection and Immunity*, *69*(5), 2988–2995. https://doi.org/10.1128/IAI.69.5.2988-2995.2001

Hurt, M., Neelam, S., Niederkorn, J., & Alizadeh, H. (2003). Pathogenic Acanthamoeba spp. Secrete a Mannose-Induced Cytolytic Protein that Correlates with the Ability to Cause Disease. *Infection and Immunity*, *71*(11), 6243–6255. https://doi.org/10.1128/IAI.71.11.6243-6255.2003

Hurt, M., Niederkorn, J., & Alizadeh, H. (2003). Effects of mannose on Acanthamoeba castellanii proliferation and cytolytic ability to corneal epithelial cells. *Investigative Ophthalmology and Visual Science*, *44*(8), 3424–3431. https://doi.org/10.1167/iovs.03-0019

Huth, S., Reverey, J. F., Leippe, M., & Selhuber-Unkel, C. (2017). Adhesion forces and mechanics in mannose-mediated acanthamoeba interactions. *PLoS ONE*, *12*(5). https://doi.org/10.1371/journal.pone.0176207

Ibrahim, Y. W., Boase, D. L., & Cree, I. A. (2009). How could contact lens wearers be at risk of Acanthamoeba infection? A review. *Journal of Optometry*, *2*(2), 60–66. https://doi.org/10.3921/joptom.2009.60

Illingworth, C. D., Cook, S. D., Karabatsas, C. H., & Easty, D. L. (1995). Acanthamoeba keratitis: risk factors and outcome. *BrJ' Ophthalmol*, *79*, 1078–1082.

Im, K., & Kim, D.-S. (1998). Acanthamoebiasis in Korea: two new cases with clinical cases review. *Yonsei Medical Journal*, *39*(5), 478–484.

Jiang, C., Sun, X., Wang, Z., & Zhang, Y. (2015). Acanthamoeba Keratitis: Clinical Characteristics and Management. *Elsevier*, *13*(2), 164–168. www.theocularsurface.com

Johnston, S. P., Sriram, R., Qvarnstrom, Y., Roy, S., Verani, J., Yoder, J., Lorick, S., Roberts, J., Beach, M. J., & Visvesvara, G. (2009). Resistance of Acanthamoeba cysts to disinfection in multiple contact lens solutions. *Journal of Clinical Microbiology*, *47*(7), 2040–2045. https://doi.org/10.1128/JCM.00575-09

Judelson, H., & Al-Mohanna, M. T. (2014). *GUIDELINES FOR DESIGNING PRIMERS*. https://www.researchgate.net/publication/315832536

Kaiserman, I., Bahar, I., McAllum, P., Srinivasan, S., Elbaz, U., Slomovic, A. R., & Rootman, D. S. (2012). Prognostic factors in Acanthamoeba keratitis. *Canadian Journal of Ophthalmology*, *47*(3), 312–317. https://doi.org/10.1016/j.jcjo.2012.03.040

Kalra, S. K., Sharma, P., Shyam, K., Tejan, N., & Ghoshal, U. (2020). Acanthamoeba and its pathogenic role in granulomatous amebic encephalitis. *Experimental Parasitology*, *208*, 1–11. https://doi.org/10.1016/j.exppara.2019.107788

Kamel Abd Ghani, M., Yusof, S., Ahmad, N., Agm, K., Raja Muda Abdul Aziz, J., & Lumpur, K. (2005). *A case of trauma related Acanthamoeba keratitis Molecular characterization of Corynebacterium Diptheria View project Mas Cotek Research group View project A case of trauma related Acanthamoeba keratitis*. 58–60. https://www.researchgate.net/publication/7284668

Karaman, U., Koloren, Z., & Karanis, P. (2022). Survey and first report of Acanthamoeba T4 genotype in natural spring water resources in the Black Sea, Turkey. *Journal of Water and Health*, *20*(1), 193–204. https://doi.org/10.2166/WH.2021.250

Karsenti, N., Lau, R., Purssell, A., Chong-Kit, A., Cunanan, M., Gasgas, J., Tian, J., Wang, A., Ralevski, F., & Boggild, A. K. (2017). Development and validation of a real-time PCR assay for the detection of clinical acanthamoebae. *BMC Research Notes*, *10*(1). https://doi.org/10.1186/s13104-017-2666-x

Kaufman, A. R., & Tu, E. Y. (2022). Advances in the management of Acanthamoeba keratitis: A review of the literature and synthesized algorithmic approach: Advances in the Management of Acanthamoeba. *Ocular Surface*, *25*, 26–36. https://doi.org/10.1016/j.jtos.2022.04.003

Kaul, D. R., Lowe, L., Visvesvara, G. S., Farmen, S., Khaled, Y. A., & Yanik, G. A. (2008). Acanthamoeba infection in a patient with chronic graft-versus-host disease occurring during treatment with voriconazole. *Transplant Infectious Disease*, *10*(6), 437–441. https://doi.org/10.1111/j.1399-3062.2008.00335.x

Kawasaki, T., & Kawai, T. (2014). Toll-like receptor signaling pathways. *Frontiers in Immunology*, *5*, 1–8. https://doi.org/10.3389/fimmu.2014.00461

Keay, L., Edwards, K., & Stapleton, F. (2009). Signs, symptoms, and comorbidities in contact lens-related microbial keratitis. *Optometry and Vision Science : Official Publication of the American Academy of Optometry*, *86*(7), 803–809. https://doi.org/10.1097/OPX.0b013e3181ae1b69

Khan, N. A. (2006). Acanthamoeba: Biology and increasing importance in human health. *FEMS Microbiology Reviews*, *30*(4), 564–595. https://doi.org/10.1111/j.1574-6976.2006.00023.x

Khan, N. A., Jarroll, E. L., & Paget, T. A. (2001). Acanthamoeba can be differentiated by the polymerase chain reaction and simple plating assays. *Current Microbiology*, *43*(3), 204–208. https://doi.org/10.1007/s002840010288

Khan, N. A., Jarroll, E. L., Panjwani, N., Cao, Z., & Paget, T. A. (2000). Proteases as Markers for Differentiation of Pathogenic and Nonpathogenic Species of Acanthamoeba. *JOURNAL OF CLINICAL MICROBIOLOGY*, *38*(8), 2858–2861.

Kidney, D. D., & Kim, S. H. (1998). CNS Infections with Free-Living Amebas: Neuroimaging Findings. *AJR*, *171*, 809–812. www.ajronline.org

Kilvington, S. (1993). ACANTHAMOEBA TROPHOZOITE AND CYST ADHERENCE TO FOUR TYPES OF SOFT CONTACT LENS AND REMOVAL BY CLE ANING AGENTS. *Eye*, *7*, 535–538.

Kim, H. K., Ha, Y. R., Yu, H. S., Kong, H. H., & Chung, D. Il. (2003). Purification and characterization of a 33 kDa serine protease from Acanthamoeba lugdunensis KA/E2 isolated from a Korean keratitis patient. *The Korean Journal of Parasitology*, *41*(4), 189–196. https://doi.org/10.3347/kjp.2003.41.4.189

Kim, J. H., Matin, A., Shin, H. J., Park, H., Yoo, K. T., Yuan, X. Z., Kim, K. S., & Jung, S. Y. (2012). Functional roles of mannose-binding protein in the adhesion, cytotoxicity and phagocytosis of Acanthamoeba castellanii. *Experimental Parasitology*, *132*(2), 287–292. https://doi.org/10.1016/j.exppara.2012.08.007

Knickelbein, J. E., Kovarik, J., Dhaliwal, D. K., & Chu, C. T. (2013). Acanthamoeba keratitis: A clinicopathologic case report and review of the literature. *Human Pathology*, *44*(5), 918–922. https://doi.org/10.1016/j.humpath.2012.10.007

Koehsler, M., Walochnik, J., Michel, R., Lugauer, J., & Wylezich, C. (2007). Molecular identification and classification of Cochlonema euryblastum , a zoopagalean parasite of Thecamoeba quadrilineata . *Mycologia*, *99*(2), 215–221. https://doi.org/10.1080/15572536.2007.11832580

Köhsler, M. (2007). *Comparative studies on the genus Acanthamoeba: Discrimination, Encystment Behaviour, Pathogenicity and Drug Susceptibility.* [Dissertation]. University of Vienna.

Köhsler, M., Leitsch, D., Fürnkranz, U., Duchêne, M., Aspöck, H., & Walochnik, J. (2008). Acanthamoeba strains lose their abilities to encyst synchronously upon prolonged axenic culture. *Parasitology Research*, *102*(5), 1069–1072. https://doi.org/10.1007/s00436-008-0885-8

Köhsler, M., Mrva, M., & Walochnik, J. (2016). Acanthamoeba. In *Molecular Parasitology: Protozoan Parasites and their Molecules* (pp. 285–324). Springer-Verlag Wien. https://doi.org/10.1007/978-3-7091-1416-2_10

Kong, H. H. (2009). Molecular Phylogeny of Acanthamoeba. *Korean Journal of Parasitology*, *47*, S21–S28. https://doi.org/10.3347/kjp.2009.47.S.S21

Kong, H.-H., Park, J.-H., & Chung, D.-I. (1995). Interstrain polymorphisms of isoenzyme profiles and mitochondrial DNA fingerprints among seven strains assigned to Acanthamoeba polyphaga. *The Korean Journal of Parasitology*, *33*(4), 331–340.

Kot, K., Łanocha-Arendarczyk, N. A., & Kosik-Bogacka, D. I. (2018). Amoebas from the genus Acanthamoeba and their pathogenic properties. *Annals of Parasitology*, *64*(4), 299–308. https://doi.org/10.17420/ap6404.164

Kot, K., Łanocha-Arendarczyk, N., & Kosik-Bogacka, D. (2021). Immunopathogenicity of acanthamoeba spp. In the brain and lungs. *International Journal of Molecular Sciences*, *22*(3), 1–21. https://doi.org/10.3390/ijms22031261

Kurna, S. A., Sengor, T., Aki, S., & Agirman, Y. (2012). Ring keratitis due to topical anaesthetic abuse in a contact lens wearer. *Clinical and Experimental Optometry*, *95*(4), 457–459. https://doi.org/10.1111/j.1444-0938.2012.00712.x

Kuzman, T., Kutija, M. B., Juri, J., Jandroković, S., Škegro, I., Olujić, S. M., Kordić, R., & Cerovski, B. (2014). Lens wearers non-compliance-Is there an association with lens case contamination? *Contact Lens and Anterior Eye*, *37*(2), 99–105. https://doi.org/10.1016/j.clae.2013.08.004

Lakhundi, S., Siddiqui, R., & Khan, N. A. (2017). Pathogenesis of microbial keratitis. *Microbial Pathogenesis*, *104*, 97–109. https://doi.org/10.1016/j.micpath.2016.12.013

Lalitha, M. K., Anandi, V., Srivastava, A., Thomas, K., Cherian, A. M., & Chandi3, S. M. (1985). Isolation of Acanthamoeba culbertsoni from a Patient with Meningitis. *JOURNAL OF CLINICAL MICROBIOLOGY*, 666–667.

Lamien-Meda, A., Köhsler, M., & Walochnik, J. (2022). Real-Time PCR for the Diagnosis of Acanthamoeba Genotype T4. *Microorganisms*, *10*(7). https://doi.org/10.3390/microorganisms10071307

Larkin, D. F. P., & Easty, D. L. (1991). Experimental Acanthamoeba keratitis: II. Immunohistochemical evaluation. *British Lournal of Ophthalmology*, *75*, 421–424.

Larkin, D. F. P., Kilvington, S., Easty, D. L., & Larkin, M. D. F. P. (1990). Contamination of contact lens storage cases by Acanthamoeba and bacteria. *BritishJournal OfOphthalmology*, *74*, 133–135.

Lee, J. J., Hutner, S. H., & Bovee, E. C. (1985). *An Illustrated Guide to the Protozoa* (Vol. 32). https://doi.org/10.1111/j.1550-7408.1985.tb03119.x

Lee, S. M., Lee, J. E., Lee, D. I., & Yu, H. S. (2018). Adhesion of Acanthamoeba on cosmetic contact lenses. *Journal of Korean Medical Science*, *33*(4). https://doi.org/10.3346/jkms.2018.33.e26

Lee, S.-M., Lee, D.-I., Park, S.-H., Yu, H.-S., Lee, J.-E., & Lee, J.-S. (2017). Effect of Multipurpose Solution Combined With Autophagy Inhibitors on Adhesion of Acanthamoeba trophozoites to Silicone Hydrogel Contact Lenses. *Cornea*, *36*(12), 1538–1543. www.corneajrnl.com

Leher, H., Kinoshita, K., Alizadeh, H., Zaragoza, F. L., He, Y., & Niederkorn, J. (1998). Impact of Oral Immunization with Acanthamoeba Antigens on Parasite Adhesion and Corneal Infection. *Investigative Ophthalmology & Visual Science*, *39*(12), 2337–2343.

Leher, H., Silvany, R., Alizadeh, H., Huang, J., & Niederkorn, J. Y. (1998). Mannose Induces the Release of Cytopathic Factors from Acanthamoeba castellanii. *INFECTION AND IMMUNITY*, *66*(1), 5–10.

Leitsch, D., Köhsler, M., Marchetti-Deschmann, M., Deutsch, A., Allmaier, G., Duchêne, M., & Walochnik, J. (2010). Major role for cysteine proteases during the early phase of Acanthamoeba castellanii encystment. *Eukaryotic Cell*, *9*(4), 611–618. https://doi.org/10.1128/EC.00300-09

Lekkla, A., Sutthikornchai, C., Bovornkitti, S., & Sukthana, Y. (2005). Free-living ameba contamination in natural hot springs in Thailand. *The Southeast Asian Journal of Tropical Medicine and Public Health*, *36 Suppl 4*, 5–9.

Linder, M., Winiecka-Krusnell, J., & Linder, E. (2002). Use of recombinant cellulose-binding domains of Trichoderma reesei cellulase as a selective immunocytochemical marker for cellulose in protozoa. *Applied and Environmental Microbiology*, *68*(5), 2503–2508. https://doi.org/10.1128/AEM.68.5.2503-2508.2002

Lindsay, R. G., Watters, G., Johnson, R., Ormonde, S. E., & Snibson, G. R. (2007). Acanthamoeba keratitis and contact lens wear. *Clinical and Experimental Optometry*, *90*(5), 351–360. https://doi.org/10.1111/j.1444-0938.2007.00172.x

Litovchick, L. (2020). Immunoblotting. *Cold Spring Harbor Protocols*, *2020*(6), 098392. https://doi.org/10.1101/pdb.top098392

Lonnen, J., Putt, K. S., Kernick, E. R., Lakkis, C., May, L., & Pugh, R. B. (2014). The efficacy of acanthamoeba cyst kill and effects upon contact lenses of a novel ultraviolet lens disinfection system. *American Journal of Ophthalmology*, *158*(3). https://doi.org/10.1016/j.ajo.2014.05.032

Lorenzo-Morales, J., Khan, N. A., & Walochnik, J. (2015). An update on Acanthamoeba keratitis: Diagnosis, pathogenesis and treatment. *Parasite*, *22*. https://doi.org/10.1051/parasite/2015010

Lorenzo-Morales, J., Kliescikova, J., Martinez-Carretero, E., De Pablos, L. M., Profotova, B., Nohynkova, E., Osuna, A., & Valladares, B. (2008). Glycogen phosphorylase in Acanthamoeba spp.: Determining the role of the enzyme during the encystment process using RNA interference. *Eukaryotic Cell*, *7*(3), 509–517. https://doi.org/10.1128/EC.00316-07

Lorenzo-Morales, J., Martín-Navarro, C. M., López-Arencibia, A., Arnalich-Montiel, F., Piñero, J. E., & Valladares, B. (2013). Acanthamoeba keratitis: An emerging disease gathering importance worldwide? *Trends in Parasitology*, *29*(4), 181–187. https://doi.org/10.1016/j.pt.2013.01.006

Ma, P., Visvesvara, G. S., Martinez, A. J., Theodore, F. H., Daggett, P. M., & Sawyer, T. K. (1990). Naegleria and Acanthamoeba infections: review. *Reviews of Infectious Diseases*, *12*(3), 490–513. https://doi.org/10.1093/clinids/12.3.490

Maghsood, A. H., Sissons, J., Rezaian, M., Holder, D., Warhurst, D., & Khan, N. A. (2005). Acanthamoeba genotype T4 from the UK and Iran and isolation of the T2 genotype from clinical isolates. *Journal of Medical Microbiology*, *54*(8), 755–759. https://doi.org/10.1099/jmm.0.45970-0

Magnet, A., Gomes, T. S., Pardinas, C., Garcia De Blas, N., Sadaba, C., Carrillo, E., Izquierdo, F., Del Castillo, J. M. B., Hurtado, C., Del Aguila, C., & Fenoy, S. (2018). Can artificial tears prevent Acanthamoeba keratitis? An in vitro approach. *Parasites and Vectors*, *11*(1). https://doi.org/10.1186/s13071-018-2639-5

Mahdavi Poor, B., Dalimi, A., Ghafarifar, F., Khoshzaban, F., & Abdolalizadeh, J. (2017). Characterization of extracellular proteases of Acanthamoeba genotype T4 isolated from different sources in Iran. *Parasitology Research*, *116*(12), 3373–3380. https://doi.org/10.1007/s00436-017-5656-y

Majid, M. A. A., Mahboob, T., Mong, B. G. J., Jaturas, N., Richard, R. L., Tian-Chye, T., Phimphila, A., Mahaphonh, P., Aye, K. N., Aung, W. L., Chuah, J., Ziegler, A. D., Yasiri, A., Sawangjaroen, N., Lim, Y. A. L., & Nissapatorn, V. (2017). Pathogenic waterborne free-living amoebae: An update from selected Southeast Asian countries. *PLoS ONE*, *12*(2). https://doi.org/10.1371/journal.pone.0169448

Marciano-Cabral, F., & Cabral, G. (2003). Acanthamoeba spp. as agents of disease in humans. *Clinical Microbiology Reviews*, *16*(2), 273–307. https://doi.org/10.1128/CMR.16.2.273-307.2003

Martinez, A. J., & Visvesvaraz, G. S. (1997). Free-living, Amphizoic and Opportunistic Amebas. *Brain Pathology*, *7*, 583–598.

Martín-Navarro, C. M., López-Arencibia, A., Sifaoui, I., Reyes-Batlle, M., Valladares, B., Martínez-Carretero, E., Piñero, J. E., Maciver, S. K., & Lorenzo-Morales, J. (2015). Statins and voriconazole induce programmed cell death in Acanthamoeba castellanii. *Antimicrobial Agents and Chemotherapy*, *59*(5), 2817–2824. https://doi.org/10.1128/AAC.00066-15

Mascarenhas, J., Lalitha, P., Prajna, N. V., Srinivasan, M., Das, M., D'Silva, S. S., Oldenburg, C. E., Borkar, D. S., Esterberg, E. J., Lietman, T. M., & Keenan, J. D. (2014). Acanthamoeba, fungal, and bacterial keratitis: A comparison of risk factors and clinical features. *American Journal of Ophthalmology*, *157*(1), 56–62. https://doi.org/10.1016/j.ajo.2013.08.032

Matsumoto, Y., A Ibrahim, O. M., Kojima, T., Wakamatsu, T. H., Dogru, M., & Tsubota, K. (2016). Microwave Irradiation as a Promising Method of Sterilization for Acanthamoeba polyphaga in Cultures. *Cornea*, *35*(11), 1478–1482. www.corneajrnl.com

Matsumoto, Y., Kodama, A., Goto, E., Kawakita, T., Dogru, M., & Tsubota, K. (2017). The relation of ocular surface irregularity and visual disturbance in early stage Acanthamoeba keratitis. *Eye and Contact Lens*, *43*(1), 51–56. https://doi.org/10.1097/ICL.0000000000000233

Mattana, A., Cappai, V., Alberti, L., Serra, C., Fiori, P. L., & Cappuccinelli, P. (2002). ADP and other metabolites released from Acanthamoeba castellanii lead to human monocytic cell death through apoptosis and stimulate the secretion of proinflammatory cytokines. *Infection and Immunity*, *70*(8), 4424–4432. https://doi.org/10.1128/IAI.70.8.4424-4432.2002

Mattar, F. E., & Byers, T. J. (1971). MORPHOLOGICAL CHANGES AND THE REQUIREMENTS FOR MACROMOLECULE SYNTHESIS DURING EXCYSTMENT OF ACANTHAMOEBA CASTELLANII. *The Journal of Cell Biology*, *49*, 507–519.

May, L. P., Sidhu, G. S., Ruth Buchness, M., & York, N. (1992). Diagnosis of Acanthamoeba infection by cutaneous manifestations in a man seropositive to HIV. *Journal of the American Academy of Dermatology* , *26*(2), 352–355.

Maycock, N. J. R., & Jayaswal, R. (2016). Update on Acanthamoeba Keratitis: Diagnosis, Treatment, and Outcomes. *Cornea*, *35*, 713–720. http://www.cdc.gov/parasites/

McKelvie, J., Patel, D., & McGhee, C. (2009). Cosmetic contact lens-related acanthamoeba keratitis. *Clinical and Experimental Ophthalmology*, *37*(4), 419–420. https://doi.org/10.1111/j.1442-9071.2009.02052.x

McLaughlin, G. L., Brandt, F. H., & Visvesvara, G. S. (1988). Restriction Fragment Length Polymorphisms of the DNA of Selected Naegleria and Acanthamoeba Amebae. *JOURNAL OF CLINICAL MICROBIOLOGY*, 1655–1658.

Megha, K., Gupta, A., Sehgal, R., & Khurana, S. (2017). An improvised medium for axenic cultivation of Acanthamoeba spp. *Indian Journal of Medical Microbiology*, *35*(4), 597–599. https://doi.org/10.4103/ijmm.IJMM_17_151

Meighani, M., Eslamirad, Z., Hajihossein, R., Ahmadi, A., & Saki, S. (2018). Isolation and genotyping of acanthamoeba from soil samples in Markazi Province, Iran. *Open Access Macedonian Journal of Medical Sciences*, *6*(12), 2290–2294. https://doi.org/10.3889/oamjms.2018.454

Michel, R., & Hauröder, B. (1997). Isolation of an Acanthamoeba Strain with Intracellular Burkholderia pickettii Infection. *Zbl. Bakt.*, *285*, 541–557.

Mirsayafov, D., Albert, T., Shmakov, A., & Asitinskaya, P. (2018). Tap Water and Risk of Acanthamoeba Keratitis in Rigid Gas-Permeable Lens Wearers: Sacred Cow or Culprit? *Eye & Contact Lens*, *44*(2), 132–136. http://journals.lww.com/claojournal

Mitra, M. M., Alizadeh, H., Gerard, R. D., & Niederkorn, J. Y. (1995). Characterization of a plasminogen activator produced by Acanthamoeba castellanii. In *Molecular and Biochemical Parasitology* (Vol. 73).

Mitro, K., Bhagavathiammai, A., Zhou, O.-M., Bobbett, G., McKerrow, J. H., Chokshi, R., Chokshi, B., & James, E. R. (1994). Partial Characterization of the Proteolytic Secretions of Acanthamoeba polyphaga. *Experimental Parasitology*, *78*, 377–385.

Moon, E. K., Hong, Y., Chung, D. Il, & Kong, H. H. (2012). Cysteine protease involving in autophagosomal degradation of mitochondria during encystation of Acanthamoeba. *Molecular and Biochemical Parasitology*, *185*(2), 121–126. https://doi.org/10.1016/j.molbiopara.2012.07.008

Moon, E. K., & Kong, H. H. (2012). Short-cut pathway to synthesize cellulose of encysting Acanthamoeba. *Korean Journal of Parasitology*, *50*(4), 361–364. https://doi.org/10.3347/kjp.2012.50.4.361

Moon, E. K., Lee, S., Quan, F. S., & Kong, H. H. (2018). Effect of 2, 6-dichlorobenzonitrile on amoebicidal activity of multipurpose contact lens disinfecting solutions. *Korean Journal of Parasitology*, *56*(5), 491–494. https://doi.org/10.3347/kjp.2018.56.5.491

Mosser, D. M., & Edwards, J. P. (2008). Exploring the full spectrum of macrophage activation. *Nature Reviews Immunology*, *8*(12), 958–969. https://doi.org/10.1038/nri2448

Moura, H., Wallace, S., & Visvesvara, G. S. (1992). Acanthamoeba healyi N. Sp. and the Isoenzyme Acanthamoeba spp., Groups and Immunoblot 1 and 3 Profiles of. *J Prolozoo*, *39*(5), 573–583.

Mullis, K. B. (1990). The unusual origin of the polymerase chain reaction. *Scientific American*, *262*(4), 56–61, 64–65. https://doi.org/10.1038/scientificamerican0490-56

Na, B. K., Kim, J. C., & Song, C. Y. (2001). Characterization and pathogenetic role of proteinase from Acanthamoeba castellanii. *Microbial Pathogenesis*, *30*(1), 39–48. https://doi.org/10.1006/mpat.2000.0403

Na, B.-K., Cho, J.-H., Song, C.-Y., & Kim, T.-S. (2002). Degradation of immunoglobulins, protease inhibitors and interleukin-1 by a secretory proteinase of Acanthamoeba castellanii. *The Korean Journal of Parasitology*, *40*(2), 93–99.

Nacapunchai, D., Kino, H., & Sriwichai, P. (2014). A brief survey of free-living amebae in Thailand and Hamamatsu District, Japan. *Southeast Asian J Trop Med Public Health*, *32*(2), 179–182. https://www.researchgate.net/publication/11330761

Nagington, J., Watson, P. G., Playfair, T. J., Mcgill, J., Jones, BarrieR., & Steele, A. D. McG. (1974). AMOEBIC INFECTION OF THE EYE. *The Lancet*, *304*(7896), 1537–1540. https://doi.org/10.1016/S0140-6736(74)90285-2

Nau, A., & Dhaliwal, D. (2018). Exposure to Tap Water Puts a Contact Lens Wearer at Greater Risk of Exposure to Acanthamoeba. *Eye & Contact Lens*, *44*(2), 136.

Neale, K. A., & Alderete, J. F. (1990). Analysis of the Proteinases of Representative Trichomonas vaginalis Isolates. *INFECTION AND IMMUNITY*, *58*(1), 157–162.

Neelam, S., & Niederkorn, J. Y. (2017). Pathobiology and Immunobiology of Acanthamoeba Keratitis: Insights from Animal Models. *YALE JOURNAL OF BIOLOGY AND MEDICINE*, *90*, 261–268.

Neff, R. J. (1957). Purification, Axenic Cultivation, and Description of a Soil Amoeba, Acanthamoeba sp. *The Journal of Protozoology*, *4*(3), 176–182. https://doi.org/10.1111/j.1550-7408.1957.tb02505.x

Neumeister, B., Reiff, G., Faigle, M., Dietz, K., Northoff, H., Lang, F., & Transfusionsmedizin, A. (2000). Influence of Acanthamoeba castellanii on Intracellular Growth of Different Legionella Species in Human Monocytes. *APPLIED AND ENVIRONMENTAL MICROBIOLOGY*, *66*(3), 914–919.

Ng, S. L., Nordin, A., Abd Ghafar, N., Suboh, Y., Ab Rahim, N., & Chua, K. H. (2017). Acanthamoeba-mediated cytopathic effect correlates with MBP and AhLBP mRNA expression. *Parasites and Vectors*, *10*(1). https://doi.org/10.1186/s13071-017-2547-0

Niederkorn, J. Y. (2021). The biology of Acanthamoeba keratitis. *Experimental Eye Research*, *202*. https://doi.org/10.1016/j.exer.2020.108365

Niederkorn, J. Y., Alizadeh, H., Leher, H., & Mcculley, J. P. (1999). The pathogenesis of Acanthamoeba keratitis. *Microbes and Infection*, *1*, 437–443.

Niyadurupola, N., & Illingworth, C. D. (2006). Acanthamoeba keratitis associated with misuse of daily disposable contact lenses. *Contact Lens and Anterior Eye*, *29*(5), 269–271. https://doi.org/10.1016/j.clae.2006.08.002

Niyyati, M., Abedkhojasteh, H., Salehi, M., Farnia, S., & Rezaeian, M. (2013). Axenic Cultivation and Pathogenic Assays of Acanthamoeba Strains Using Physical Parameters. *Iranian J Parasitol*, *8*(2), 186–189. http://ijpa.tums.ac.ir

Niyyati, M., Dodangeh, S., & Lorenzo-Morales, J. (2016). A Review of the Current Research Trends in the Application of Medicinal Plants as a Source for Novel Therapeutic Agents Against Acanthamoeba Infections. *Iranian Journal of Pharmaceutical Research*, *15*(4), 893–900.

Nowakowski, A. B., Wobig, W. J., & Petering, D. H. (2014). Native SDS-PAGE: high resolution electrophoretic separation of proteins with retention of native properties including bound metal ions. *Metallomics : Integrated Biometal Science*, *6*(5), 1068–1078. https://doi.org/10.1039/c4mt00033a

Oldenburg, C. E., Acharya, N. R., Tu, E. Y., Zegans, M. E., Mannis, M. J., Gaynor, B. D., Whitcher, J. P., Lietman, T. M., & Keenan, J. D. (2011). Practice patterns and opinions in the treatment of acanthamoeba keratitis. *Cornea*, *30*(12), 1363–1368. https://doi.org/10.1097/ICO.0b013e31820f7763

Olson, J. K., & Miller, S. D. (2004). Microglia Initiate Central Nervous System Innate and Adaptive Immune Responses through Multiple TLRs 1. *The Journal of Immunology*, *173*, 3916–3924. http://journals.aai.org/jimmunol/article-pdf/173/6/3916/1189450/3916.pdf

Omaña-Molina, M., González-Robles, A., Iliana Salazar-Villatoro, L., Lorenzo-Morales, J., Cristóbal-Ramos, A. R., Hernández-Ramírez, V. I., Talamás-Rohana, P., Méndez Cruz, A. R., & Martínez-Palomo, A. (2013). Reevaluating the role of acanthamoeba proteases in tissue invasion: Observation of cytopathogenic mechanisms on MDCK cell monolayers and hamster corneal cells. *BioMed Research International*, *2013*. https://doi.org/10.1155/2013/461329

Orosz, E., Szentmáry, N., Kiss, H. J., Farkas, Á., Kucsera, I., & Nagy, Z. Z. (2018). First report of acanthamoeba genotype T8 human keratitis. *Acta Microbiologica et Immunologica Hungarica*, *65*(1), 73–79. https://doi.org/10.1556/030.65.2018.007

Ortega-Rivas, A., Lorenzo-Morales, J., Alonso, V., Abreu, N. J., Foronda, P., Del Castillo, A., & Valladares, B. (2003). Random amplified polymorphic DNA profiles as a tool for the identification of Acanthamoeba divionensis. *Current Microbiology*, *47*(2), 84–86. https://doi.org/10.1007/s00284-002-3939-7

Page, M. A., & Mathers, W. D. (2013). Acanthamoeba keratitis: A 12-Year experience covering a wide spectrum of presentations, diagnoses, and outcomes. *Journal of Ophthalmology*, *2013*. https://doi.org/10.1155/2013/670242

Panjwani, N. (2010). Pathogenesis of Acanthamoeba Keratitis. *Ocul Surf*, *8*(2), 70–79.

Parija, S., Venugopal, H., & KP, D. (2015). Management of granulomatous amebic encephalitis: Laboratory diagnosis and treatment. *Tropical Parasitology*, *5*(1), 23. https://doi.org/10.4103/2229-5070.149889

Park, K. W., & Song, C. Y. (1996). Purification and Characterization of a Serine Proteinase from Acanthamoeba culbertsoni. *J. Biochem. Mol. Biol.*, *29*(5), 455–461.

Parks, W. C., Wilson, C. L., & López-Boado, Y. S. (2004). Matrix metalloproteinases as modulators of inflammation and innate immunity. *Nature Reviews Immunology*, *4*(8), 617–629. https://doi.org/10.1038/nri1418

Patel, D. V., & McGhee, C. N. J. (2009). Acanthamoeba keratitis: A comprehensive photographic reference of common and uncommon signs. *Clinical and Experimental Ophthalmology*, *37*(2), 232–238. https://doi.org/10.1111/j.1442-9071.2008.01913.x

Pélandakis, M., Kaundun, S. S., Jonckheere, J. F., & Pernin, P. (2006). DNA diversity among the free-living amoeba, Naegleria fowleri, detected by the random amplified polymorphic DNA method. *FEMS Microbiology Letters*, *151*(1), 31–39. https://doi.org/10.1111/j.1574-6968.1997.tb10391.x

Philippe, N., Shukla, A., Abergel, C., & Bisio, H. (2023). Genetic manipulation of giant viruses and their host, Acanthamoeba castellanii. *Nature Protocols*. https://doi.org/10.1038/s41596-023-00910-y

Pollard, T. D., & Borisy, G. G. (2003). Review Cellular Motility Driven by Assembly and Disassembly of Actin Filaments to decipher. Recent excitement in the motility field is focused on a convergence of structural, biochemical, genetic,and theoretical studies which have, for the first. *Cell*, *112*, 453–465.

Por, Y. M., Mehta, J. S., Chua, J. L. L., Koh, T. H., Khor, W. B., Fong, A. C. Y., Lim, J. W. K., Heng, W. J., Loh, R. S. K., Lim, L., & Tan, D. T. H. (2009). Acanthamoeba Keratitis Associated with Contact Lens Wear in Singapore. *American Journal of Ophthalmology*, *148*(1). https://doi.org/10.1016/j.ajo.2009.02.030

Preston, T. M., & King, C. A. (1984). Amoeboid Locomotion of Acanthamoeba castellanii with Special Reference to Cell-Substratum Interactions. *Journal of General Microbiology*, *130*, 23–40.

Preston, T. M., Richards, H., & Wotton, R. S. (2001). Locomotion and feeding of Acanthamoeba at the water-air interface of ponds. *FEMS Microbiology Letters*, *194*(2), 143–147. https://doi.org/10.1111/j.1574-6968.2001.tb09459.x

Pumidonming, W., Koehsler, M., Leitsch, D., & Walochnik, J. (2014). Protein profiles and immunoreactivities of Acanthamoeba morphological groups and genotypes. *Experimental Parasitology*, *145*(S), S50–S56. https://doi.org/10.1016/j.exppara.2014.05.006

Pumidonming, W., Koehsler, M., & Walochnik, J. (2010). Acanthamoeba strains show reduced temperature tolerance after long-term axenic culture. *Parasitology Research*, *106*(3), 553–559. https://doi.org/10.1007/s00436-009-1694-4

Pussard, M., & Pons, R. (1977). MORPHOLOGIE DE LA PAROI KYSTIQUE ET TAXONOMIE DU GENRE ACANTHAMOEBA (PROTOZOA, AMOEBIDA). *PROTISTOLOGICA*, *14*(4), 557–598.

Putaporntip, C., Kuamsab, N., Nuprasert, W., Rojrung, R., Pattanawong, U., Tia, T., Yanmanee, S., & Jongwutiwes, S. (2021). Analysis of Acanthamoeba genotypes from public freshwater sources in Thailand reveals a new genotype, T23 Acanthamoeba bangkokensis sp. nov. *Scientific Reports*, *11*(1). https://doi.org/10.1038/s41598-021-96690-0

Qvarnstrom, Y., Visvesvara, G. S., Sriram, R., & Da Silva, A. J. (2006). Multiplex real-time PCR assay for simultaneous detection of Acanthamoeba spp., Balamuthia mandrillaris, and Naegleria fowleri. *Journal of Clinical Microbiology*, *44*(10), 3589–3595. https://doi.org/10.1128/JCM.00875-06

Radford, C. F., Minassian, D. C., & Dart, J. K. G. (2002). Acanthamoeba keratitis in England and Wales: incidence, outcome, and risk factors. *Br J Ophthalmol*, *86*, 536–542. www.bjophthalmol.com

Raghavan, A., Bellamkonda, P., Mendoza, L., & Rammohan, R. (2018). Pythium insidiosum and Acanthamoeba keratitis in a contact lens user. *BMJ Case Reports*, *11*(1). https://doi.org/10.1136/bcr-2018-226386

Ramírez-Rico, G., Martínez-Castillo, M., De La Garza, M., Shibayama, M., & Serrano-Luna, J. (2015). Acanthamoeba castellanii proteases are capable of degrading iron-binding proteins as a possible mechanism of pathogenicity. *Journal of Eukaryotic Microbiology*, *62*(5), 614–622. https://doi.org/10.1111/jeu.12215

Randag, A. C., van Rooij, J., van Goor, A. T., Verkerk, S., Wisse, R. P. L., Saelens, I. E. Y., Stoutenbeek, R., van Dooren, B. T. H., Cheng, Y. Y. Y., & Eggink, C. A. (2019). The rising incidence of Acanthamoeba keratitis: A 7-year nationwide survey and clinical assessment of risk factors and functional outcomes. *PLOS ONE*, *14*(9), e0222092. https://doi.org/10.1371/journal.pone.0222092

Rayamajhee, B., Williams, N. L. R., Siboni, N., Rodgers, K., Willcox, M., Henriquez, F. L., Seymour, J. R., Potts, J., Johnson, C., Scanes, P., & Carnt, N. (2023). Identification and quantification of Acanthamoeba spp. within seawater at four coastal lagoons on the east coast of Australia. *Science of The Total Environment*, *901*, 165862. https://doi.org/10.1016/j.scitotenv.2023.165862

Reverey, J. F., Fromme, R., Leippe, M., & Selhuber-Unkel, C. (2014). In vitro adhesion of Acanthamoeba castellanii to soft contact lenses depends on water content and disinfection procedure. *Contact Lens and Anterior Eye*, *37*(4), 262–266. https://doi.org/10.1016/j.clae.2013.11.010

Rivière, D., Szczebara, F. M., Berjeaud, J.-M., Frère, J., & Héchard, Y. (2006). Development of a real-time PCR assay for quantification of Acanthamoeba trophozoites and cysts. *Journal of Microbiological Methods*, *64*(1), 78–83. https://doi.org/10.1016/j.mimet.2005.04.008

Robinson, D. S., & O'garra, A. (2002). Minireview Further Checkpoints in Th1 Development of Th1 responses. Chen et al. showed that upon chal-lenge with protein antigen, TCCR-deficient (TCCR /) mice had impaired Th1 responses, as measured by IFN. *Immunity*, *16*, 755–758.

Rus, H., Cudrici, C., & Niculescu, F. (2005). The role of the complement system in innate immunity. *Immunologic Research*, *33*(2), 103–112. https://doi.org/10.1385/IR:33:2:103

Sawyer, T. K., & Griffin, J. L. (1975). A Proposed New Family, Acanthamoebidae n. fam. (Order Amoebida), for Certain Cyst-Forming Filose Amoebae. *Transactions of the American Microscopical Society*, *94*(1), 93. https://doi.org/10.2307/3225534

Schein, O. D., Glynn, R. J., Poggio, E. C., Seddon, J. M., & Kenyon, K. R. (1989). The Relative Risk of Ulcerative Keratitis among Users of Daily-Wear and Extended-Wear Soft Contact Lenses. *New England Journal of Medicine*, *321*(12), 773–778. https://doi.org/10.1056/NEJM198909213211201

Schroeder, J. M., Booton, G. C., Hay, J., Niszl, I. A., Seal, D. V., Markus, M. B., Fuerst, P. A., & Byers, T. J. (2001). Use of subgenic 18S ribosomal DNA PCR and sequencing for genus and genotype identification of Acanthamoebae from humans with keratitis and from sewage sludge. *Journal of Clinical Microbiology*, *39*(5), 1903–1911. https://doi.org/10.1128/JCM.39.5.1903-1911.2001

Schuster, F. L. (2002). Cultivation of pathogenic and opportunistic free-living amebas. *Clinical Microbiology Reviews*, *15*(3), 342–354. https://doi.org/10.1128/CMR.15.3.342-354.2002

Seal, D. V. (2003). Acanthamoeba keratitis update - Incidence, molecular epidemiology and new drugs for treatment. *Eye*, *17*(8), 893–905. https://doi.org/10.1038/sj.eye.6700563

Seal, D. V, & Hay, J. (1997). Acanthamoeba keratitis: early diagnosis, rational drug intervention and prevention. *HKJO*, *1*(1), 46–52.

Serrano-Luna, J. de J., Cervantes-Sandoval, I., Calderón, J., Navarro-García, F., Tsutsumi, V., & Shibayama, M. (2006). Protease activities of Acanthamoeba polyphaga and Acanthamoeba castellanii. *Canadian Journal of Microbiology*, *52*(1), 16–23. https://doi.org/10.1139/w05-114

Sharma, S., Rao, G., & Garg, P. (2000). Article in The British journal of ophthalmology. *The British Journal of Ophthalmology*, *84*, 1103–1108. https://doi.org/10.1136/bjo.2006.096230#_blank

Siddiqui, R., Aqeel, Y., & Khan, N. A. (2016). The use of dimethyl sulfoxide in contact lens disinfectants is a potential preventative strategy against contracting Acanthamoeba keratitis. *Contact Lens and Anterior Eye*, *39*(5), 389–393. https://doi.org/10.1016/j.clae.2016.04.004

Siddiqui, R., & Khan, N. A. (2012). Biology and pathogenesis of Acanthamoeba. *Parasites & Vectors*, *5*, 6. https://doi.org/10.1186/1756-3305-5-6

Singh, D., Naik, S. R., & Naik, S. (2004). Role of cysteine proteinase of Entamoeba histolytica in target cell death. *Parasitology*, *129*(2), 127–135. https://doi.org/10.1017/S0031182004005451

Sissons, J., Alsam, S., Goldsworthy, G., Lightfoot, M., Jarroll, E. L., & Khan, N. A. (2006). Identification and properties of proteases from an Acanthamoeba isolate capable of producing granulomatous encephalitis. *BMC Microbiology*, *6*(42). https://doi.org/10.1186/1471-2180-6-42

Sissons, J., Alsam, S., Jayasekera, S., & Khan, N. A. (2004). Ecto-ATPases of clinical and non-clinical isolates of Acanthamoeba. *Microbial Pathogenesis*, *37*(5), 231–239. https://doi.org/10.1016/j.micpath.2004.01.004

Sissons, J., Alsam, S., Jayasekera, S., Kim, K. S., Stins, M., & Khan, N. A. (2004). Acanthamoeba induces cell-cycle arrest in host cells. *Journal of Medical Microbiology*, *53*(8), 711–717. https://doi.org/10.1099/jmm.0.45604-0

Sissons, J., Kwang, S. K., Stins, M., Jayasekera, S., Alsam, S., & Khan, N. A. (2005). Acanthamoeba castellanii induces host cell death via a phosphatidylinositol 3-kinase-dependent mechanism. *Infection and Immunity*, *73*(5), 2704–2708. https://doi.org/10.1128/IAI.73.5.2704-2708.2005

Snider, J., Lin, F., Zahedi, N., Rodionov, V., Yu, C. C., & Gross, S. P. (2004). Intracellular actin-based transport: How far you go depends on how often you switch. *PNAS*, *101*(36), 13204–13209. www.pnas.orgcgidoi10.1073pnas.0403092101

Somani, S. N., Ronquillo, Y., & Moshirfar, M. (2023). Acanthamoeba Keratitis. In *StatPearls*. http://www.ncbi.nlm.nih.gov/pubmed/26989955

Sriram, R., Shoff, M., Booton, G., Fuerst, P., & Visvesvara, G. S. (2008). Survival of Acanthamoeba cysts after desiccation for more than 20 years. *Journal of Clinical Microbiology*, *46*(12), 4045–4048. https://doi.org/10.1128/JCM.01903-08

Stan, C., Vlăduțiu, C., & Popovici, M. (2016). Acanthamoeba keratitis challenges a case report. *Romanian Journal of Ophthalmology*, *60*(1), 40–42.

Stapleton, F., & Carnt, N. (2012). Contact lens-related microbial keratitis: How have epidemiology and genetics helped us with pathogenesis and prophylaxis. *Eye*, *26*(2), 185–193. https://doi.org/10.1038/eye.2011.288

Startford, M. P., & Griffiths, A. J. (1978). Variations in the Properties and Morphology of Cysts of Acanthamoeba castellanii. *Journal of General Microbiology*, *108*, 33–37.

Sternlicht, M. D., & Werb, Z. (2001). How matrix metalloproteinases regulate cell behavior. *Annual Review of Cell and Developmental Biology*, *17*, 463–516. https://doi.org/10.1146/annurev.cellbio.17.1.463

Stevens, A. R., & O'Dell, W. D. (1974). In vitro growth and virulence of Acanthamoeba. *The Journal of Parasitology*, *60*(5), 884–885.

Stothard, D. R., Schroeder-Diedrich, J. M., Awwad, M. H., Gast,', R. J., Ledee, D. R., Rodriguez-Zaragoza, S., Dean, C. L., Fuerst, P. A., & Byers, T. J. (1998). The Evolutionary History of the Genus Acanthamoeba and the Identification of Eight New 18s rRNA Gene Sequence Types. *J. Euk. Microbiol.*, *45*, 45–54. www.bio-sci.ohio-state.edu/-pfuerst/!acanth.htm,

Sundar, S., & Olliaro, P. L. (2007). Miltefosine in the treatment of leishmaniasis: Clinical evidence for informed clinical risk management. *Therapeutics and Clinical Risk Management*, *3*(5), 733–740.

Sütçü, M., Aktürk, H., Gülümser-şişko, S., Acar, M., Erol, O. B., Somer, A., Bilgiç, B., & Salman, N. (2018). Granulomatous amebic encephalitis caused by acanthamoeba in an immuncompetent child. *Turkish Journal of Pediatrics*, *60*(3), 340–343. https://doi.org/10.24953/turkjped.2018.03.019

Taher, E. E., Méabed, E. M. H., Abdallah, I., & Abdel Wahed, W. Y. (2018). Acanthamoeba keratitis in noncompliant soft contact lenses users: Genotyping and risk factors, a study from Cairo, Egypt. *Journal of Infection and Public Health*, *11*(3), 377–383. https://doi.org/10.1016/j.jiph.2017.09.013

Tan, E. M., Starr, M. R., Henry, M. R., & Pritta, B. S. (2018). The brief case: A "fresh" pair of contact lenses. *Journal of Clinical Microbiology*, *56*(5). https://doi.org/10.1128/JCM.00790-17

Tanaka, A., Era, M., Obata, Y., Masuda, M., Kawahara, T., Kanyama, T., & Morita, H. (2017). Role of fatty acid salts as anti Acanthamoeba agents for disinfecting contact lens. *Biocontrol Science*, *22*(3), 153161.

Tanaka, Y., Suguri, S., Harada, M., Hayabara, T., Suzumori, R., & Ohta, N. (1994). Acanthamoeba-specific human T-cell clones isolated from healthy individuals. *Parasitology Research*, *80*(7), 549–553. https://doi.org/10.1007/BF00933001

Tang, S.-C., Arumugam, T. V, Xu, X., Cheng, A., Mughal, M. R., Gyu Jo, D., Lathia, J. D., Siler, D. A., Chigurupati, S., Ouyang, X., Magnus, T., Camandola, S., & Mattson, M. P. (2007). Pivotal role for neuronal Toll-like receptors in ischemic brain injury and functional deficits. *PNAS*, *104*(34), 13798–13803. www.pnas.org/cgi/content/full/

Thong, Y. H., & Ferrante, A. (1986a). Migration Patterns of Pathogenic and Nonpathogenic Naegleria spp. *INFECTION AND IMMUNITY*, *51*(1), 177–180.

Thong, Y. H., & Ferrante, A. (1986b). Migration Patterns of Pathogenic and Nonpathogenic Naegleria spp. *INFECTION AND IMMUNITY*, *51*(1), 177–180. https://journals.asm.org/journal/iai

Tomlinson, G., & Jones, E. A. (1962). Isolation of cellulose from the cyst wall of a soil amoeba. *Biochimica et Biophysica Acta*, *63*(1), 194–200. https://doi.org/10.1016/0006-3002(62)90353-0

Tu, E. Y., & Joslin, C. E. (2010). Recent outbreaks of atypical contact lens-related keratitis: What have we learned? *American Journal of Ophthalmology*, *150*(5). https://doi.org/10.1016/j.ajo.2010.06.045

Tu, E. Y., Joslin, C. E., & Shoff, M. E. (2010). Successful treatment of chronic stromal acanthamoeba keratitis with oral voriconazole monotherapy. *Cornea*, *29*(9), 1066–1068. https://doi.org/10.1097/ICO.0b013e3181cbfa2c

Tu, E. Y., Joslin, C. E., Sugar, J., Booton, G. C., Shoff, M. E., & Fuerst, P. A. (2008). The Relative Value of Confocal Microscopy and Superficial Corneal Scrapings in the Diagnosis of Acanthamoeba Keratitis. *Cornea*, *27*(7), 764–772. http://journals.lww.com/corneajrnl

Tu, E. Y., Joslin, C. E., Sugar, J., Shoff, M. E., & Booton, G. C. (2008). Prognostic Factors Affecting Visual Outcome in Acanthamoeba Keratitis. *Ophthalmology*, *115*(11), 1998–2003. https://doi.org/10.1016/j.ophtha.2008.04.038

Tu, E. Y., Shoff, M. E., Gao, W., & Joslin, C. E. (2013). Effect of low concentrations of benzalkonium chloride on acanthamoebal survival and its potential impact on empirical therapy of infectious keratitis. *JAMA Ophthalmology*, *131*(5), 595–600. https://doi.org/10.1001/jamaophthalmol.2013.1644

Tuska-Szalay, B., Kelly, H., Takács, N., Kontschán, J., Votýpka, J., & Hornok, S. (2022). Molecular evidence of Monocercomonas and Acanthamoeba in the feces of captive reptiles. *Parasitology Research*, *121*(12), 3681–3687. https://doi.org/10.1007/s00436-022-07677-3

Vernon, S. E., Acar, B. C., Pham, S. M., & Fertel, D. (2005). Acanthamoeba infection in lung transplantation: Report of a case and review of the literature. *Transplant Infectious Disease*, *7*(3–4), 154–157. https://doi.org/10.1111/j.1399-3062.2005.00113.x

Visvesvara, G. S., Mirra-f H Brandt, S. S., Moss, D. M., Mathews, H. M., & Martin Ez, A. J. (1983). Isolation of Two Strains of Acanthamoeba castellanii from Human Tissue and Their Pathogenicity and Isoenzyme Profiles. *JOURNAL OF CLINICAL MICROBIOLOGY*, *18*(6), 1405–1412.

Walochnik, J., Aichelburg, A., Assadian, O., Steuer, A., Visvesvara, G., Vetter, N., & Aspöck, H. (2008). Granulomatous amoebic encephalitis caused by Acanthamoeba amoebae of genotype T2 in a human immunodeficiency virus-negative patient. *Journal of Clinical Microbiology*, *46*(1), 338–340. https://doi.org/10.1128/JCM.01177-07

Walochnik, J., & Aspöck, H. (2002). Amöben und Amöbosen: Gefährliche biologische und medizinische Sammelsurien. *Denisia 6*, *184*, 229–263. www.biologiezentrum.at

Walochnik, J., & Aspöck, H. (2021). Akanthamöben-Keratitis (AK) (engl. Acanthamoeba keratitis). In *Entzündliche Augenerkrankungen* (pp. 181–193). Springer Berlin Heidelberg. https://doi.org/10.1007/978-3-662-60399-4_10

Walochnik, J., & Obwaller, A. (2001). Acanthamoeba-Keratitis in Österreich: Klinische, mikrobiologische und epidemiologische Befunde. *Mitt. Österr. Ges. Tropenmed. Parasitol.*, *23*, 17–26. https://www.researchgate.net/publication/318724471

Walochnik, J., Obwaller, A., & Aspock, H. (2000). Correlations between morphological, molecular biological, and physiological characteristics in clinical and nonclinical isolates of Acanthamoeba spp. *Applied and Environmental Microbiology*, *66*(10), 4408–4413. https://doi.org/10.1128/AEM.66.10.4408-4413.2000

Walochnik, J., Scheikl, U., & Haller-Schober, E. M. (2015). Twenty years of Acanthamoeba diagnostics in Austria. *Journal of Eukaryotic Microbiology*, *62*(1), 3–11. https://doi.org/10.1111/jeu.12149

Walochnik, J., Sommer, K., Obwaller, A., Haller-Schober, E. M., & Aspöck, H. (2004). Characterisation and differentiation of pathogenic and non-pathogenic Acanthamoeba strains by their protein and antigen profiles. *Parasitology Research*, *92*(4), 289–298. https://doi.org/10.1007/s00436-003-1041-0

Wang, Y., Jiang, L., Zhao, Y., Ju, X., Wang, L., Jin, L., Fine, R. D., & Li, M. (2023). Biological characteristics and pathogenicity of Acanthamoeba. *Frontiers in Microbiology*, *14*, 1–23. https://doi.org/10.3389/fmicb.2023.1147077

Wara-Asawapati, S., Intapan, P. M., & Chotmongkol, V. (2017). Images in clinical tropical medicine acanthamoeba brain abscess confirmed by molecular identification. *American Journal of Tropical Medicine and Hygiene*, *97*(2), 307–308. https://doi.org/10.4269/ajtmh.16-0375

Weisman, R. A. (1976). Differentiation in Acanthamoeba castellanii. *Annual Review of Microbiology*, *30*, 189–219. https://doi.org/10.1146/annurev.mi.30.100176.001201

Wilhelmus, K. R., Jones, D. B., Matoba, A. Y., Hamill, M. B., Pflugfelder, S. C., & Weikert, M. P. (2008). Bilateral Acanthamoeba Keratitis. *American Journal of Ophthalmology*, *145*(2). https://doi.org/10.1016/j.ajo.2007.09.037

Willcox, M. (2010). Multipurpose Disinfecting Solution and Acanthamoeba Keratitis. *Cornea*, *29*(1), 120–121. www.cdc.gov/ncidod/dpd/parasites/

Wong, M. M., Karr, S. L., & Chow, C. K. (1977). Changes in the virulence of Naegleria fowleri maintained in vitro. *The Journal of Parasitology*, *63*(5), 872–878.

Yang, Z., Cao, Z., & Panjwani, N. (1997). Pathogenesis of Acanthamoeba Keratitis: Carbohydrate-Mediated Host-Parasite Interactions. *INFECTION AND IMMUNITY*, *65*(2), 439–445.

Yarar, D., Waterman-Storer, C. M., & Schmid, S. L. (2005). A Dynamic Actin Cytoskeleton Functions at Multiple Stages of Clathrin-mediated Endocytosis □ V. *Molecular Biology of the Cell*, *16*, 964–975. https://doi.org/10.1091/mbc

Yoo, K. T., & Jung, S. Y. (2012). Effects of mannose on pathogenesis of Acanthamoeba castellanii. *Korean Journal of Parasitology*, *50*(4), 365–369. https://doi.org/10.3347/kjp.2012.50.4.365

Zhang, H., & Cheng, X. (2021). Various brain-eating amoebae: the protozoa, the pathogenesis, and the disease. *Frontiers of Medicine*, *15*(6), 842–866. https://doi.org/10.1007/s11684-021-0865-2

Zimmerman, A. B., Richdale, K., Mitchell, G. L., Kinoshita, B. T., Lam, D. Y., Wagner, H., Sorbara, L., Chalmers, R. L., Collier, S. A., Cope, J. R., Rao, M. M., Beach, M. J., & Yoder, J. S. (2017). Water Exposure is a Common Risk Behavior Among Soft and Gas-Permeable Contact Lens Wearers. *Cornea*, *36*, 995–1001. www.corneajrnl.com

XIV. Appendix

Table 7. PCR program “SequNeu”

Step	**Temperature**	**Time (in mins)**	**Cycles**
Initial denaturation	96°C	0:30	1x
Denaturation	96°C	0:10	30x
Annealing	50°C	0:05	
Elongation	60°C	4:00	
Final extension	4°C	Hold	1x

Table 8. PCR program "GastB/54” and “GastB/56”

Step	**Temperature**	**Time (in mins)**	**Cycles**
Initial denaturation	95°C	15:00	1x
Denaturation	95°C	1:00	35x
Annealing	54°/56°C	1:00	
Elongation	72°C	1:00	
Final extension	72°C 4°C	7:00 Hold	1x

Table 9. PCR program “JDP”

Step	**Temperature**	**Time (in mins)**	**Cycles**
Initial denaturation	95°C	15:00	1x
Denaturation	95°C	1:00	35x
Annealing	62°C	2:00	
Elongation	72°C	3:00	
Final extension	72°C 4°C	7:00 Hold	1x

Table 10. Adjusted PCR program (from GastB/56°C)

Step	**Temperature**	**Time (in mins)**	**Cycles**
Initial denaturation	95°C	15:00	1x
Denaturation	95°C	1:00	40x
Annealing	54°C	0:45	
Elongation	72°C°C	0:25	
Final extension	72°C 4°C	7:00 Hold	1x

Table 11. Real-time PCR program

Step	**Temperature**	**Time (in mins)**	**Cycles**
Initial denaturation	95°C	5:00	1x
Denaturation	60°C	0:45	39x
Annealing	65°C → 95°C	0:05, 0.5°C/cycle	
Elongation	30°C	0:01	
Final extension	4°C	Hold	1x